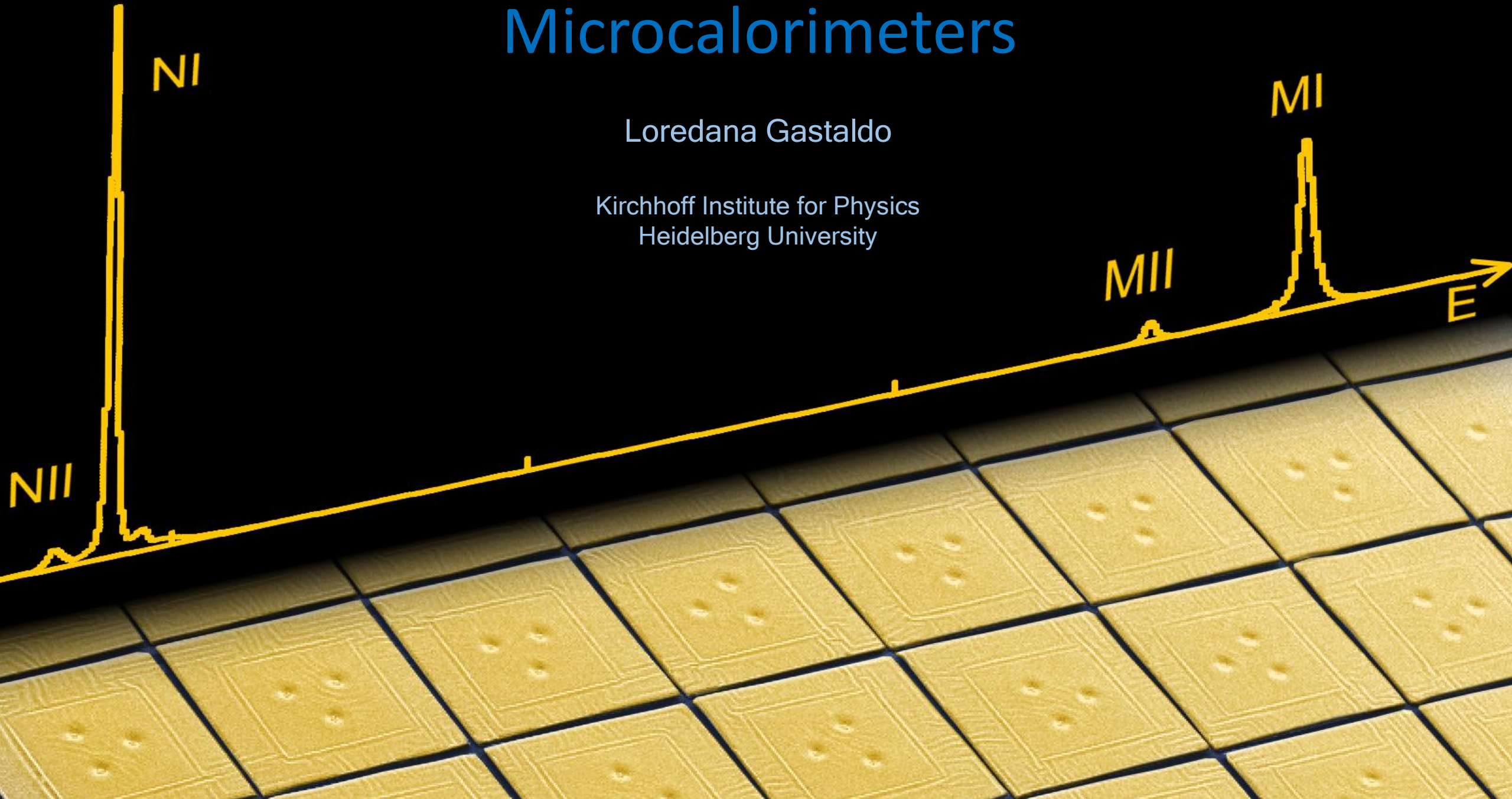


Microcalorimeters

Loredana Gastaldo

Kirchhoff Institute for Physics
Heidelberg University



Outline

- Basic of low temperature detectors
 - TES
 - MMC
- Overview on some applications
 - Photon detection
 - Neutrino physics
 - Search for Dark Matter interactions

Low temperature microcalorimeters

How do they fit to the quantum sensing school?

Low temperature microcalorimeters

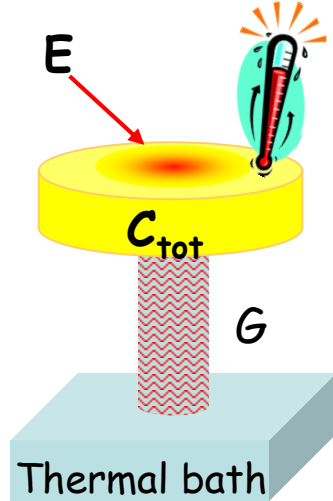
How do they fit to the quantum sensing school?

They precisely detect quanta of energy

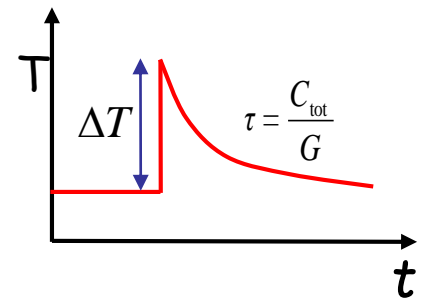
Low temperature microcalorimeters

How do they fit to the quantum sensing school?

They precisely detect quanta of energy ... as an increase of temperature



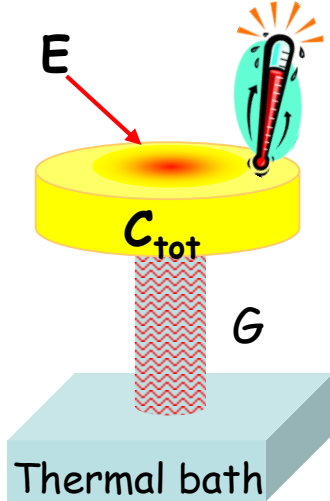
$$\Delta T \cong \frac{E}{C_{\text{tot}}}$$



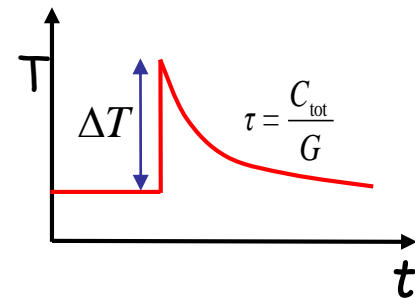
Low temperature microcalorimeters

How do they fit to the quantum sensing school?

They precisely detect quanta of energy ... as an increase of temperature



$$\Delta T \cong \frac{E}{C_{\text{tot}}}$$



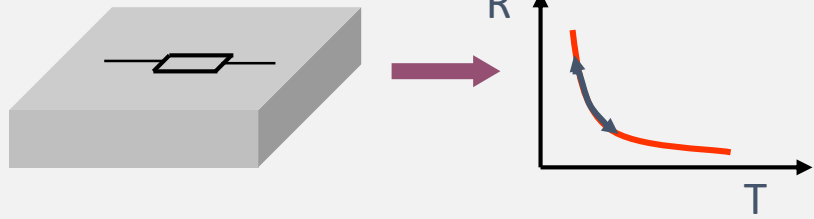
- Very small volume
- Working temperature below 100 mK
small specific heat
small thermal noise
- Very sensitive temperature sensors

Temperature sensors

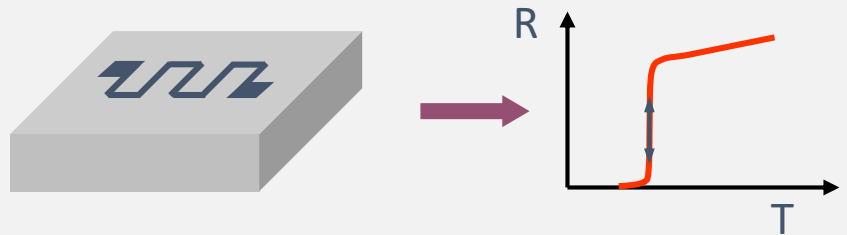
Near equilibrium sensors

Athermal sensors

Resistance of highly doped semiconductors



Resistance at superconducting transition, TES



Magnetization of paramagnetic material, MMC

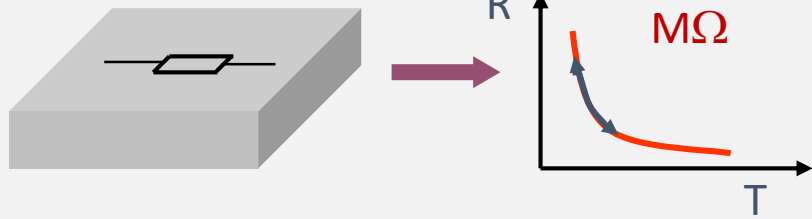


Temperature sensors

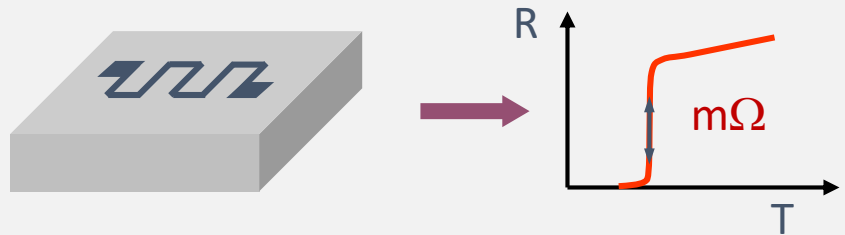
Near equilibrium sensors

Athermal sensors

Resistance of highly doped semiconductors



Resistance at superconducting transition, TES



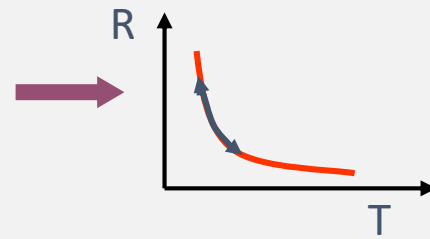
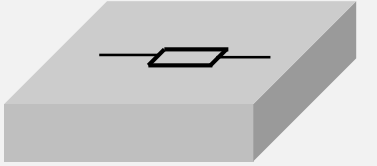
Magnetization of paramagnetic material, MMC



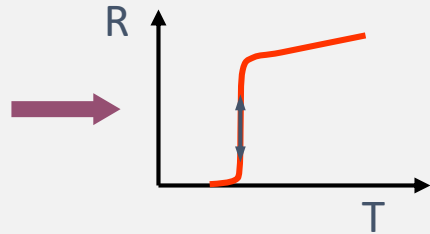
Temperature sensors

Near equilibrium sensors

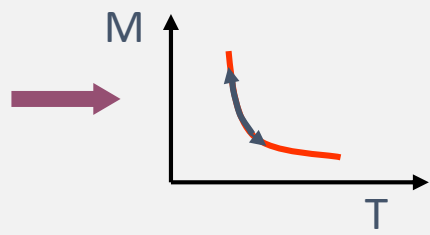
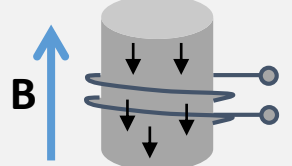
Resistance of highly doped semiconductors



Resistance at superconducting transition, TES

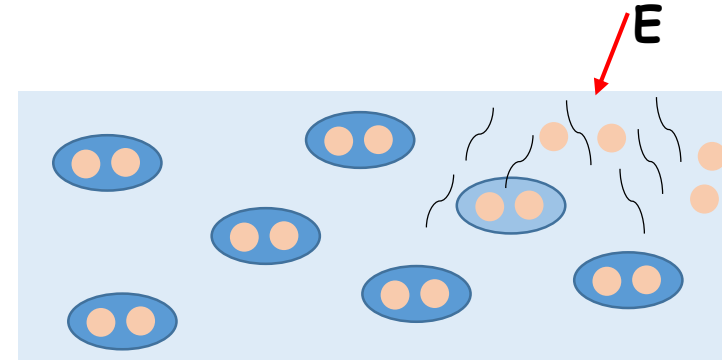


Magnetization of paramagnetic material, MMC



Athermal sensors (based on superconducting films)

Temperature increase induces breaking of Cooper pairs



- Very thin superconducting films
- Working at mK
„no“ quasi-particles @ equilibrium
long quasi-particle half-life
- High efficiency of „counting“ quasi-particles

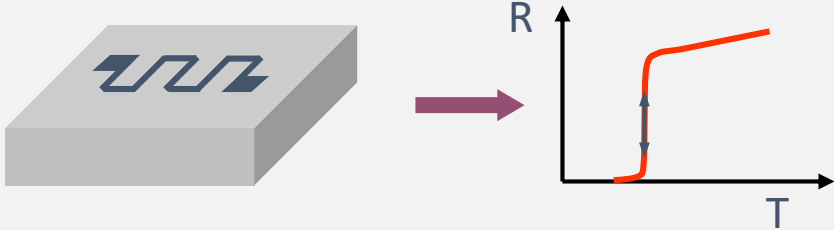
Temperature sensors

Near equilibrium sensors

Resistance of highly doped semiconductors



Resistance at superconducting transition, TES

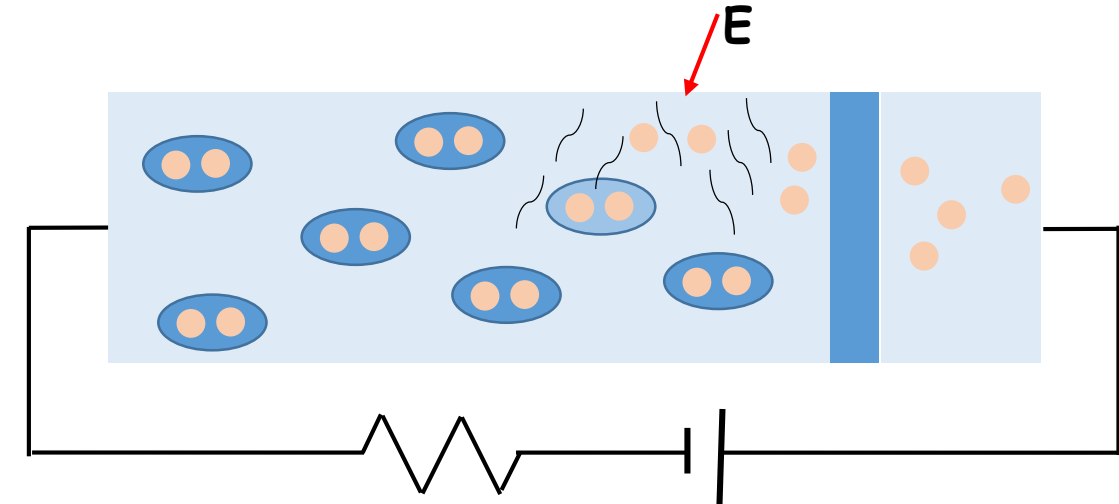


Magnetization of paramagnetic material, MMC



Athermal sensors (based on superconducting films)

Temperature increase induces breaking of Cooper pairs



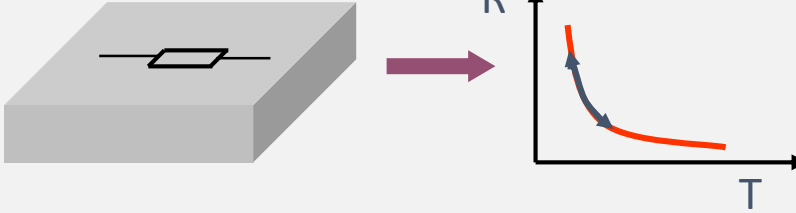
Superconducting Tunnel Junctions - STJ

Quasi-particles tunneling through a thin isolating barrier
Measurement of current

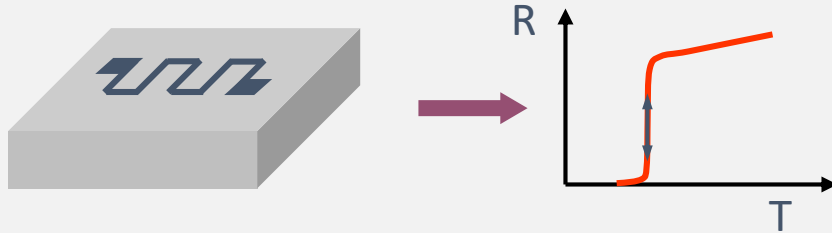
Temperature sensors

Near equilibrium sensors

Resistance of highly doped semiconductors



Resistance at superconducting transition, TES

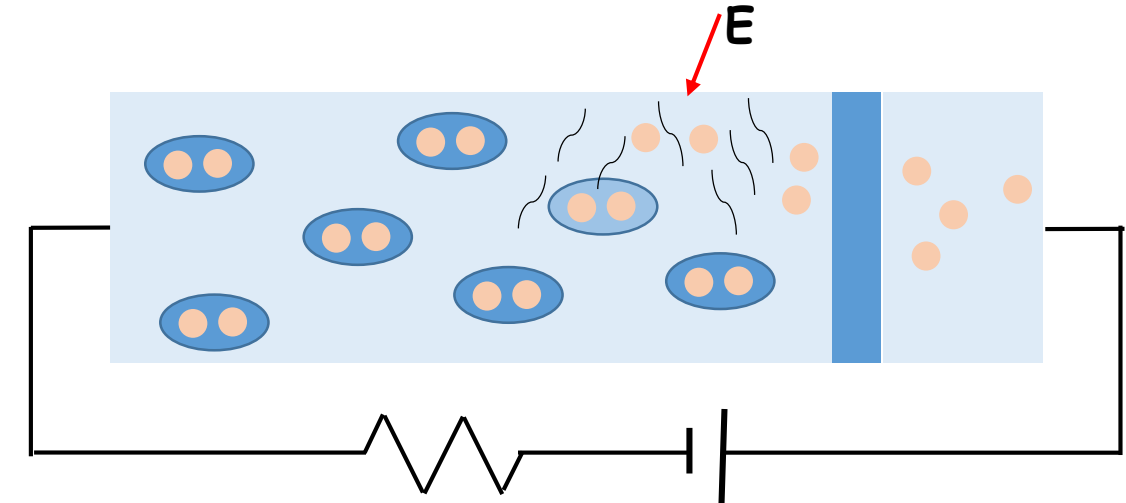


Magnetization of paramagnetic material, MMC

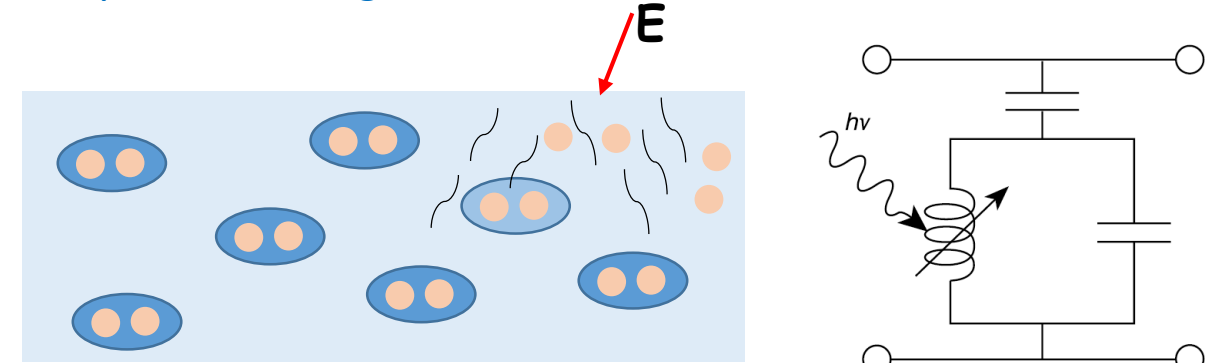


Athermal sensors (based on superconducting films)

Temperature increase induces breaking of Cooper pairs



Superconducting Tunnel Junctions - STJ

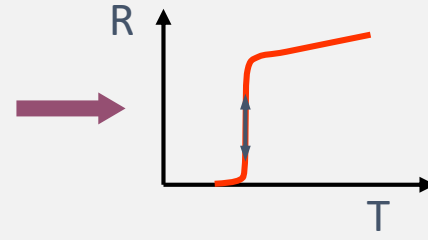


Kinetic Inductance Detectors – KID

Breaking Cooper pairs → change of kinetic inductance

Transition Edge Sensors – superconducting film

Resistance at superconducting transition, TES



Superconducting film operated at the transition temperature

Operating temperature defines:

- heat capacity
- thermal conductance
- thermal noise

In the periodic table only 18 elements with $T_c < 2 \text{ K}$ \rightarrow only 5 are actually used in TES

Al	$T_c \sim 1.1 \text{ K}$
Ti	$T_c \sim 0.39 \text{ K}$
Mo	$T_c \sim 0.92 \text{ K}$
W	$T_c \sim 0.012 \text{ K}$
Ir	$T_c \sim 0.140 \text{ K}$

only elemental superconductor routinely used as TES

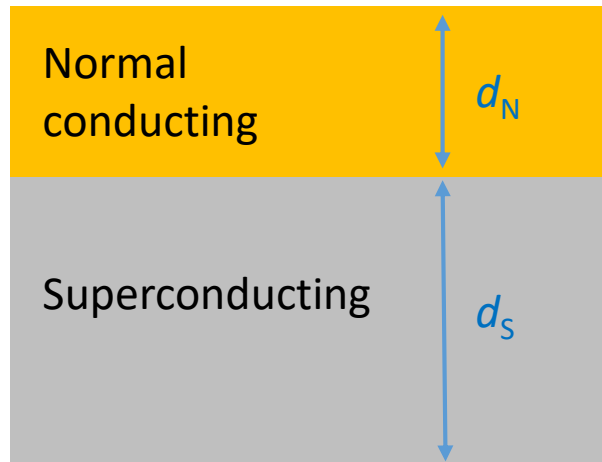
How to reduce the transition temperature of superconducting films to be $\sim 100 \text{ mK}???$

Proximity effect

Magnetic impurities

Transition Edge Sensors – superconducting film

Proximity effect: Lowering the transition temperature of a superconducting film by the presence of a normal metal layer in good electrical contact



If d_N is smaller than the coherence length ξ
→ the bilayer behaves as a homogeneous
superconducting film

Superconductors	Normal
Ti	Cu
Mo	Ag
Al	Au
Ir	

Different model have been developed for the description of the physics of bilayer system. As an example [Usadel theory](#):

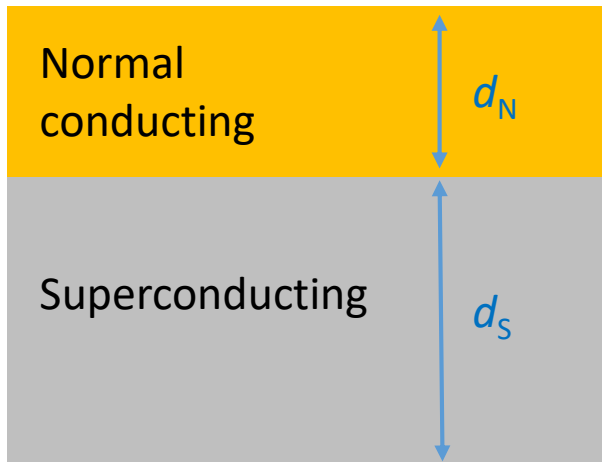
$$T_C = T_{C0} \left[\frac{d_S}{d_0} \frac{1}{1.13(1 + 1/\alpha)} \frac{1}{t} \right]^\alpha$$

$$\alpha = \frac{d_N n_N}{d_S n_S}$$
$$\frac{1}{d_0} = \frac{\pi}{2} K_B T_{C0} \lambda_F^2 n_S$$

λ_F = Fermi wavelength
 n_S, n_N = density of electronic states
 t = transmission coefficient

Transition Edge Sensors – superconducting film

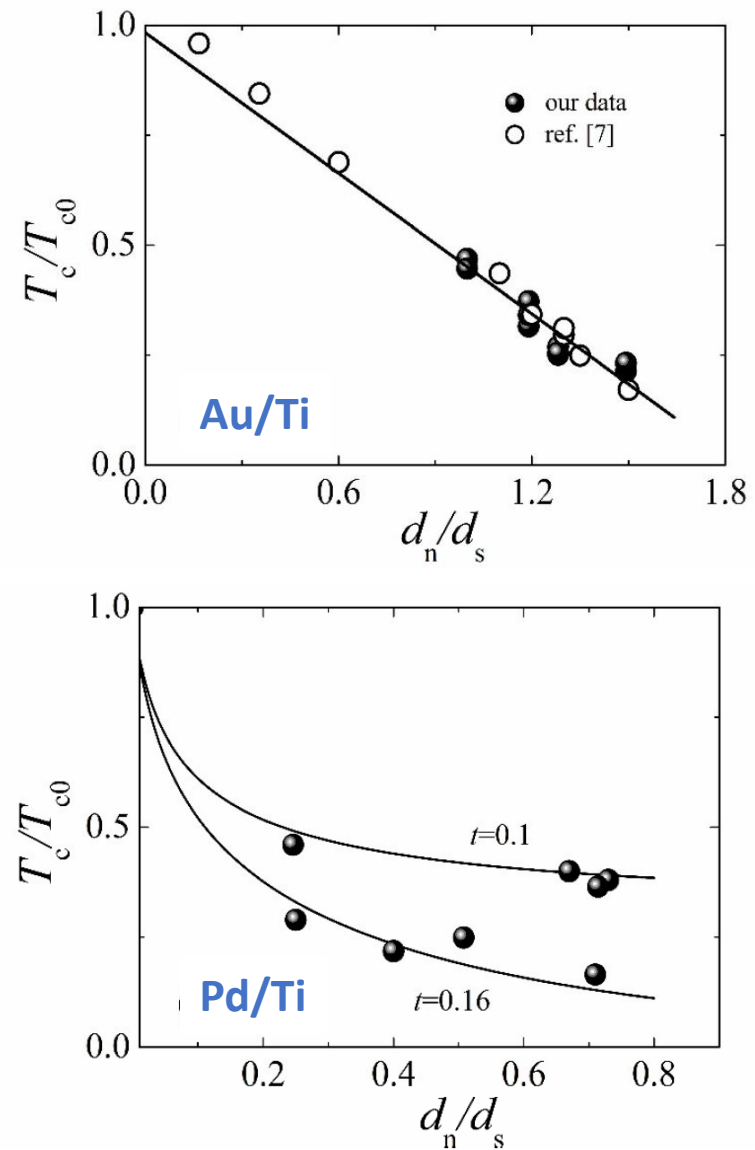
Proximity effect: Lowering the transition temperature of a superconducting film by the presence of a normal metal layer in good electrical contact



If d_N is smaller than the coherence length ξ
→ the bilayer behaves as a homogeneous superconducting film

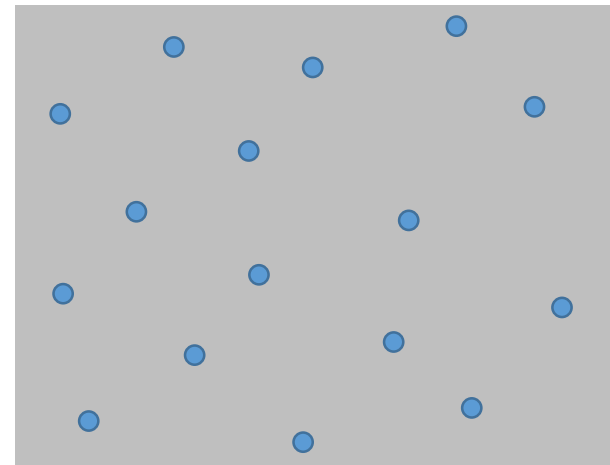
Different model have been developed for the description of the physics of bilayer system. As an example [Usadel theory](#):

$$T_c = T_{c0} \left[\frac{d_s}{d_0} \frac{1}{1.13(1 + 1/\alpha)} \frac{1}{t} \right]^\alpha$$



Transition Edge Sensors – superconducting film

Magnetic impurities: in a superconducting film magnetic impurities induce pair breaking
→ the film thickness is not limited by coherence length



Superconductors
Al
Mo
Ti

Normal
Mn
Fe

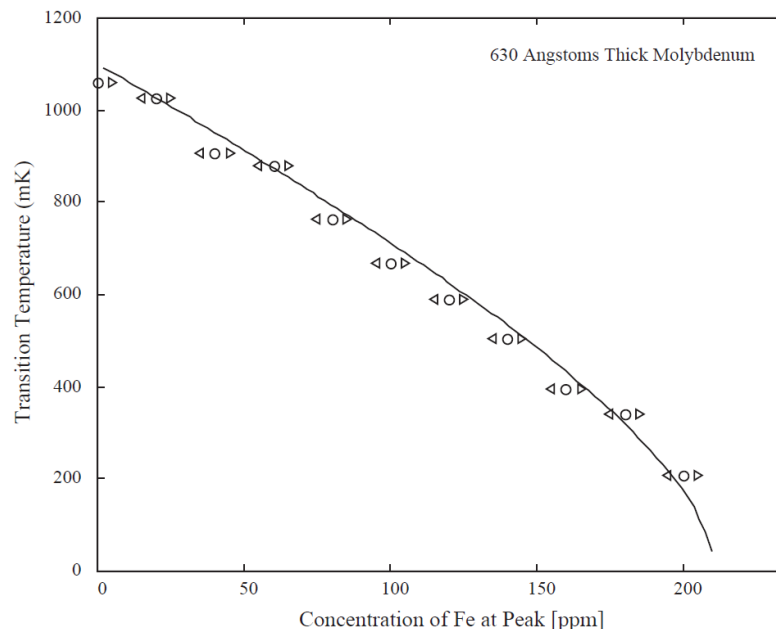


Fig. 2. Reduction of molybdenum film T_c as a function of dopant $^{56}\text{Fe}^+$ concentration. The curve shown is a fit to the data using an Abrikosov-Gor'kov model.

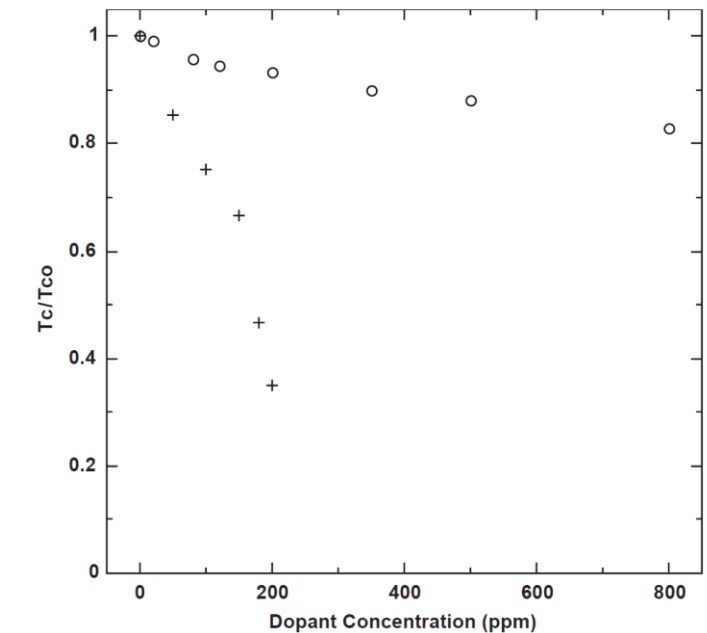


Fig. 3. Titanium film results. Implanting $^{55}\text{Mn}^+$ suppressed T_c dramatically (+). $^{56}\text{Fe}^+$ had only limited effect (o).

Transition Edge Sensors - signal

$R = R(T, I)$: TES resistance

T : TES temperature

C : Heat capacity TES + absorber

G : thermal conductivity to the bath – $G = nkT^{m-1}$

R_{SH} = shunt resistance $R_{SH} < R$

V = applied constant voltage

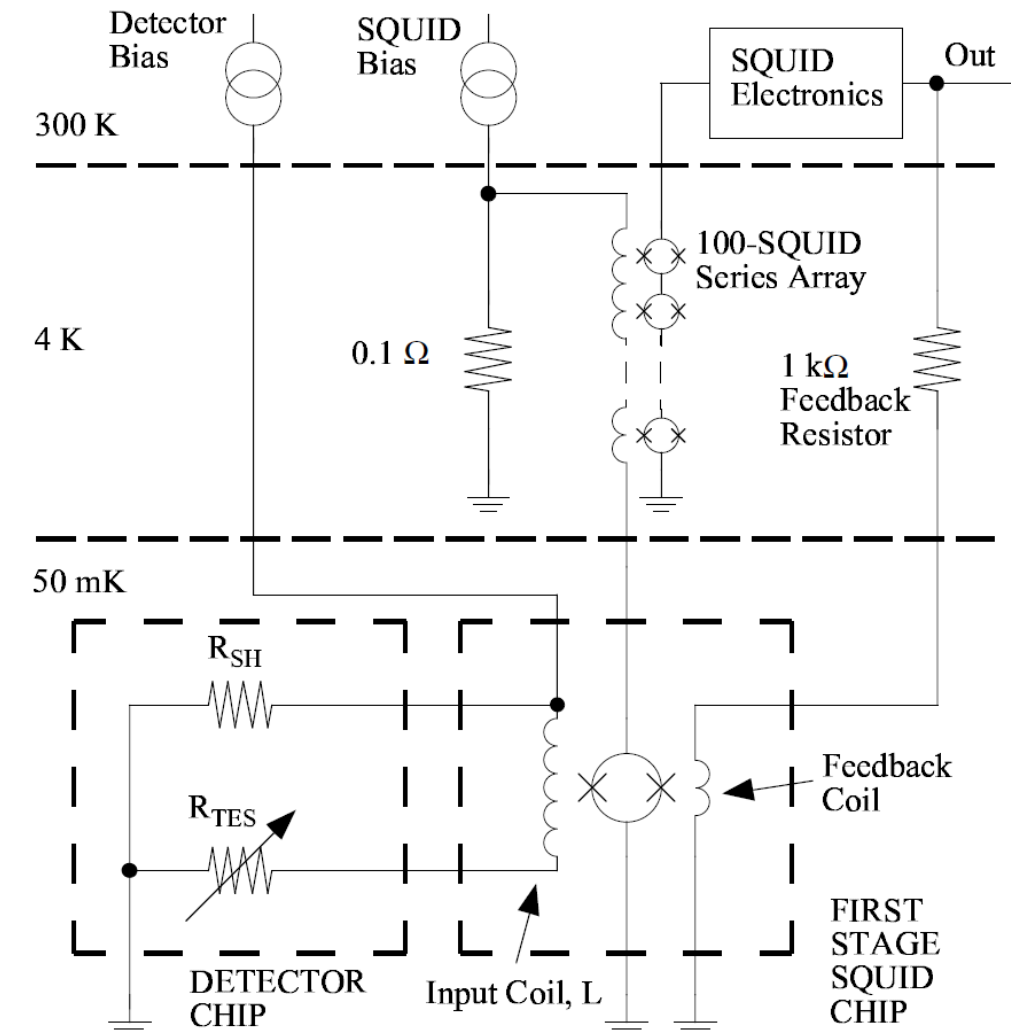
I : current through the TES

L : inductance of the input coil of the SQUID

P_{bath} : power flowing to the bath

P_j : Joule power in R

P : signal power



Transition Edge Sensors - signal

$R = R(T, I)$: TES resistance

T : TES temperature

C : Heat capacity TES + absorber

G : thermal conductivity to the bath – $G = nkT^{n-1}$

R_{SH} = shunt resistance $R_{SH} < R$

V = applied constant voltage

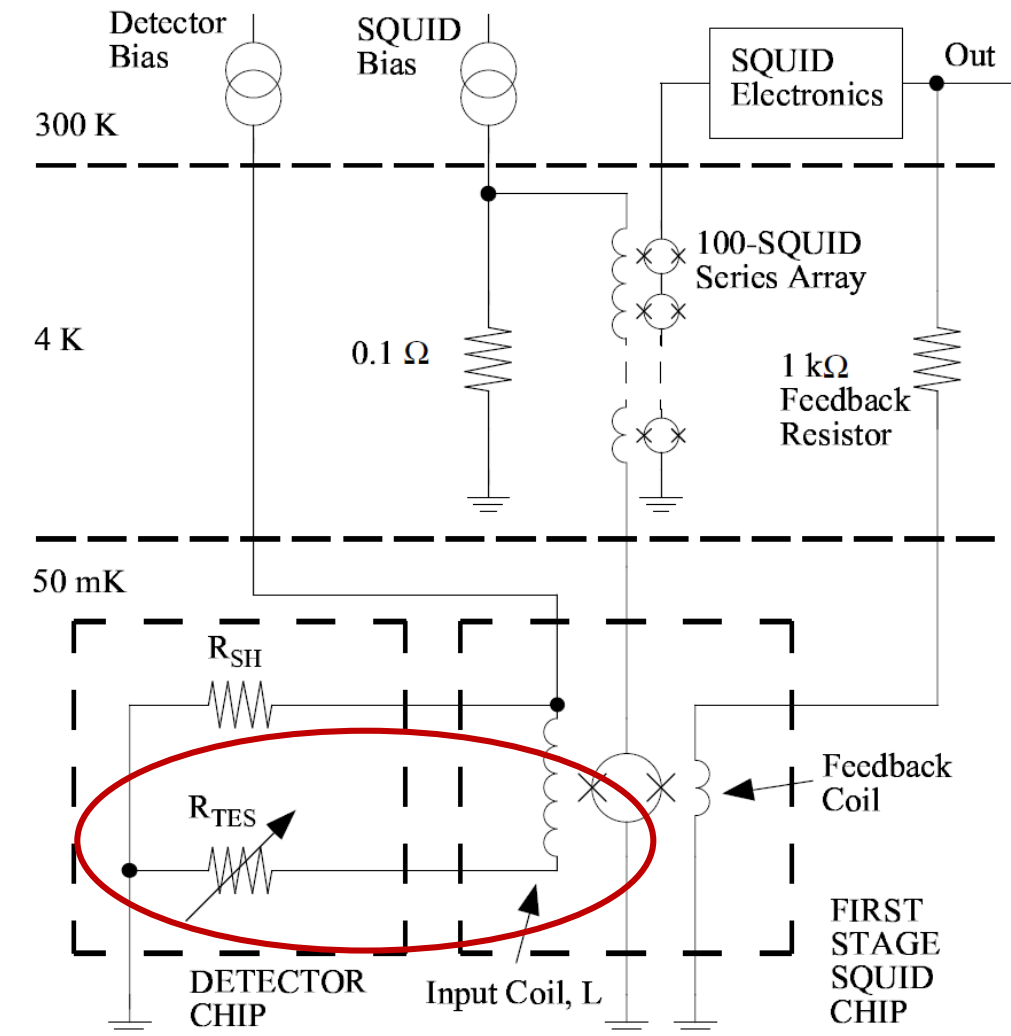
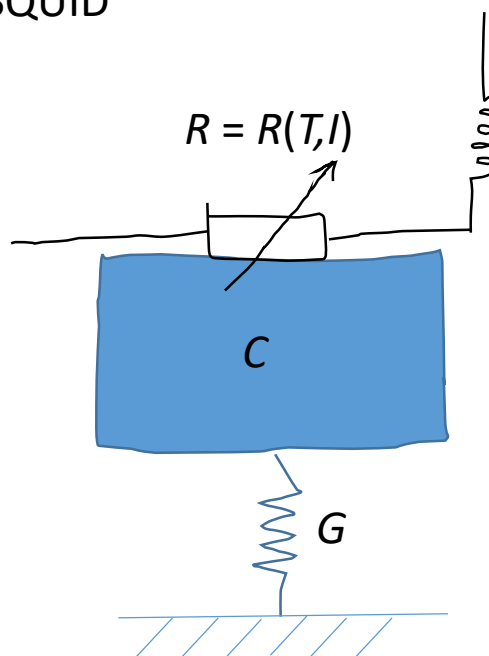
I : current through the TES

L : inductance of the input coil of the SQUID

P_{bath} : power flowing to the bath

P_j : Joule power in R

P : signal power



Transition Edge Sensors - signal

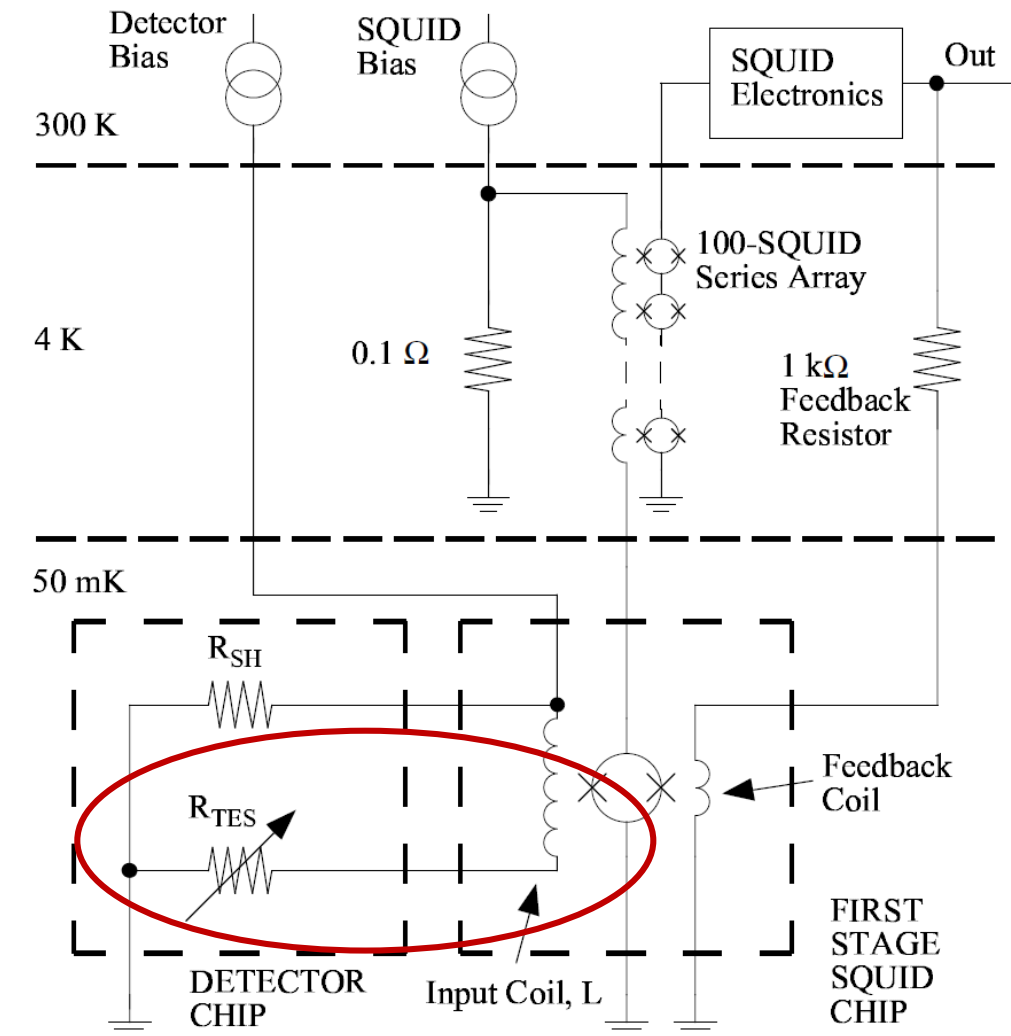
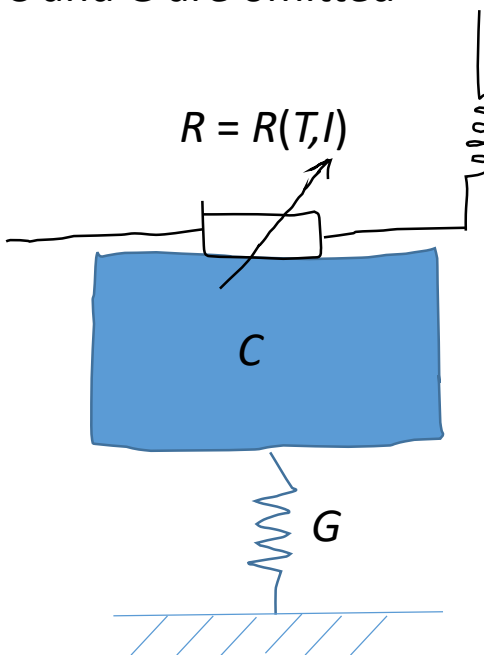
Thermal differential equation:

$$C \frac{dT}{dt} = -P_{bath} + P_J + P$$

Electrical differential equation:

$$L \frac{dI}{dt} = V - IR_{SH} - IR(T, I)$$

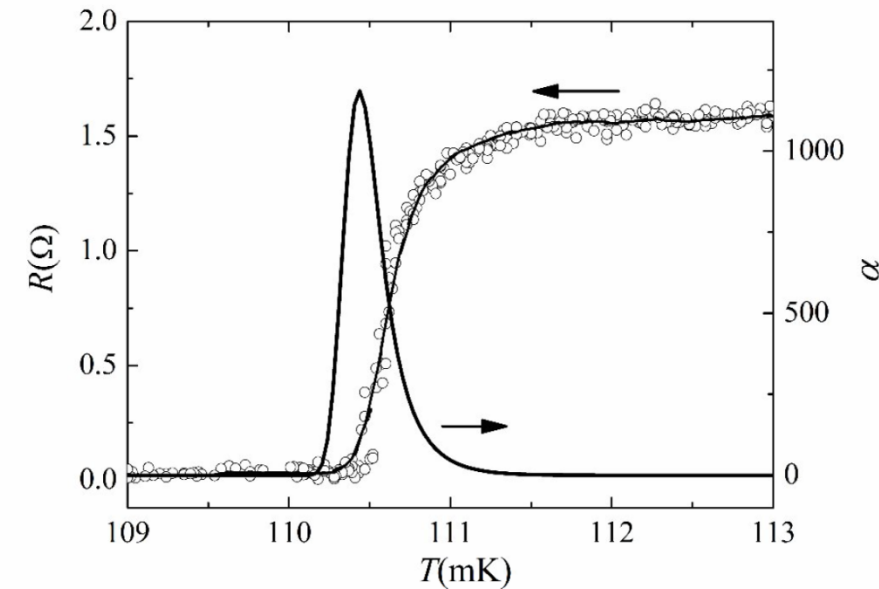
Solution in the **small signal limit** around the values R_0 , T_0 , I_0 and the temperature dependences of C and G are omitted



Transition Edge Sensors - signal

$$R(T, I) \approx R_0 + \left. \frac{\partial R}{\partial T} \right|_{I_0} \delta T + \left. \frac{\partial R}{\partial I} \right|_{T_0} \delta I$$

$$\alpha_I = \left. \frac{\partial \log R}{\partial \log T} \right|_{I_0} = \frac{T_0}{R_0} \left. \frac{\partial R}{\partial T} \right|_{I_0}$$



Transition Edge Sensors - signal

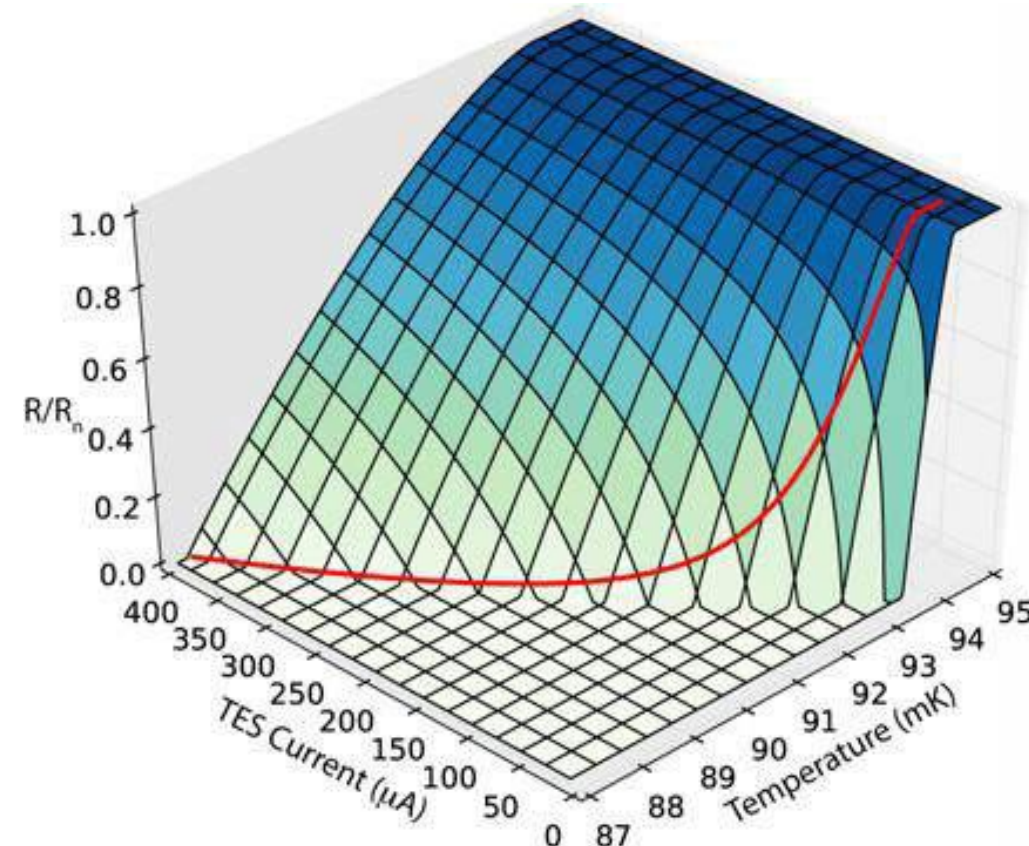
$$R(T, I) \approx R_0 + \frac{\partial R}{\partial T} \Big|_{I_0} \delta T + \frac{\partial R}{\partial I} \Big|_{T_0} \delta I$$

$$R(T, I) = R_0 + \alpha_I \frac{R_0}{T_0} \delta T + \beta_I \frac{R_0}{I_0} \delta I$$

$$\alpha_I = \frac{\partial \log R}{\partial \log T} \Big|_{I_0} = \frac{T_0}{R_0} \frac{\partial R}{\partial T} \Big|_{I_0}$$

$$\beta_I = \frac{\partial \log R}{\partial \log I} \Big|_{T_0} = \frac{I_0}{R_0} \frac{\partial R}{\partial I} \Big|_{T_0}$$

$$R_{\text{dyn}} = \frac{\partial V}{\partial I} \Big|_{T_0} = R_0 (1 + \beta_I)$$



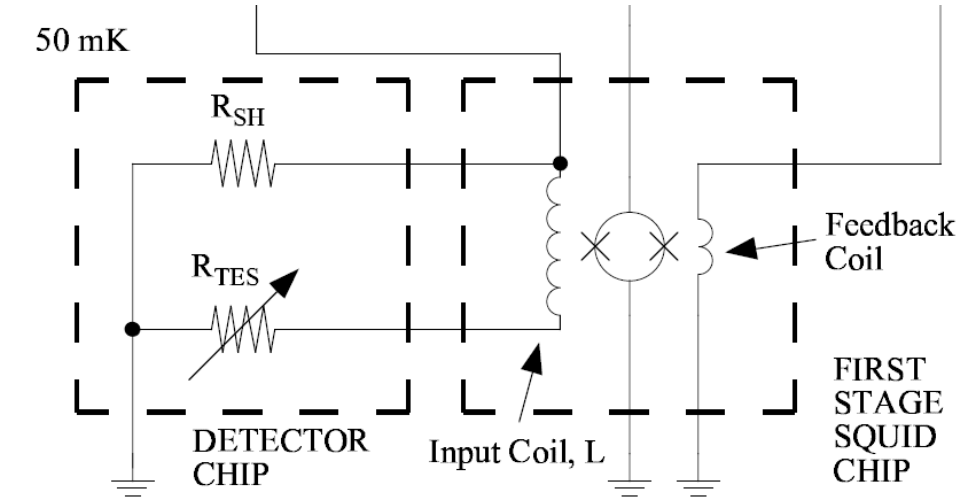
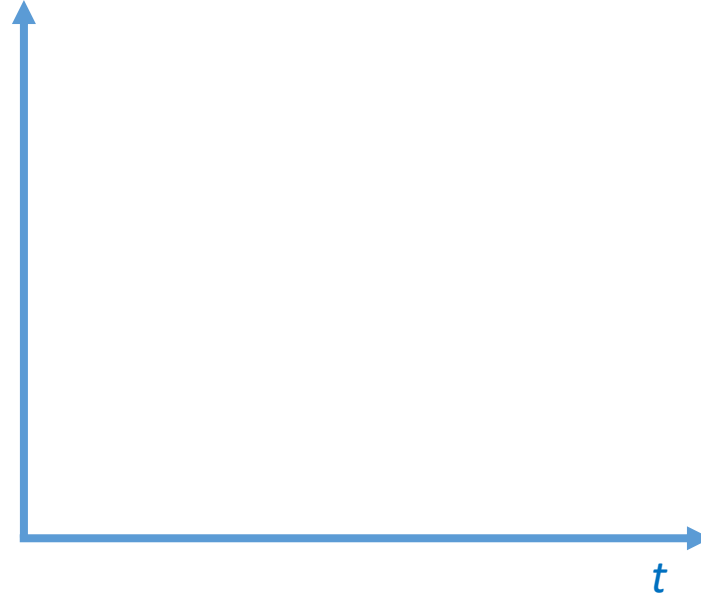
Transition Edge Sensors - signal

If $R_{SH} \gg R(T,I)$

- $\rightarrow I \sim \text{constant} \rightarrow P_j = I^2 R$
- $\rightarrow R \text{ increases} \rightarrow P_j \text{ increases}$
- $\rightarrow \text{positive feedback}$

If $R_{SH} \ll R(T,I)$

- $\rightarrow V \sim \text{constant} \rightarrow P_j = V^2/R$
 - $\rightarrow R \text{ increases} \rightarrow P_j \text{ decreases}$
 - $\rightarrow \text{negative feedback}$
- Negative electro-thermal feedback



The negative electro-thermal feedback makes the working point more stable and decreases the decay time of the current signal with respect to the thermal time constant $\tau_0 = C/G$:

$$\tau_{eff} = \frac{\tau_0}{1 + \alpha/n}$$

Transition Edge Sensors - signal

Pulse shape:

$$\delta I(t) \propto \left(-e^{-\frac{t}{\tau_+}} + e^{-\frac{t}{\tau_-}} \right)$$

rise time

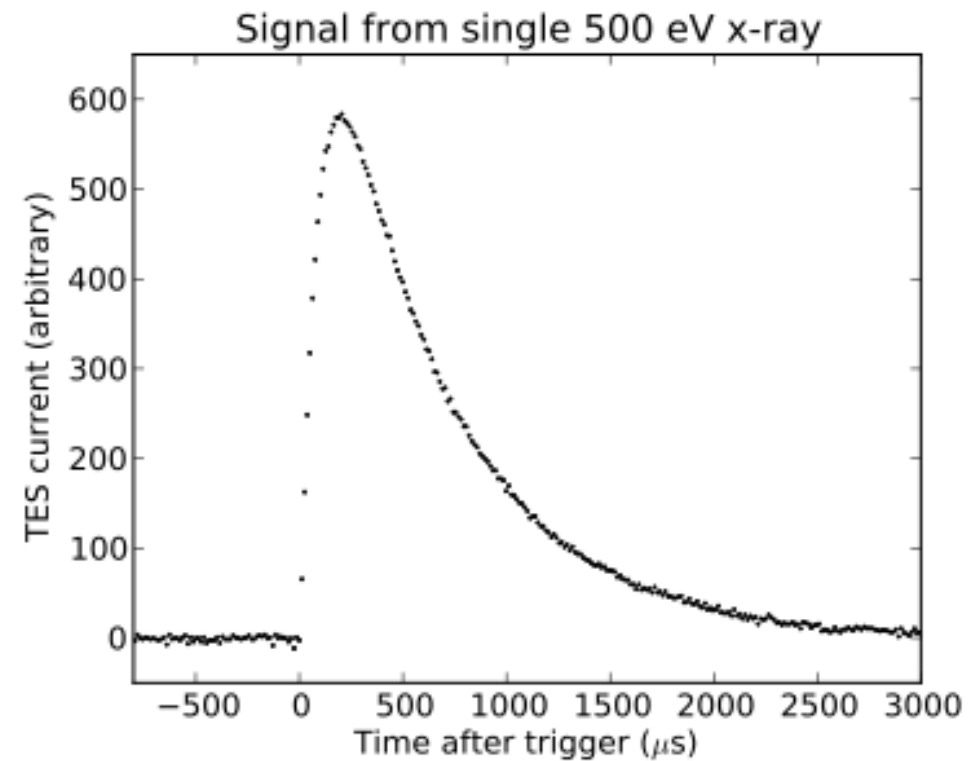
$$\tau_+ \sim \tau_{el} = \frac{L}{R_{SH} + R_{dyn}}$$

decay time

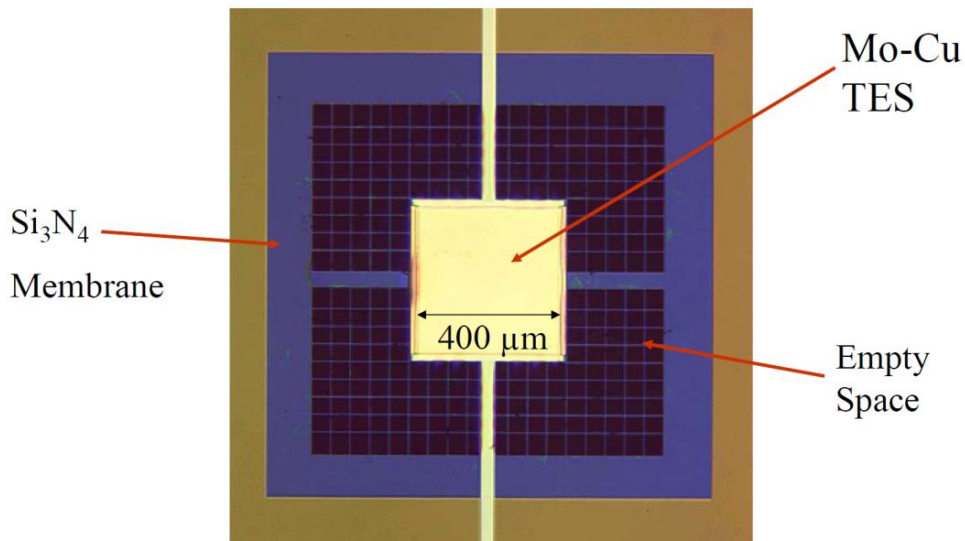
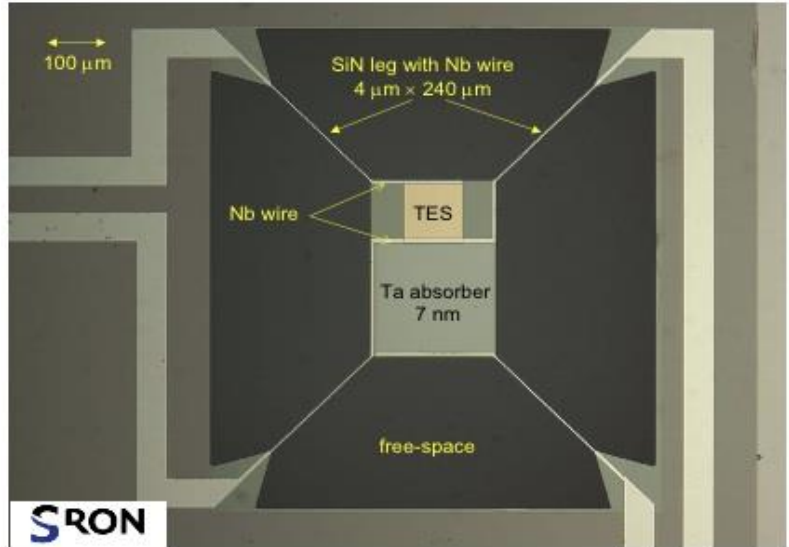
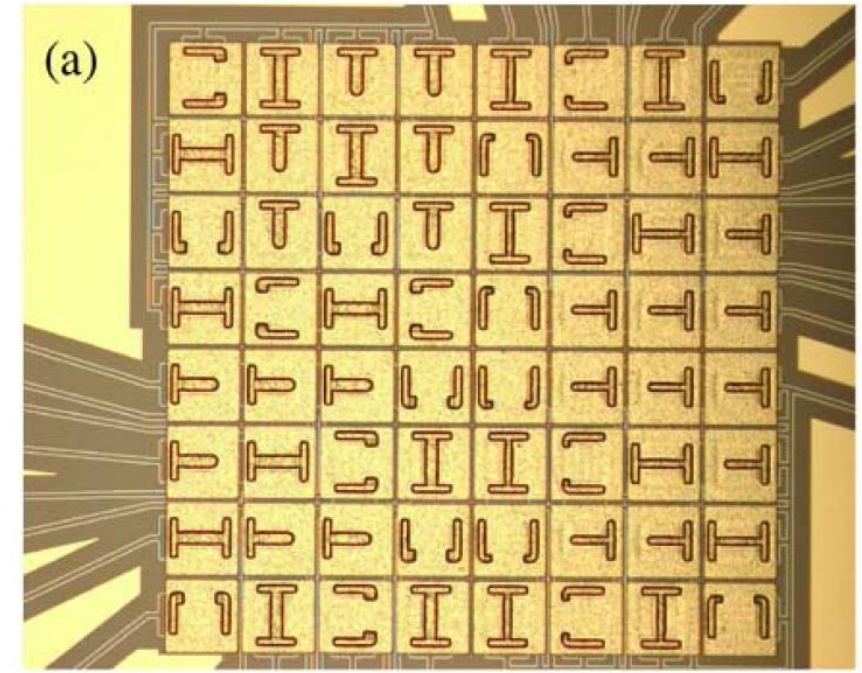
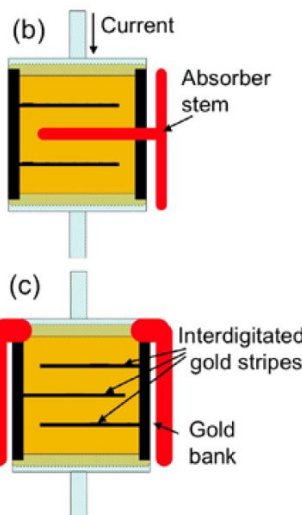
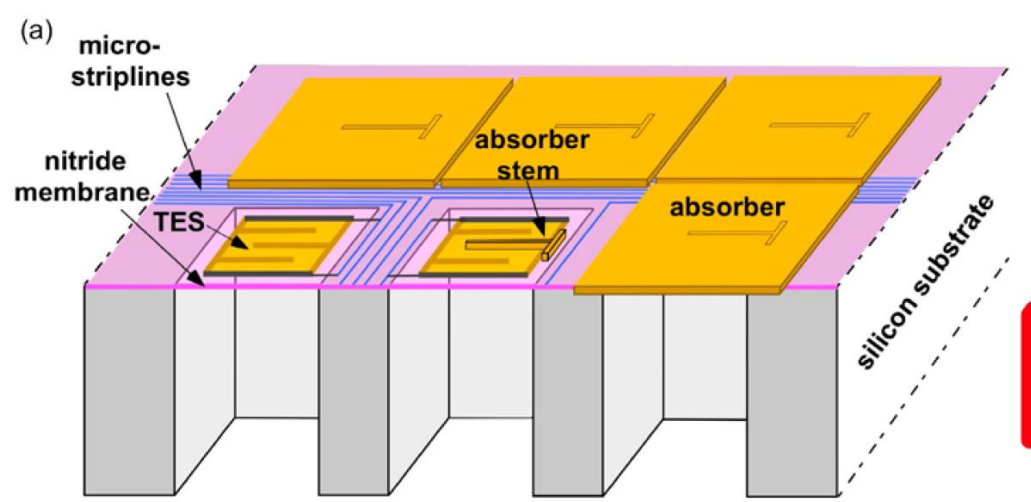
$$\tau_- = \tau_{eff} = \frac{\tau_0}{1+\alpha/n}$$

For **strong electro-thermal feedback** → best energy resolution:

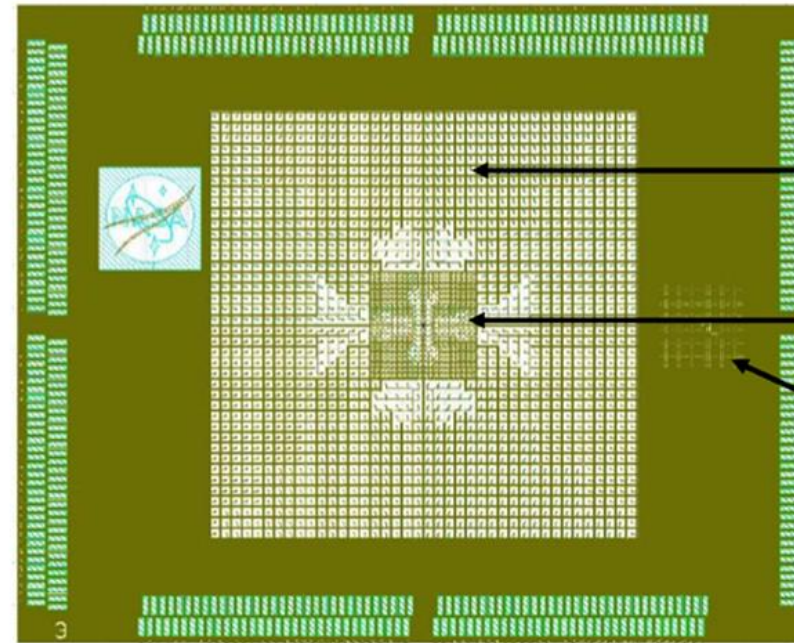
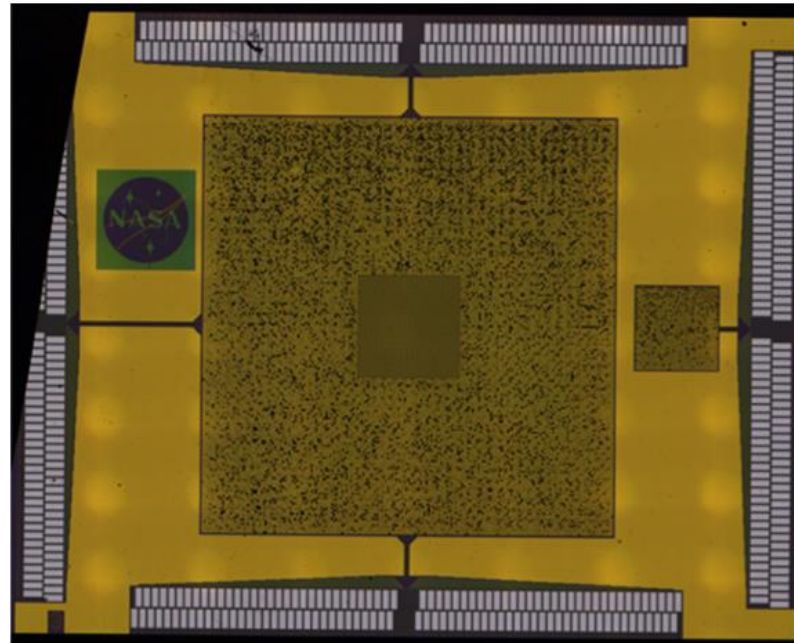
$$\Delta E_{FWHM} = 2\sqrt{2\ln 2} \sqrt{4k_B T^2 \frac{C}{\alpha} \sqrt{\frac{n}{2}}}$$



Transition Edge Sensors - fabrication



Transition Edge Sensors – Lynx array



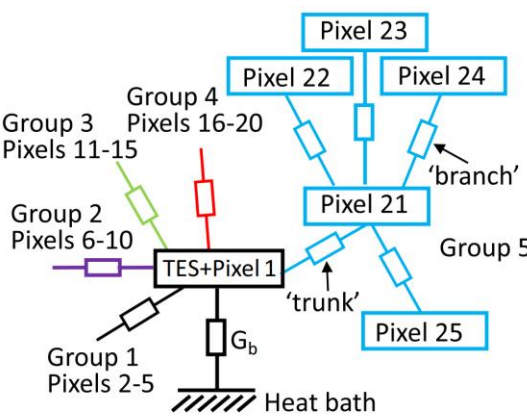
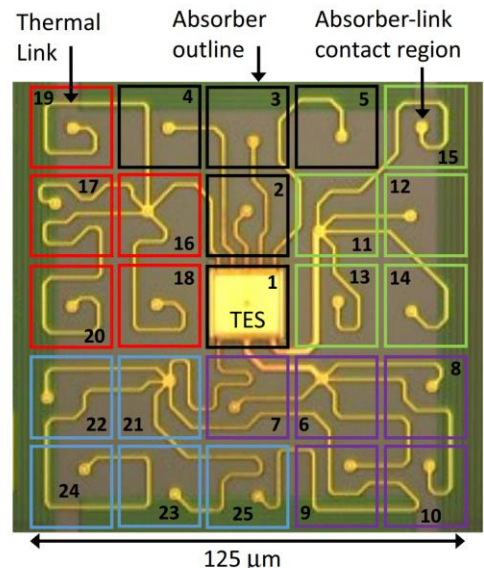
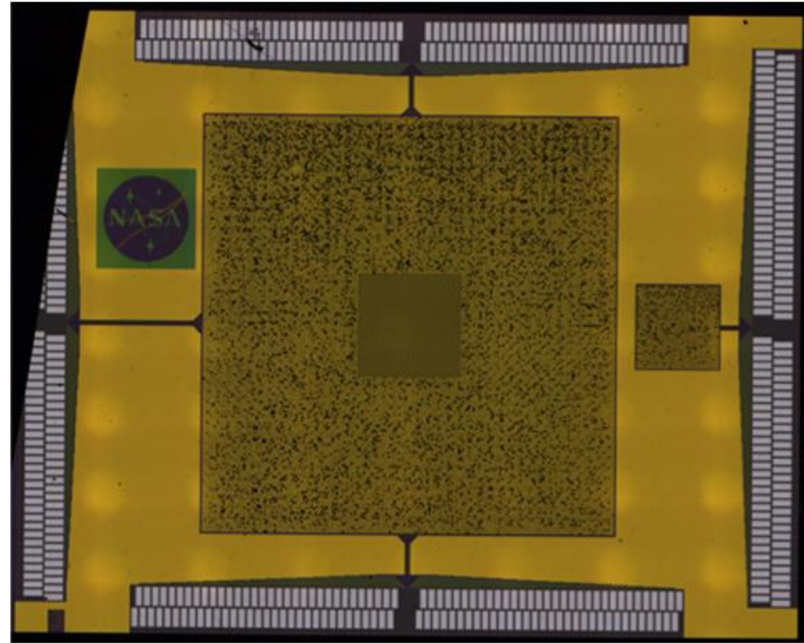
40x40 Main Array
250 μm pitch TES
25-hydra

20x20 Enhanced Main array
125 μm pitch TES
25-hydra

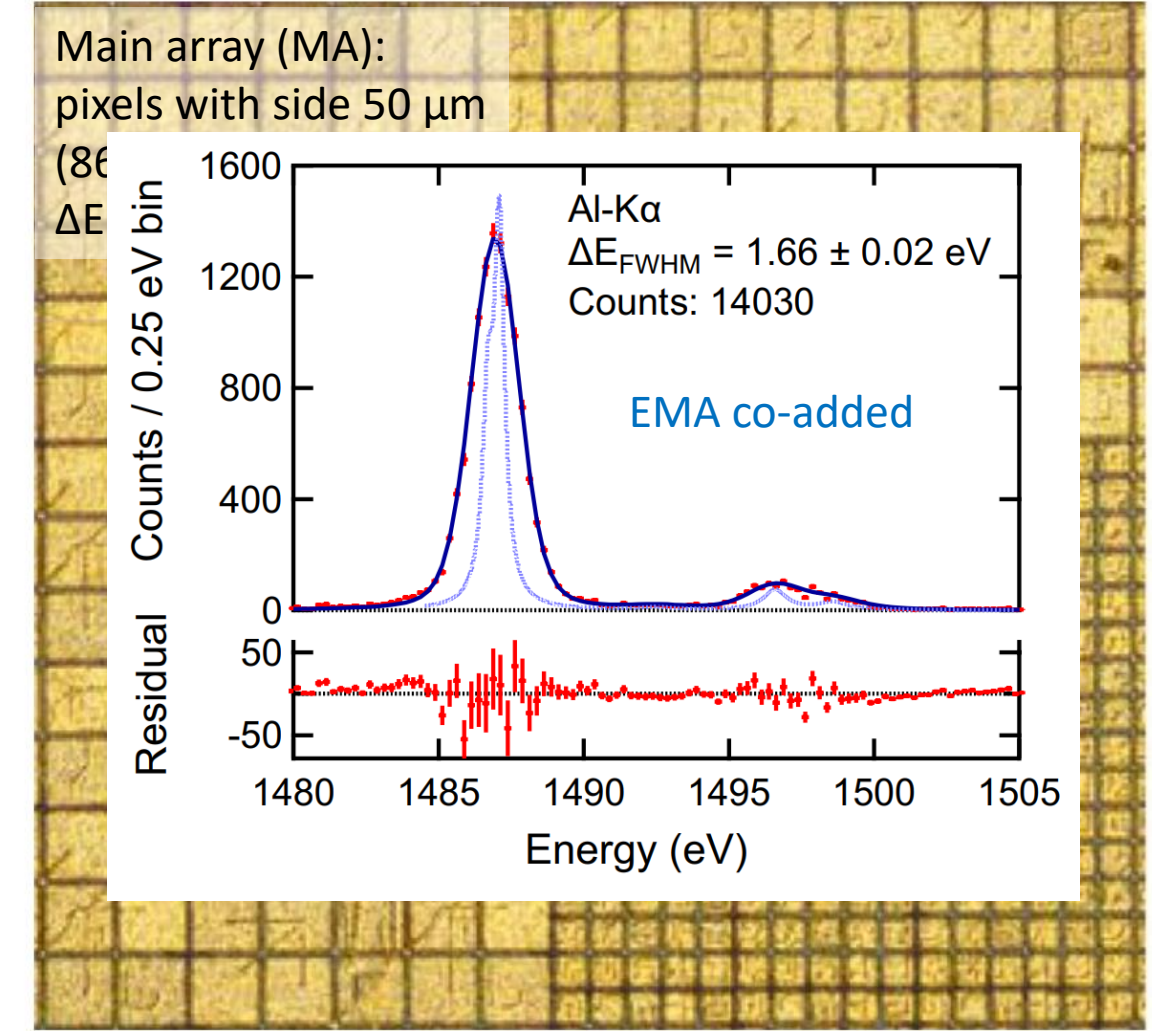
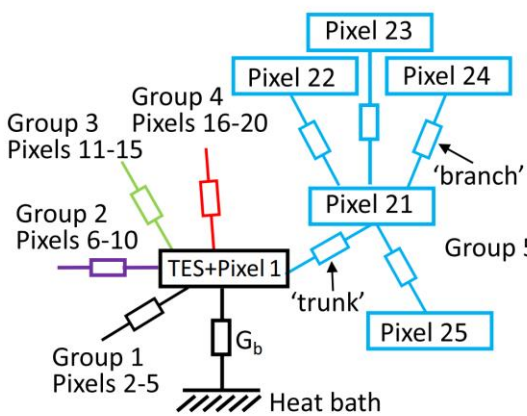
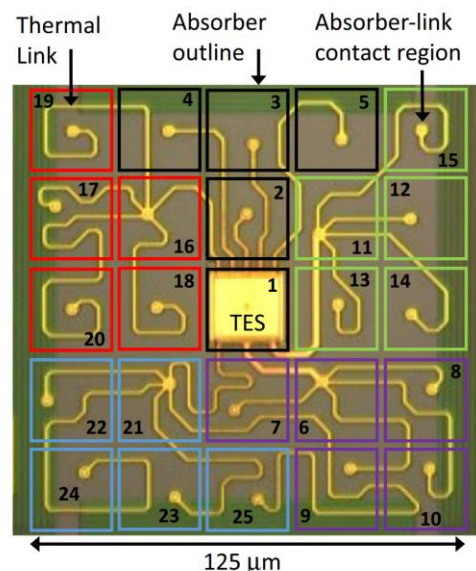
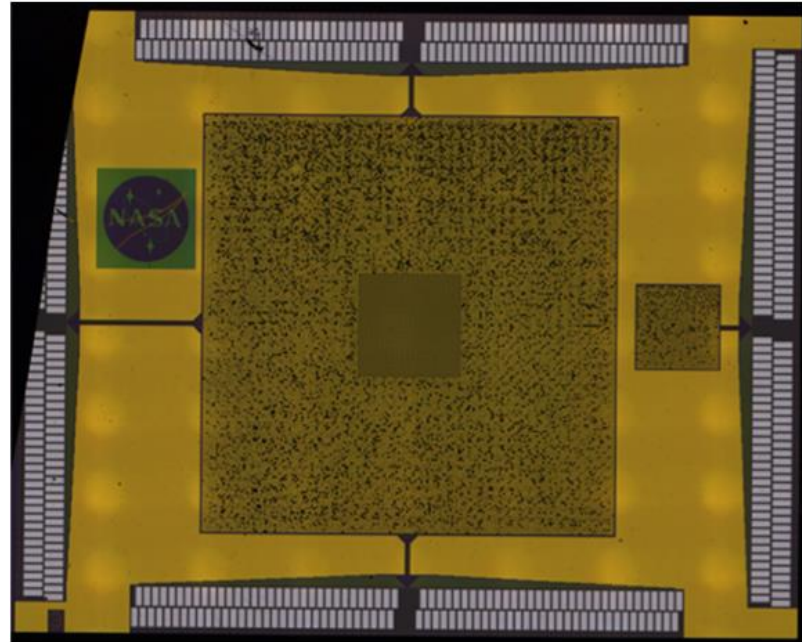
40x40 Ultra-Hi-Res Array
50 μm pitch TES

Lynx microcalorimeter array for future NASA mission for soft x-ray astronomy:
< 1" angular resolution optic
~ 100,000-pixel with energy resolution of $\Delta E_{\text{FWHM}} \sim 3$ eV

Transition Edge Sensors – Lynx array

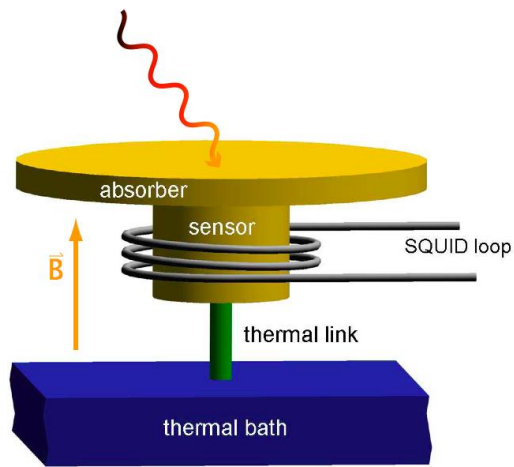


Transition Edge Sensors – Lynx array

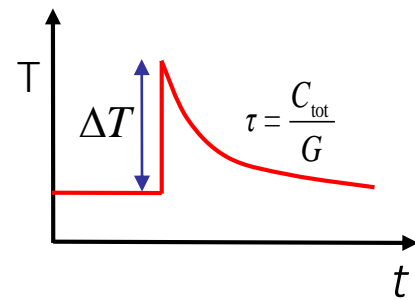


Metallic Magnetic Calorimeters

Paramagnetic temperature sensor



$$\Delta T \approx \frac{E}{C_{\text{tot}}} \quad \xrightarrow{\text{MMC}} \quad \Delta \Phi_s \propto \frac{\partial M}{\partial T} \Delta T$$

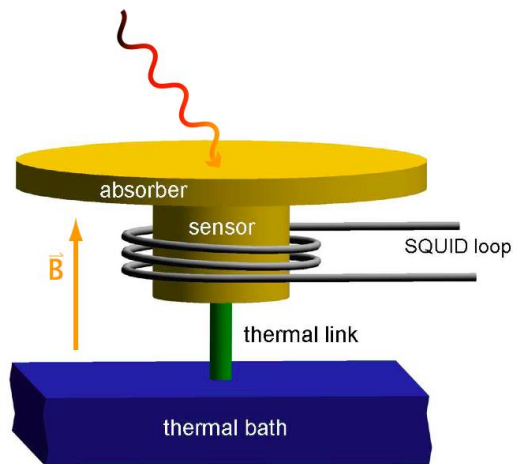


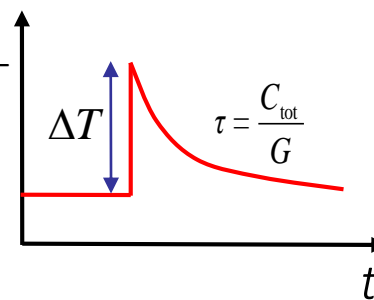
A.Fleischmann, C. Enss and G. M. Seidel,
Topics in Applied Physics **99** (2005) 63

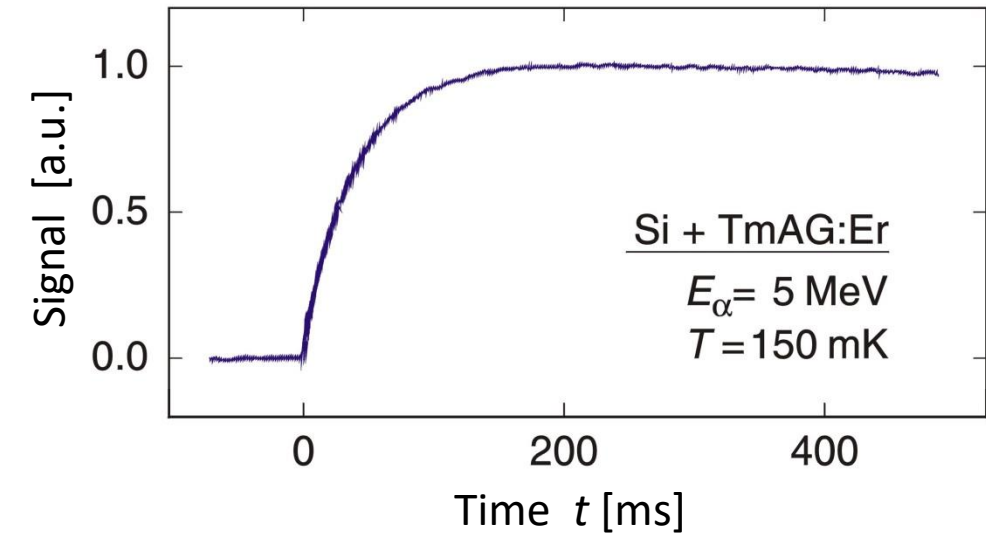
A.Fleischmann et al.,
AIP Conf. Proc. **1185** (2009) 571

Metallic Magnetic Calorimeters

Paramagnetic temperature sensor

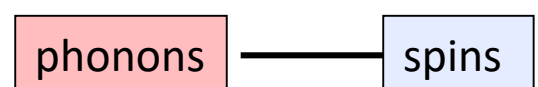


$$\Delta T \approx \frac{E}{C_{\text{tot}}} \xrightarrow{\text{MMC}} \Delta \Phi_s \propto \frac{\partial M}{\partial T} \Delta T$$

$$\tau = \frac{C_{\text{tot}}}{G}$$



dielectric sensor:

Bühler & Umlauf '93



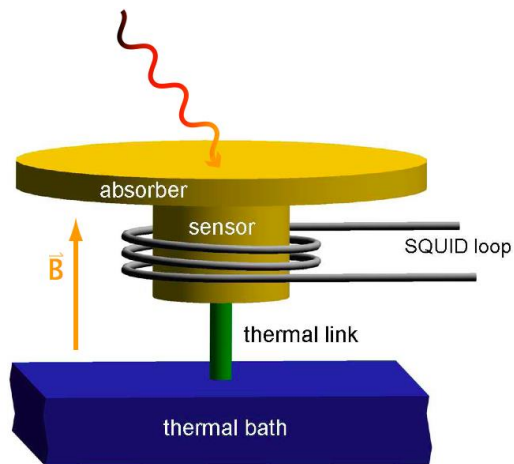
$\tau \approx 50 \text{ ms}$

A.Fleischmann, C. Enss and G. M. Seidel,
Topics in Applied Physics **99** (2005) 63

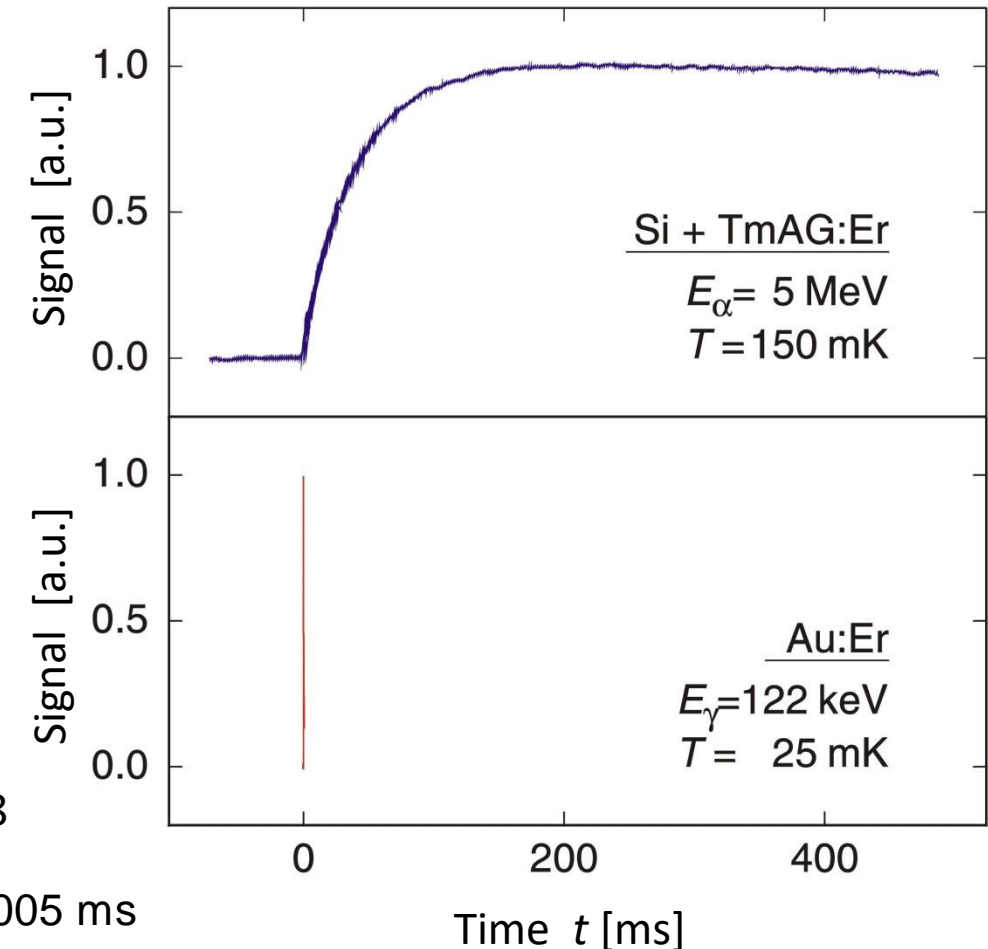
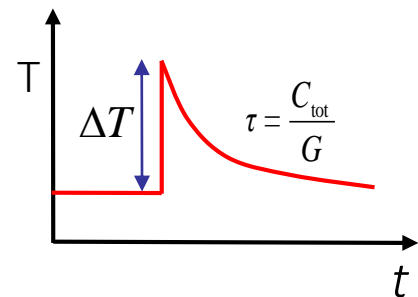
A.Fleischmann et al.,
AIP Conf. Proc. **1185** (2009) 571

Metallic Magnetic Calorimeters

Paramagnetic temperature sensor



$$\Delta T \approx \frac{E}{C_{\text{tot}}} \xrightarrow{\text{MMC}} \Delta \Phi_s \propto \frac{\partial M}{\partial T} \Delta T$$



A.Fleischmann, C. Enss and G. M. Seidel,
Topics in Applied Physics **99** (2005) 63

A.Fleischmann et al.,
AIP Conf. Proc. **1185** (2009) 571

metallic sensor:

electrons

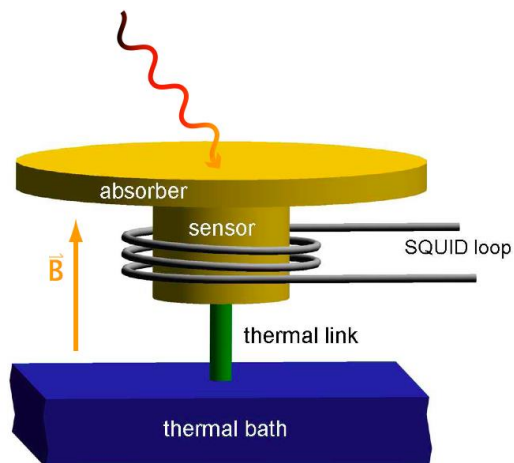
Heidelberg '98

spins

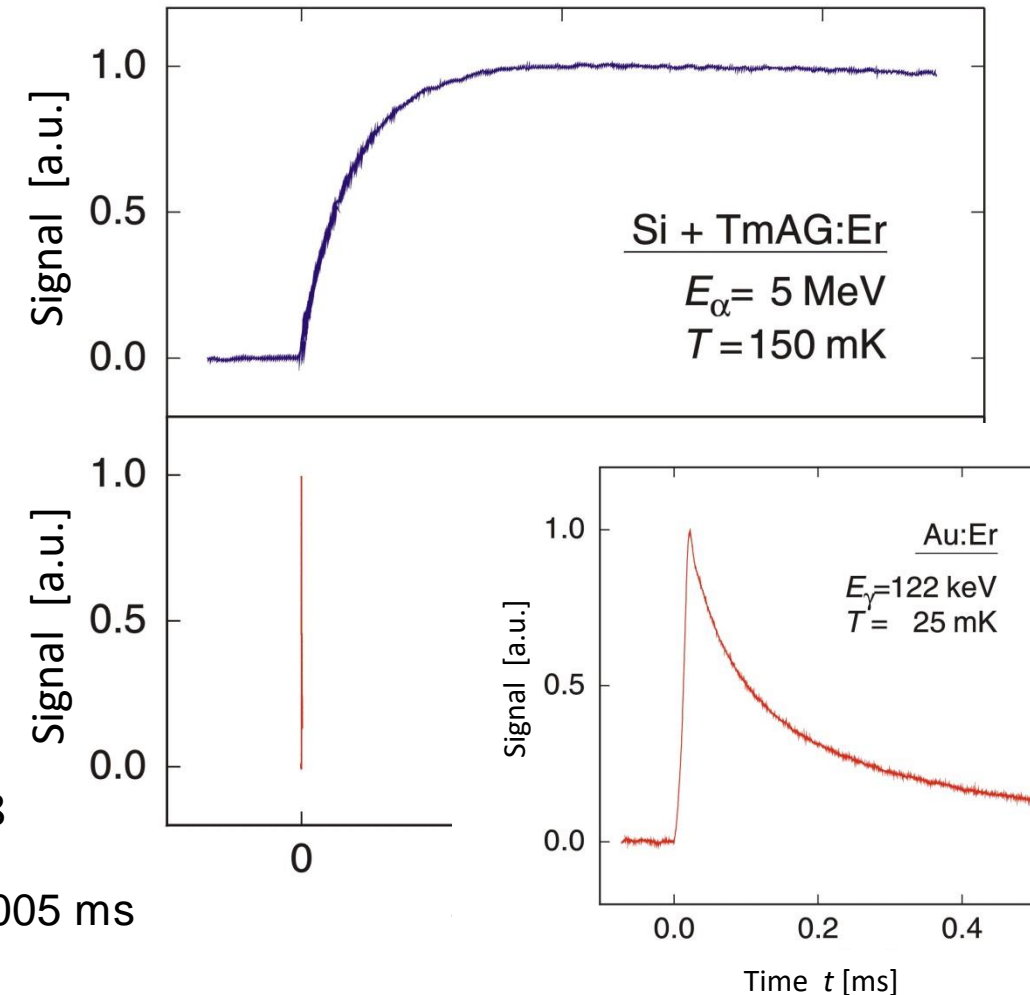
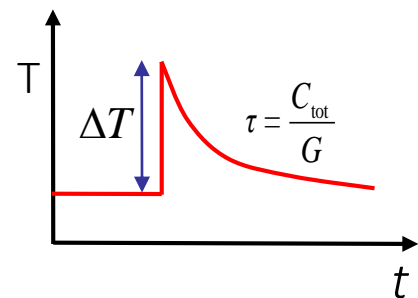
$\tau \approx 0,005 \text{ ms}$

Metallic Magnetic Calorimeters

Paramagnetic temperature sensor



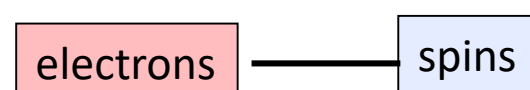
$$\Delta T \approx \frac{E}{C_{\text{tot}}} \quad \xrightarrow{\text{MMC}} \quad \Delta \Phi_s \propto \frac{\partial M}{\partial T} \Delta T$$



A.Fleischmann, C. Enss and G. M. Seidel,
Topics in Applied Physics **99** (2005) 63

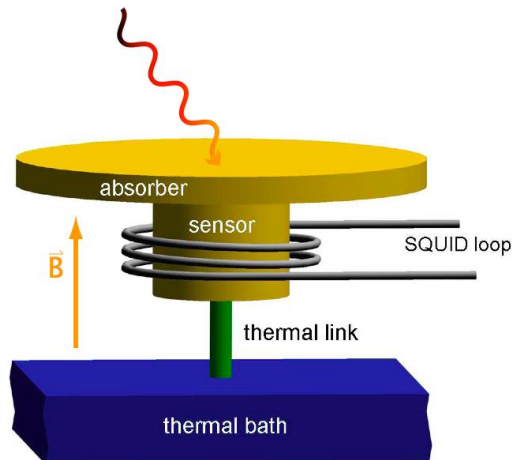
A.Fleischmann et al.,
AIP Conf. Proc. **1185** (2009) 571

metallic sensor: Heidelberg '98

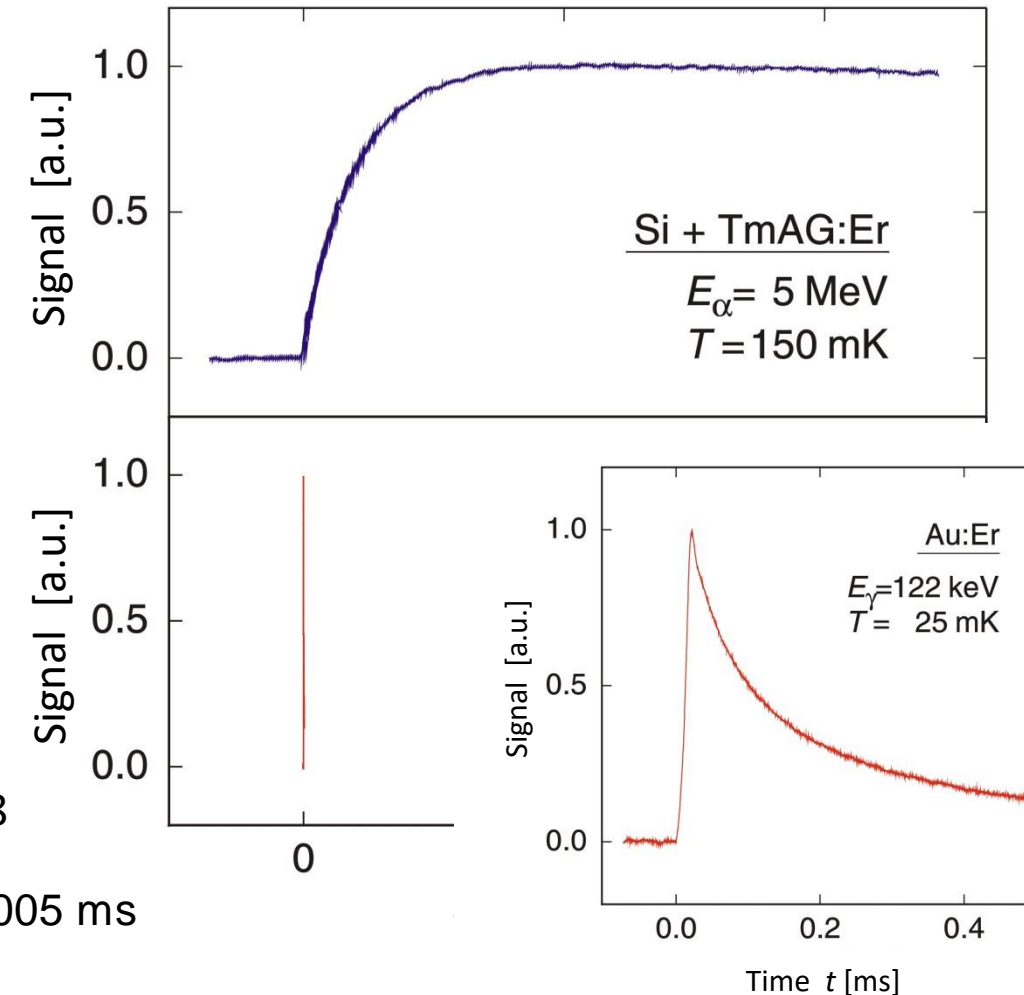
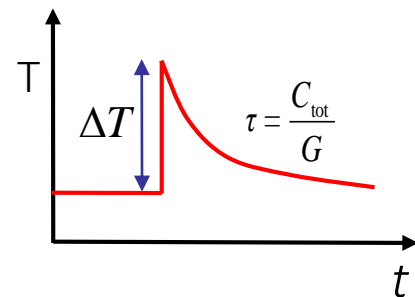


Metallic Magnetic Calorimeters

Paramagnetic temperature sensor → Dilute alloy Au:Er or Ag:Er (Er concentration: a few hundred ppm)



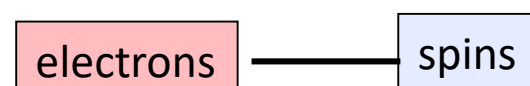
$$\Delta T \approx \frac{E}{C_{\text{tot}}} \xrightarrow{\text{MMC}} \Delta \Phi_s \propto \frac{\partial M}{\partial T} \Delta T$$



A.Fleischmann, C. Enss and G. M. Seidel,
Topics in Applied Physics **99** (2005) 63

A.Fleischmann et al.,
AIP Conf. Proc. **1185** (2009) 571

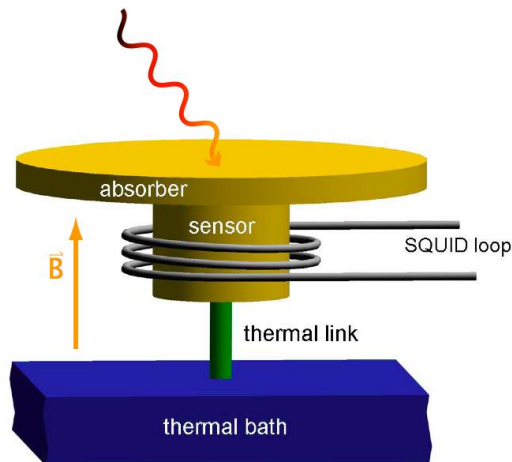
metallic sensor: Heidelberg '98



$\tau \approx 0,005 \text{ ms}$

Metallic Magnetic Calorimeters

Signal

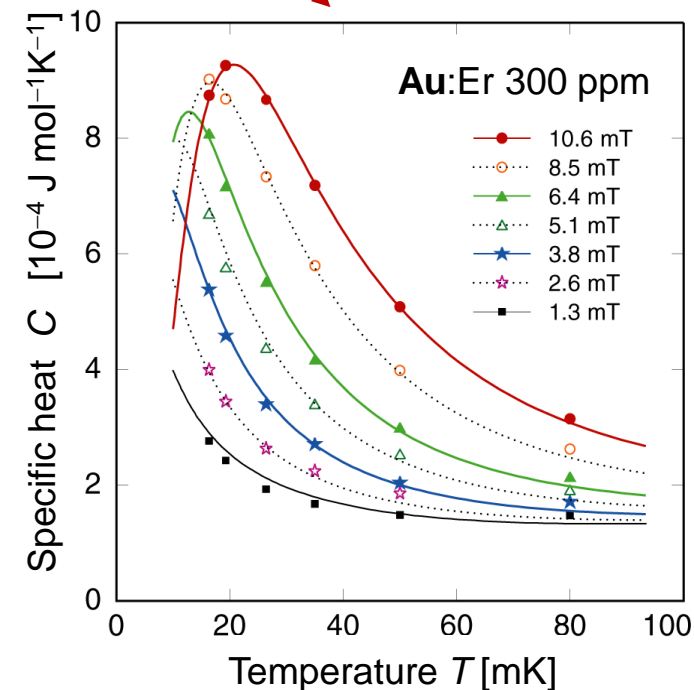
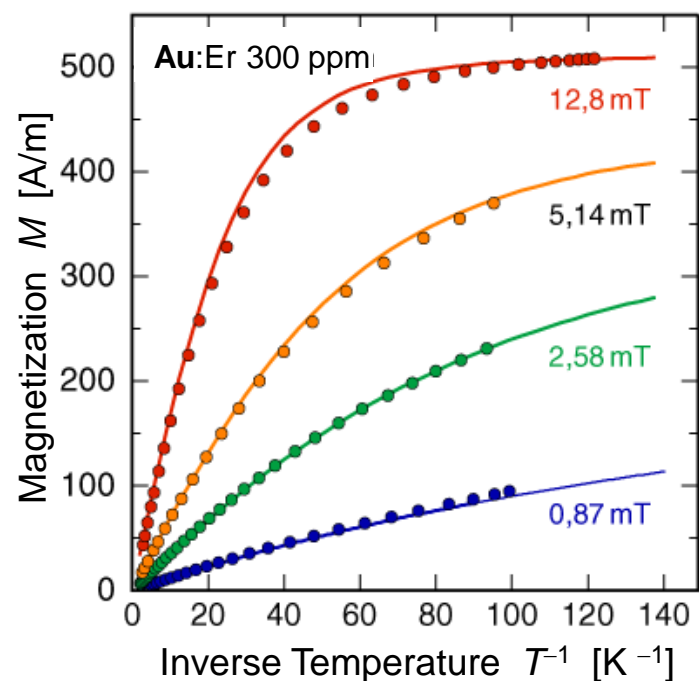


$$\Delta T \approx \frac{E}{C_{\text{tot}}} \xrightarrow{\text{MMC}} \Delta \Phi_s \propto \frac{\partial M}{\partial T} \Delta T \rightarrow \Delta \Phi_s \propto \frac{\partial M}{\partial T} \frac{E}{C_{\text{tot}}}$$

The diagram illustrates the signal generation process. On the left, a plot of Temperature T versus time t shows a step-like increase in temperature ΔT after a magnetic pulse. The relaxation time constant is given by $\tau = \frac{C_{\text{tot}}}{G}$. The middle part shows the relationship between the magnetic flux change $\Delta \Phi_s$, magnetization M , and the calorimeter parameters. The right part shows a red curve representing the signal $\Delta \Phi_s$ as a function of time t .

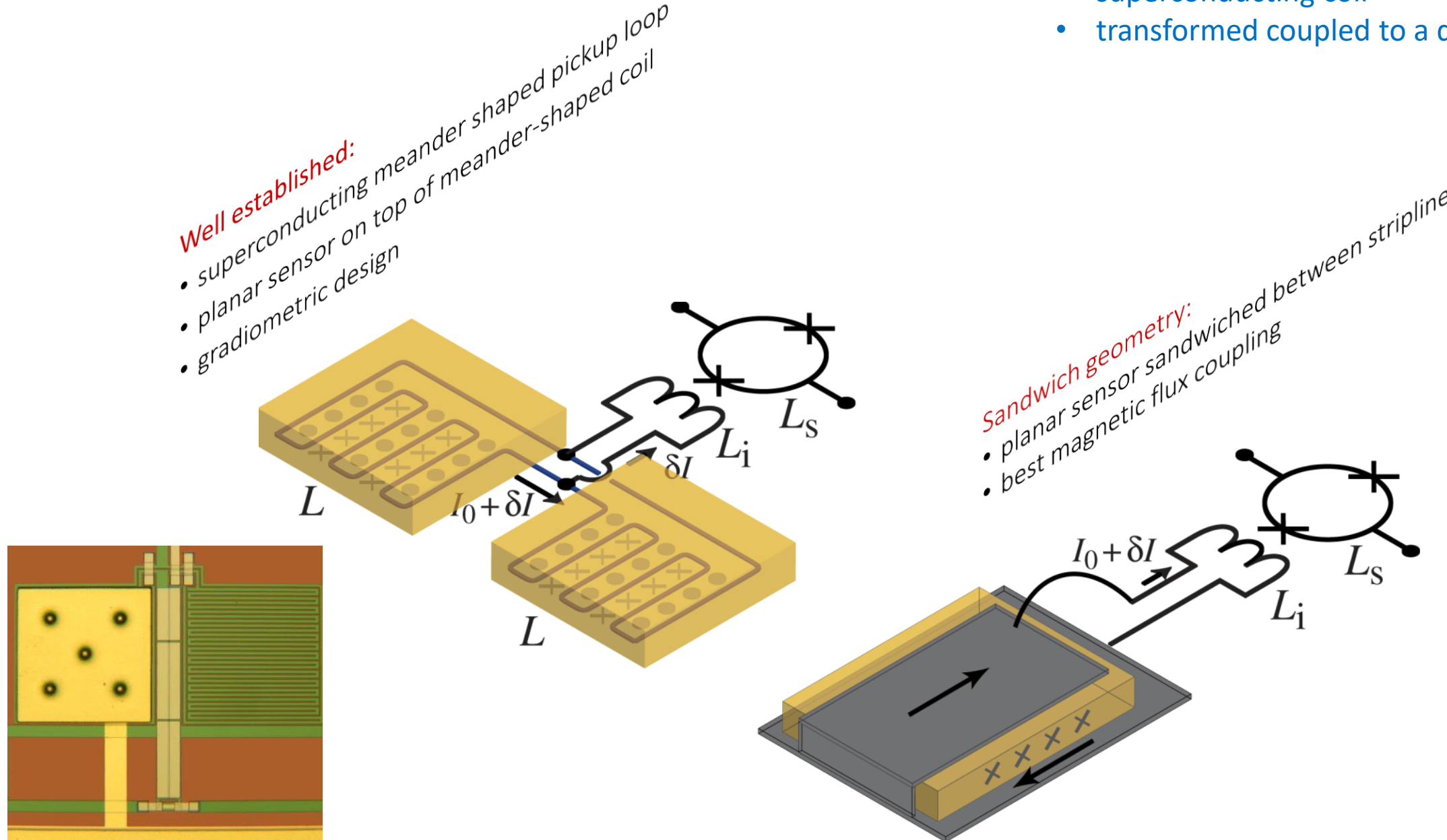
Very good agreement between data and theoretical expectation for interacting spin system

Optimization of detector geometries for different applications



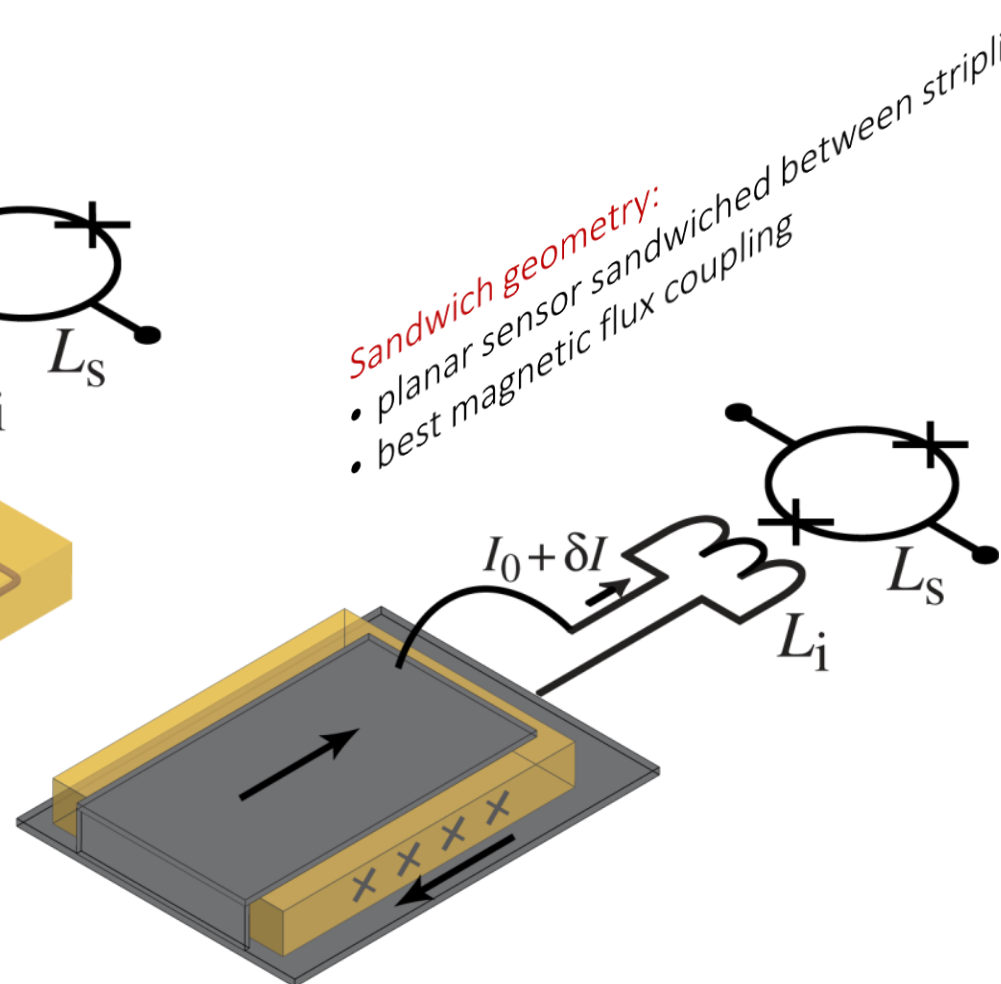
Detector geometries

- planar paramagnetic sensor
- superconducting coil
- transformed coupled to a dc SQUID

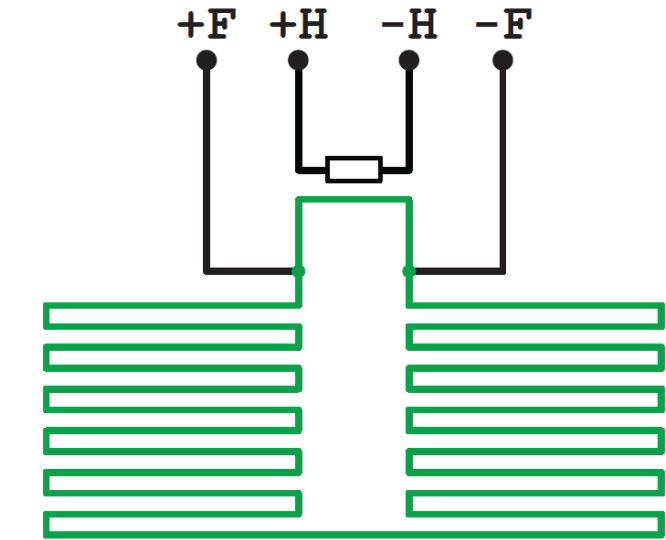
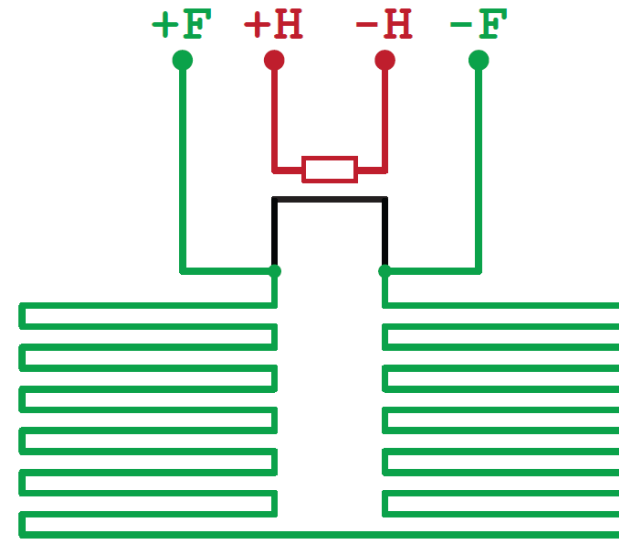
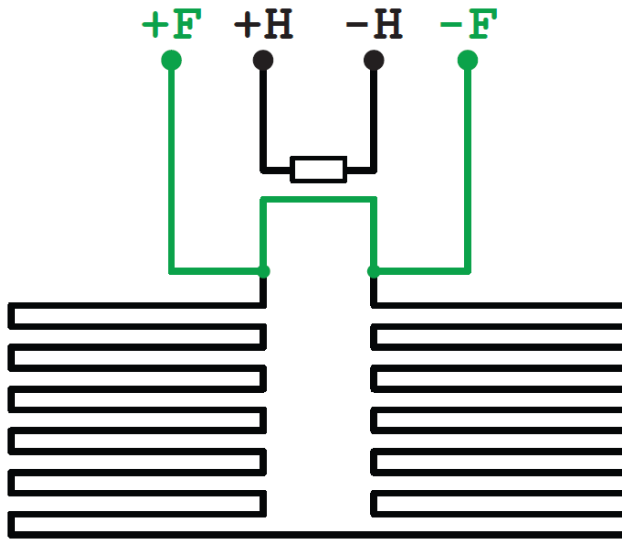


Sandwich geometry:

- planar sensor sandwiched between stripline
- best magnetic flux coupling

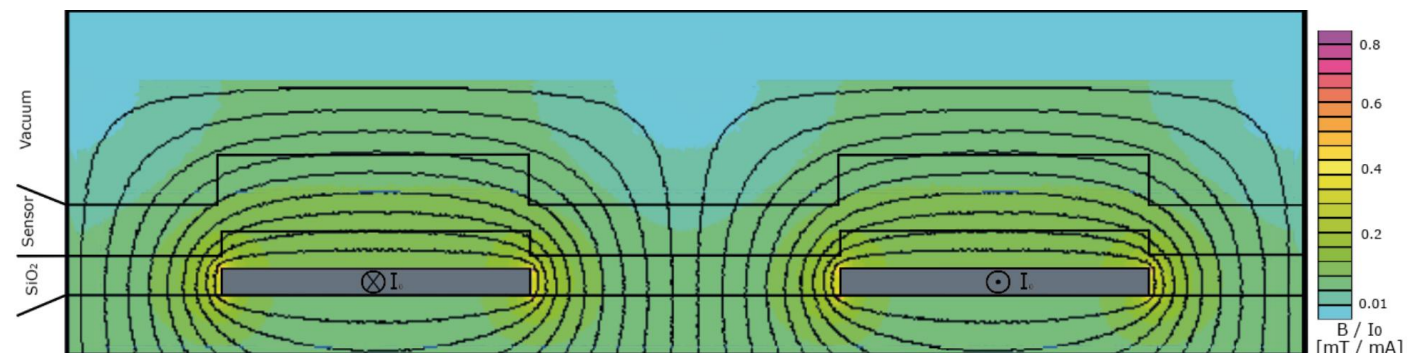


Persistent current



Reliable injection of a persistent current in
the superconducting coil:

Achievable critical current density: $\sim 10 \text{ MA/cm}^2$

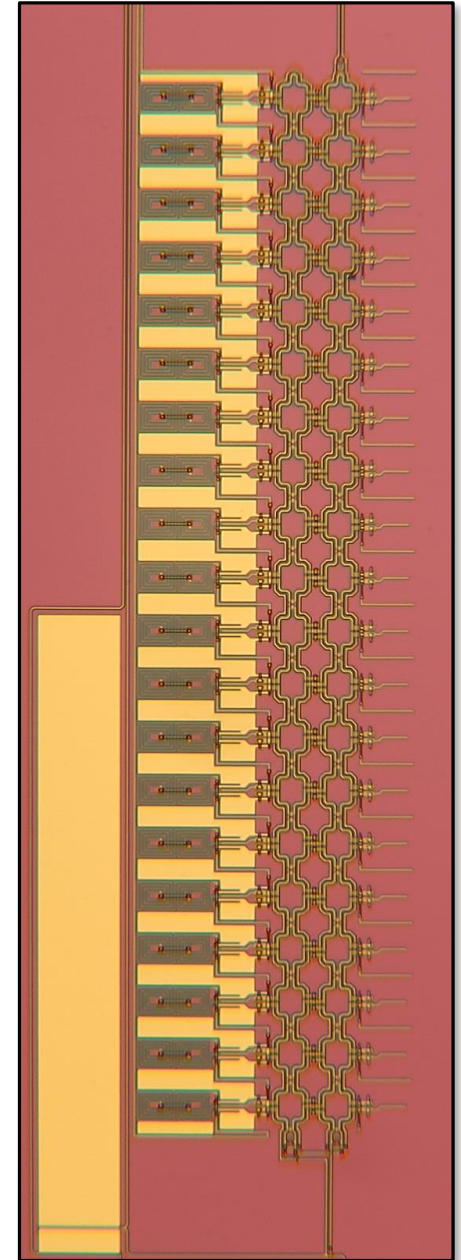
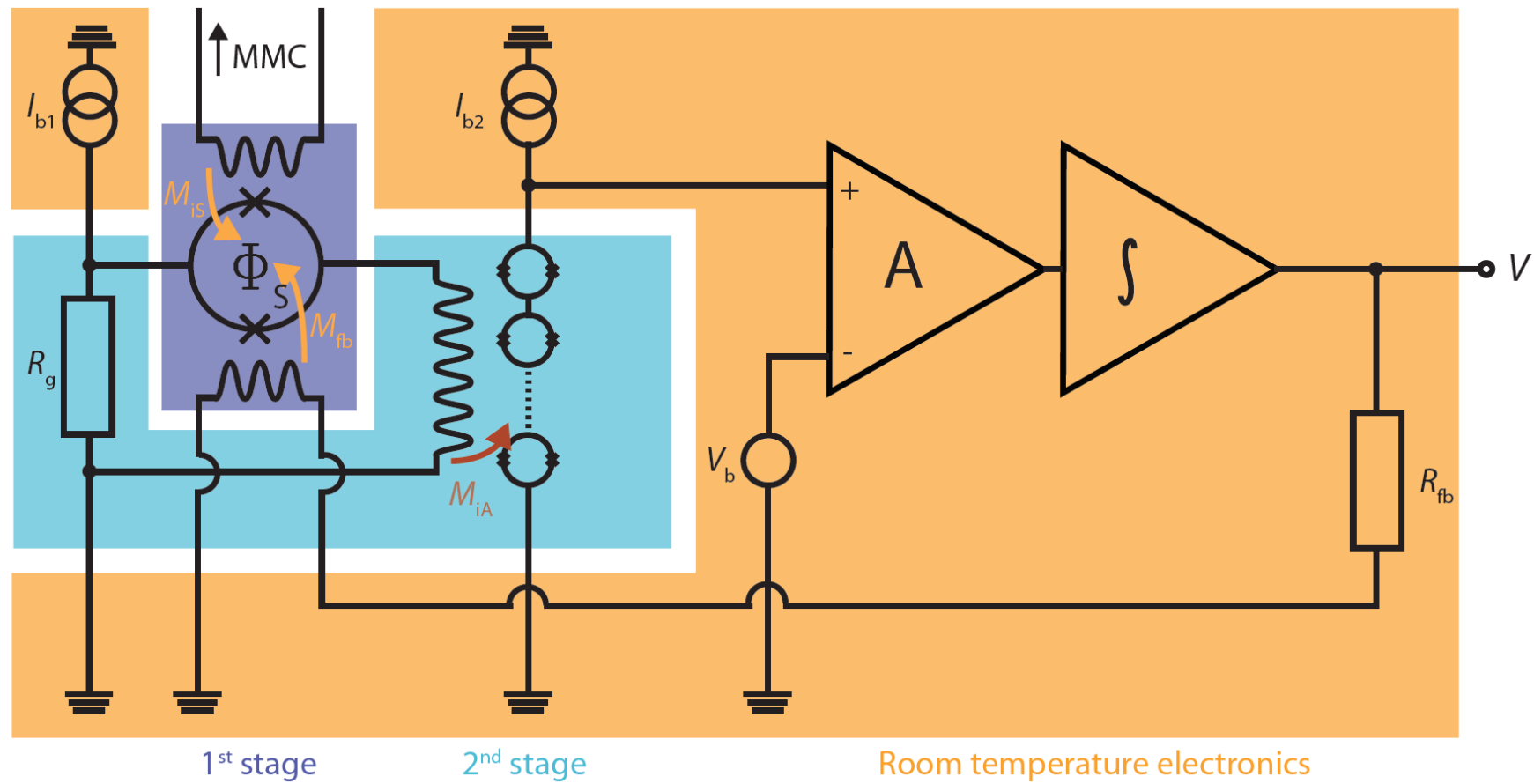


MMC readout

Two-stage dc-SQUID readout with flux-locked loop

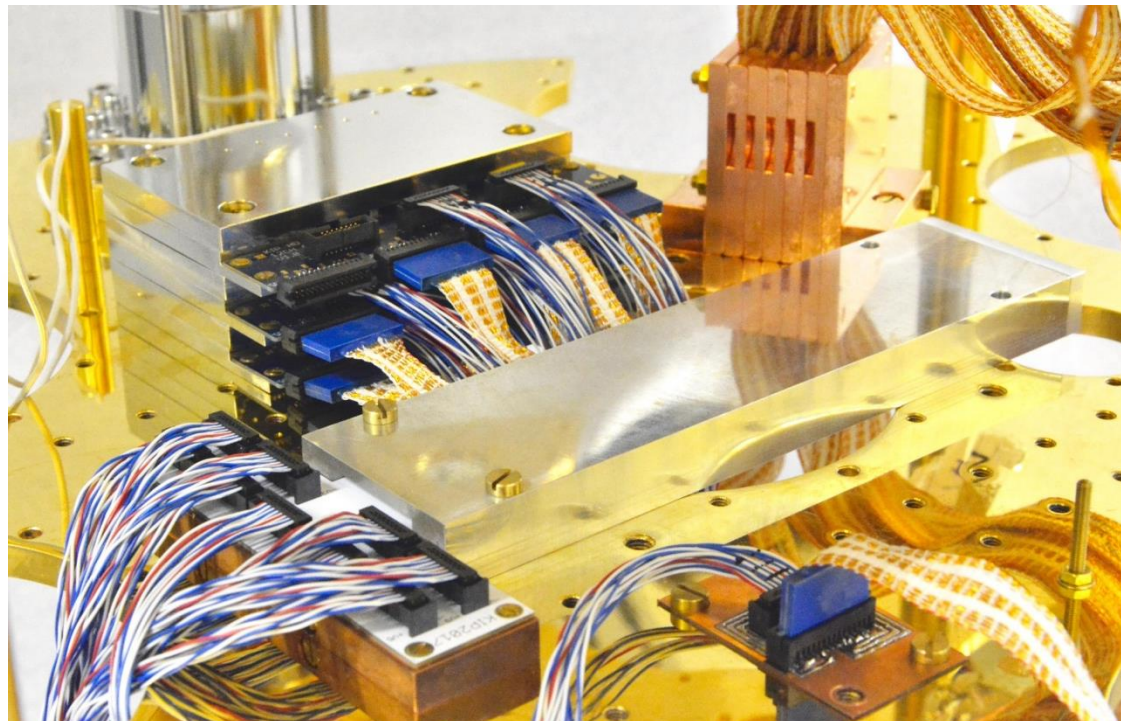
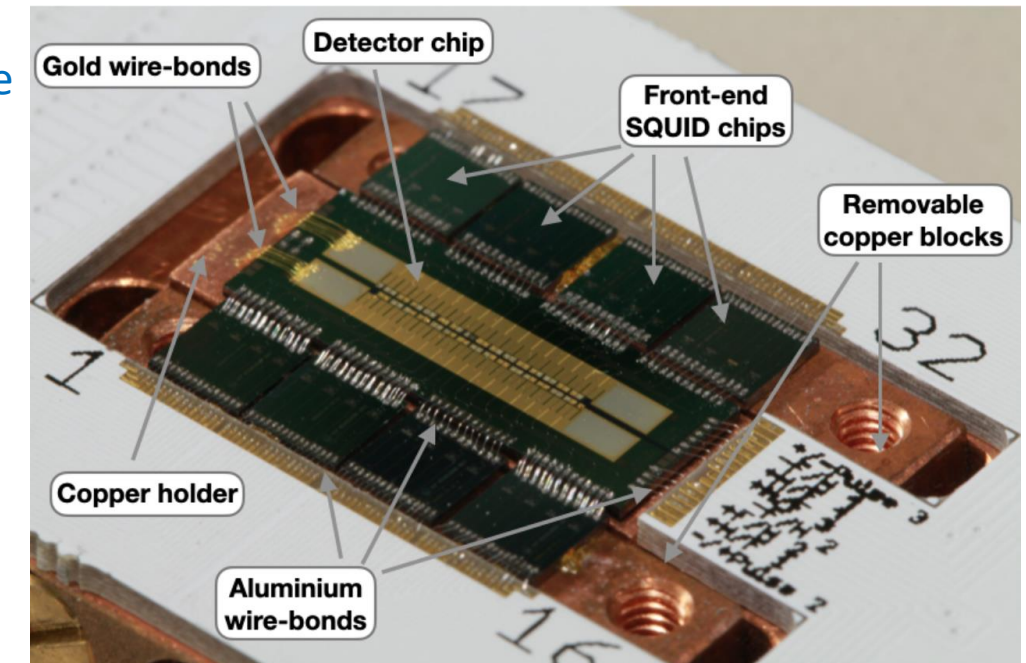
low noise

small power dissipation on detector SQUID chip (voltage bias 1st stage)



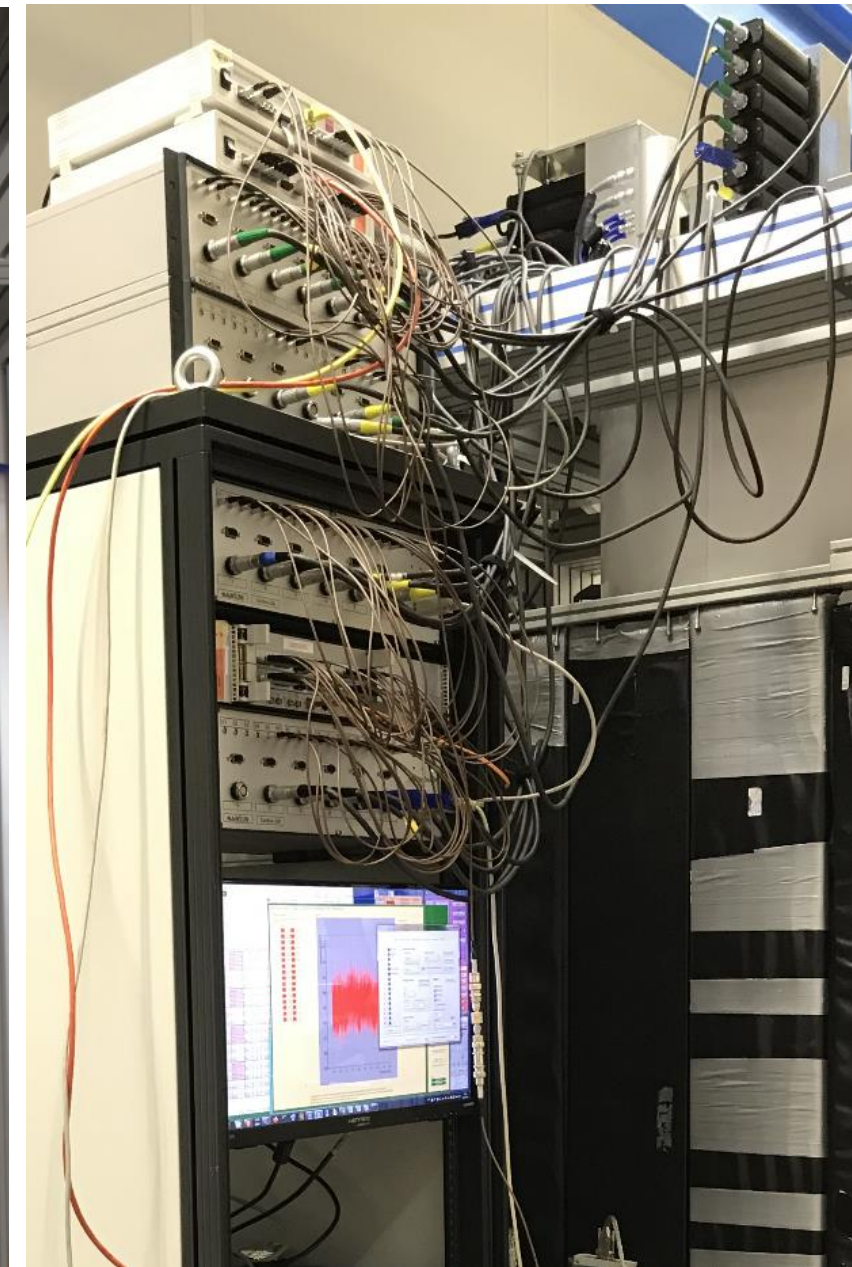
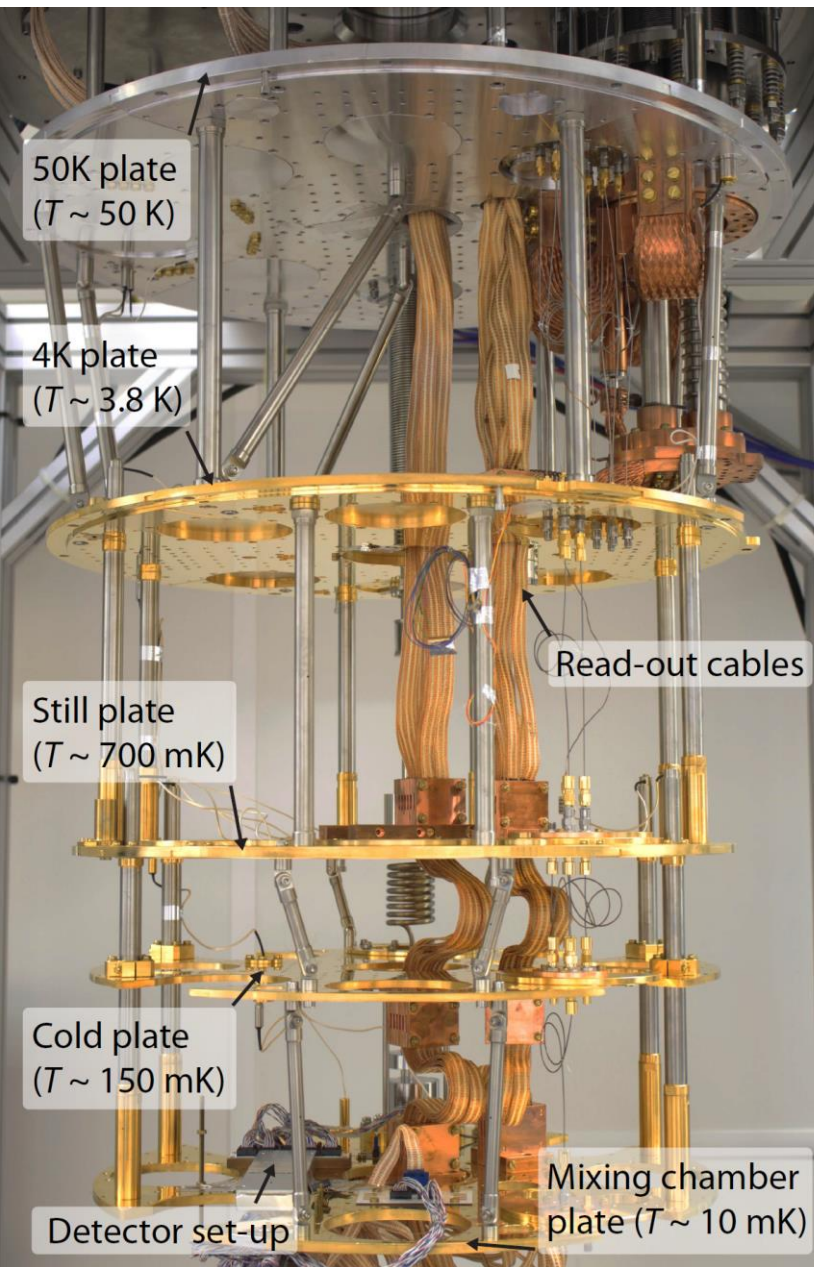
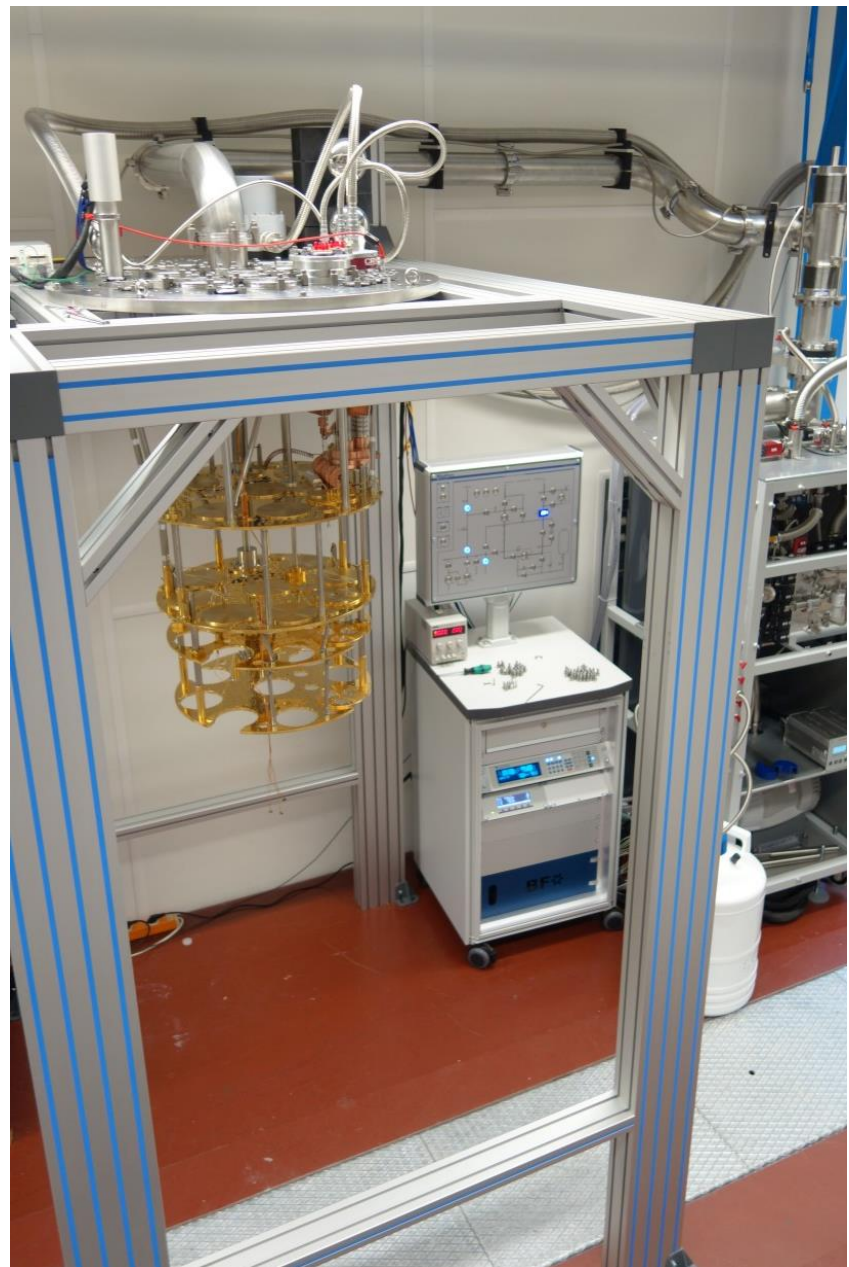
In house produced SQUID array

MMC readout

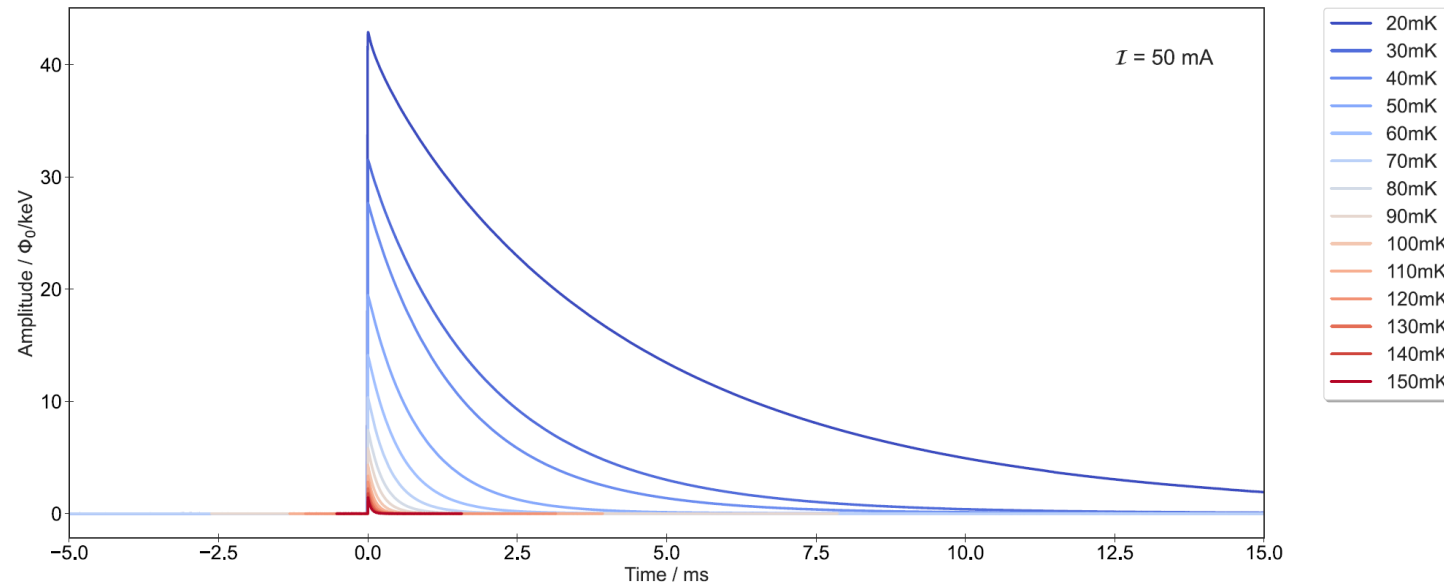


Detector and amplifier module
mounted on the
mixing chamber plate

MMC readout



Performance



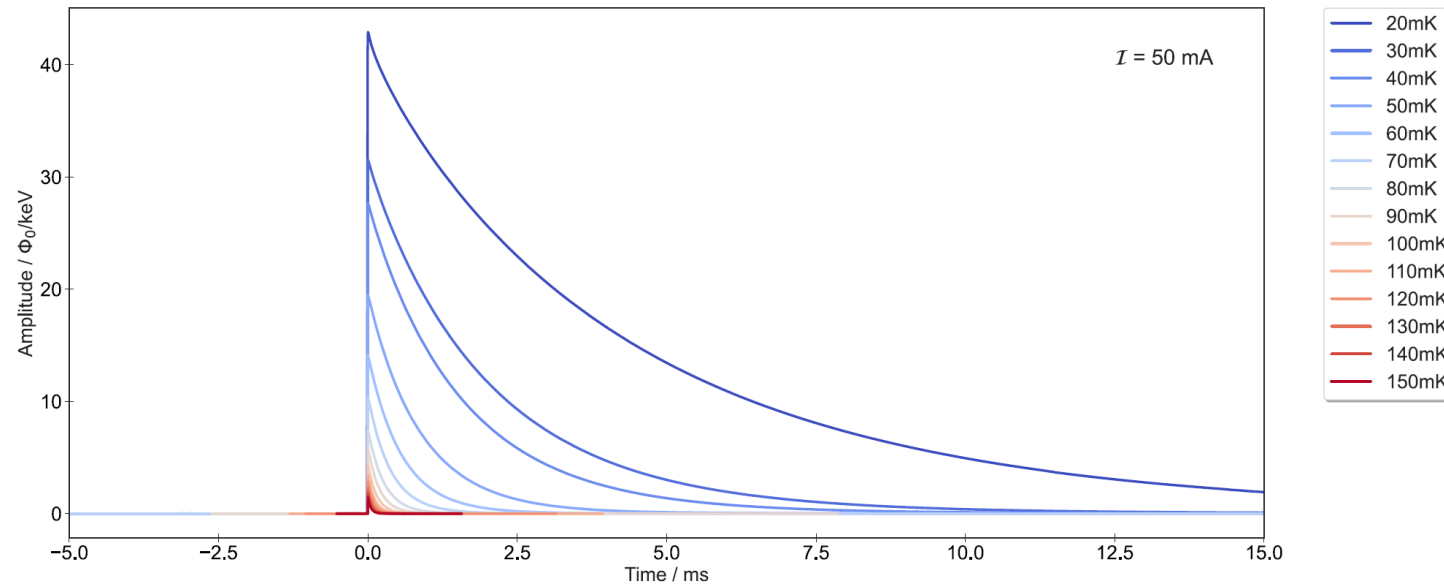
Amplitude proportional to energy

Rise time limited by the electron spin coupling

Decay time given by C/G

→ thermal link optimized for
detector heat capacity at operating
temperature

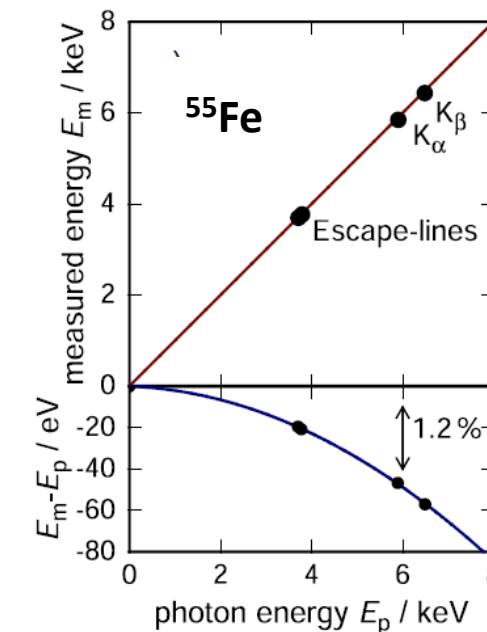
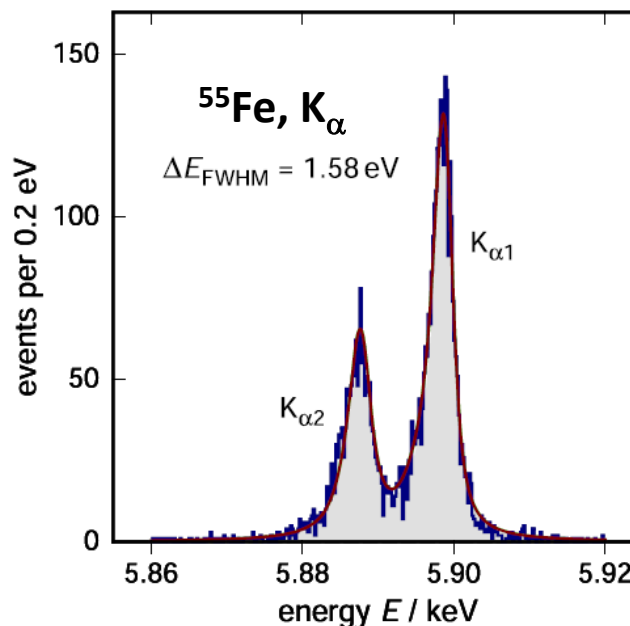
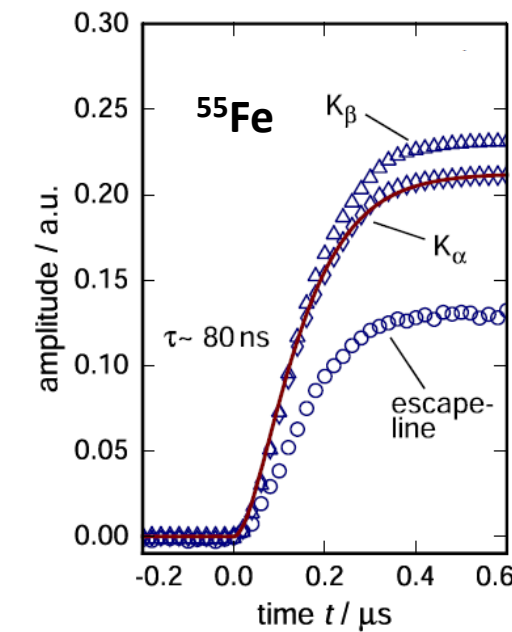
Performance



Operation over a large temperature range
→ operation of large arrays

Large dynamic range
→ no saturation of the signal

$$\Delta E_{FWHM} \sim 2.35 \sqrt{4k_B T^2 C_e} \left(\frac{1}{\beta(1-\beta)} \frac{\tau_r}{\tau_d} \right)^{1/4}$$



Fast risetime
→ Reduction un-resolved pile-up

Extremely good energy resolution
→ identification of small structures

Excellent linearity
→ precise definition of the energy scale

MMC fabrication

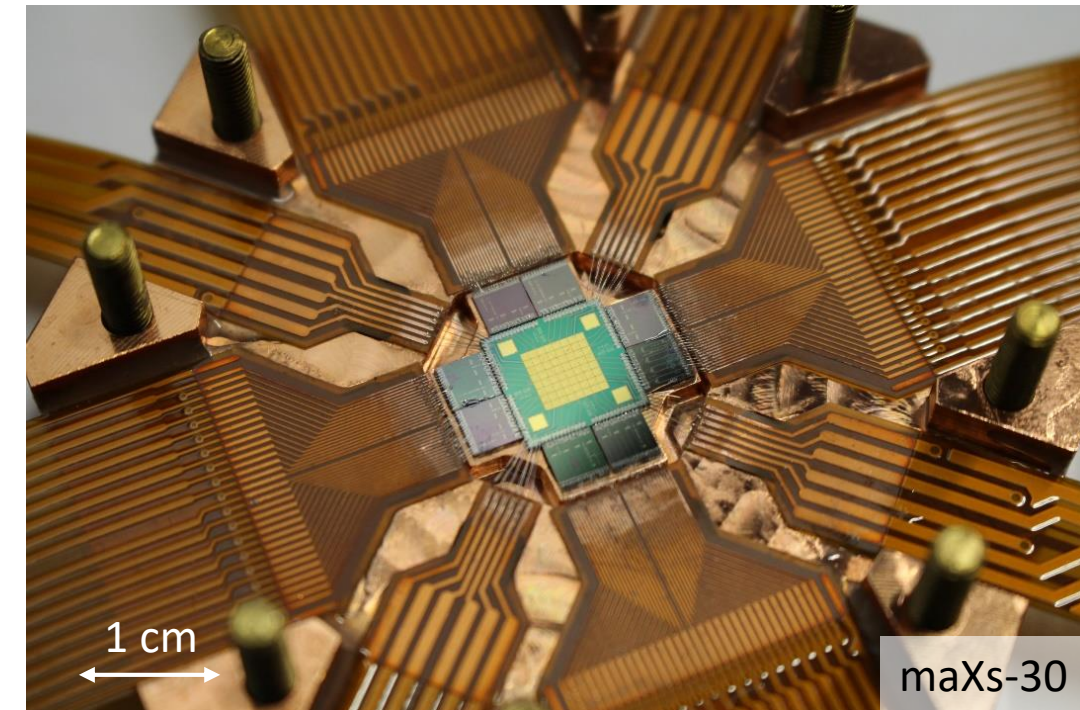
40 m² Cleanroom class 100
at Kirchhoff Institute for Physics

Wet bench
Chemistry bench
Maskless aligner
UHV sputtering system
Dry etching system

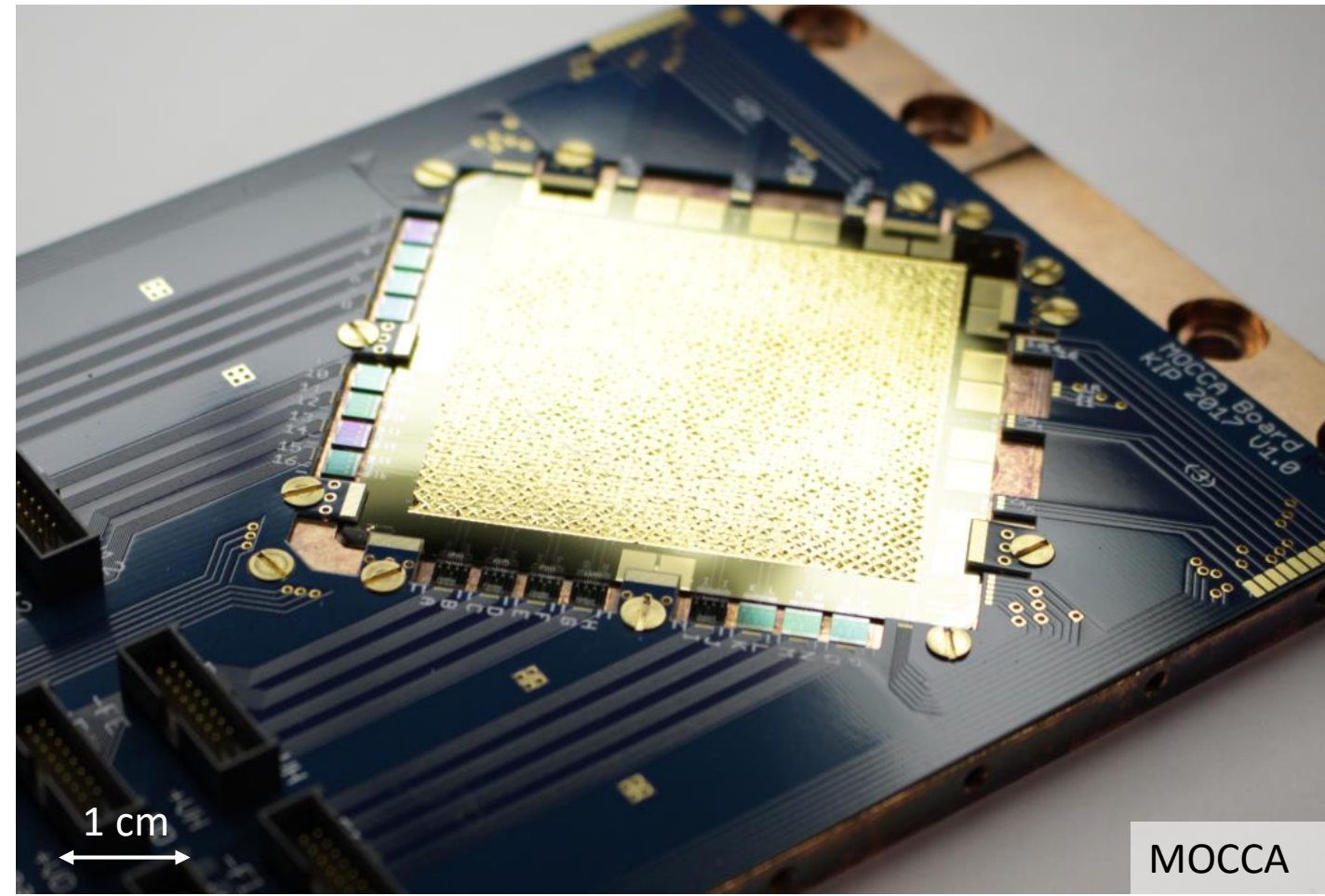
- Flexibility in design and fabrication
- Reliable processes for thin films
- Production of MMC array and superconducting electronics



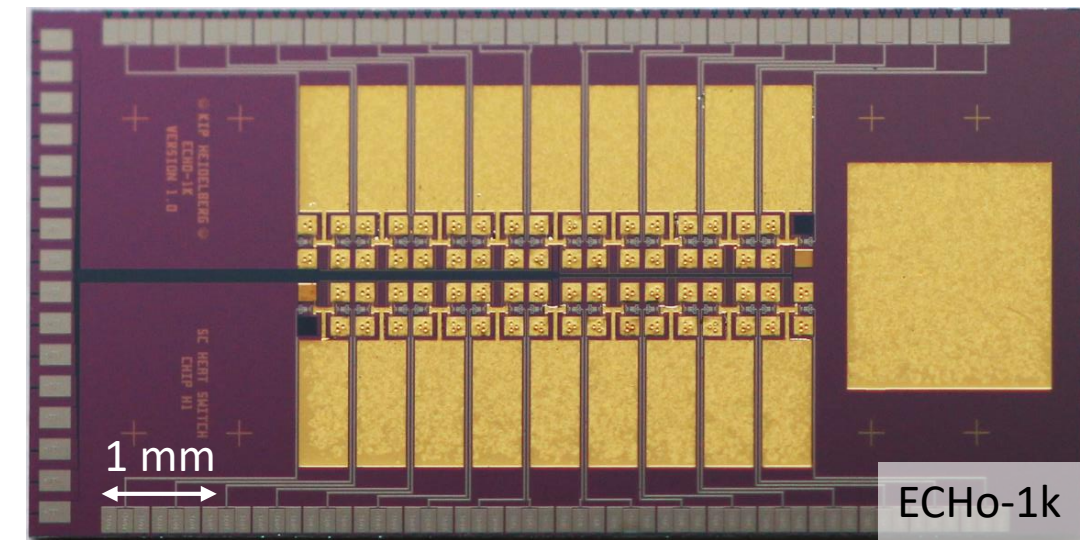
MMC Arrays



maXs-30

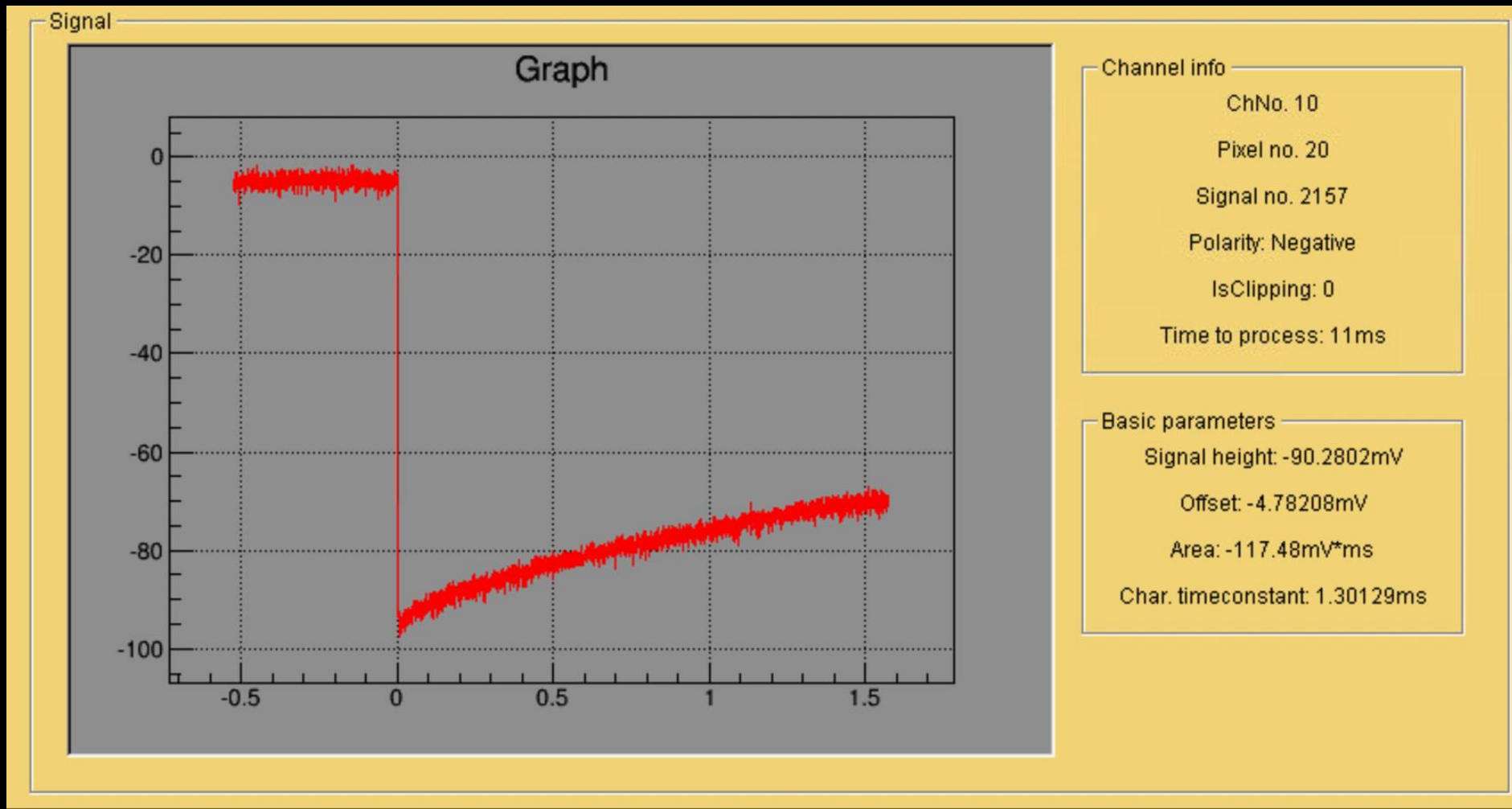


MOCCA



ECHo-1k

ECHO-1k data – Live!



mk temperatures



mK temperatures



Necessary instrumentation

Dilution refrigerators

Adiabatic demagnetization refrigerators

Before ~ 2000 Wet systems

“Complex systems”

Require liquid helium
continuous maintenance

Low temperature detectors mainly for “niche” experiment

mK temperatures



Necessary instrumentation

Dilution refrigerators

Adiabatic demagnetization refrigerators

Before ~ 2000 **Wet systems**

“Complex systems”
Require liquid helium
continuous maintenance

Low temperature detectors mainly for “niche” experiment

After ~ 2000 **Dry system**

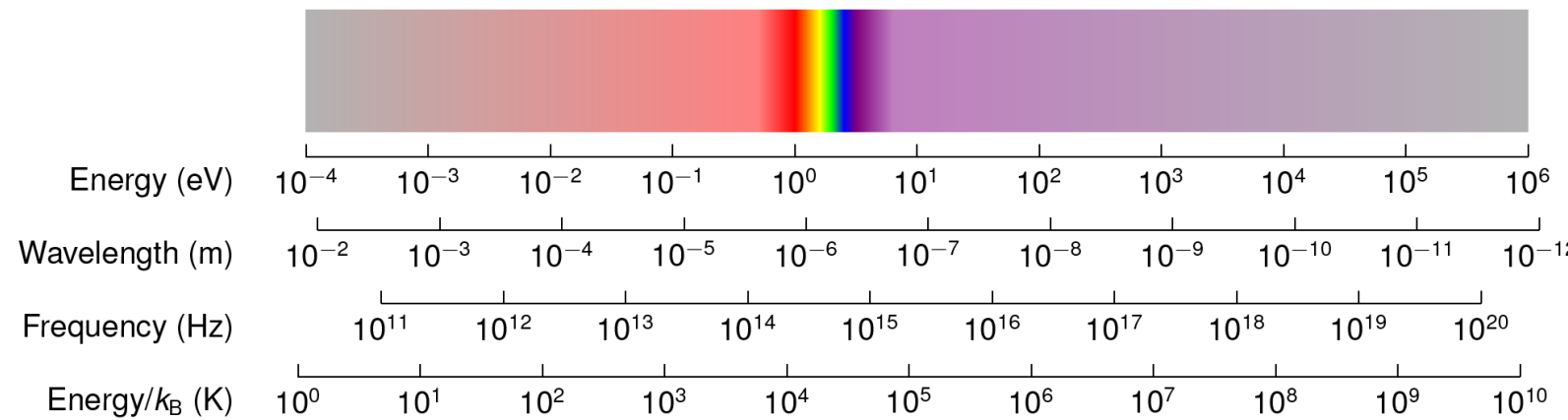
easier handling of operation
no liquid helium is required (even not liquid nitrogen)
possible full remote control – no maintenance

Low temperature detectors in many applications

Outline

- Basic of low temperature detectors
 - TES
 - MMC
- Overview on some applications
 - Photon detection
 - Neutrino physics
 - Search for Dark Matter interactions

What can LTDs measure - Photons



What can LTDs measure - Photons

TES, mKID, Ge-thermistors, STJ

TES, MMC, Si- Ge- thermistors



Energy (eV) $10^{-4} \ 10^{-3} \ 10^{-2} \ 10^{-1} \ 10^0 \ 10^1 \ 10^2 \ 10^3 \ 10^4 \ 10^5 \ 10^6$

Wavelength (m) $10^{-2} \ 10^{-3} \ 10^{-4} \ 10^{-5} \ 10^{-6} \ 10^{-7} \ 10^{-8} \ 10^{-9} \ 10^{-10} \ 10^{-11} \ 10^{-12}$

Frequency (Hz) $10^{11} \ 10^{12} \ 10^{13} \ 10^{14} \ 10^{15} \ 10^{16} \ 10^{17} \ 10^{18} \ 10^{19} \ 10^{20}$

Energy/ k_B (K) $10^0 \ 10^1 \ 10^2 \ 10^3 \ 10^4 \ 10^5 \ 10^6 \ 10^7 \ 10^8 \ 10^9 \ 10^{10}$

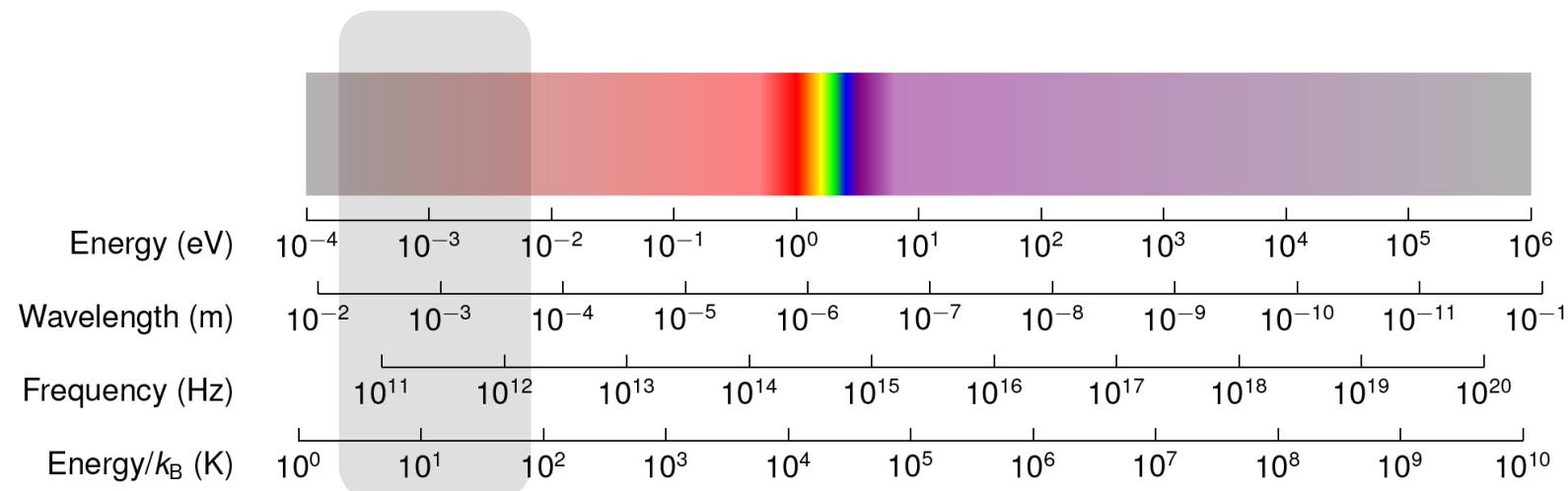
Astronomy
Cosmology

Quantum
information

Astrophysics
QED test
Material analysis
...

Nuclear
forensic

What can LTDs measure - Photons



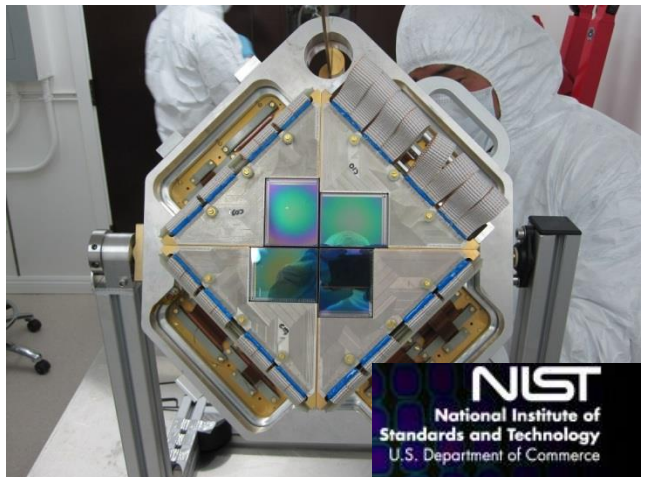
mm and sub-mm cameras

Astrophysics: studying the generation of stars and galaxies from cold gas

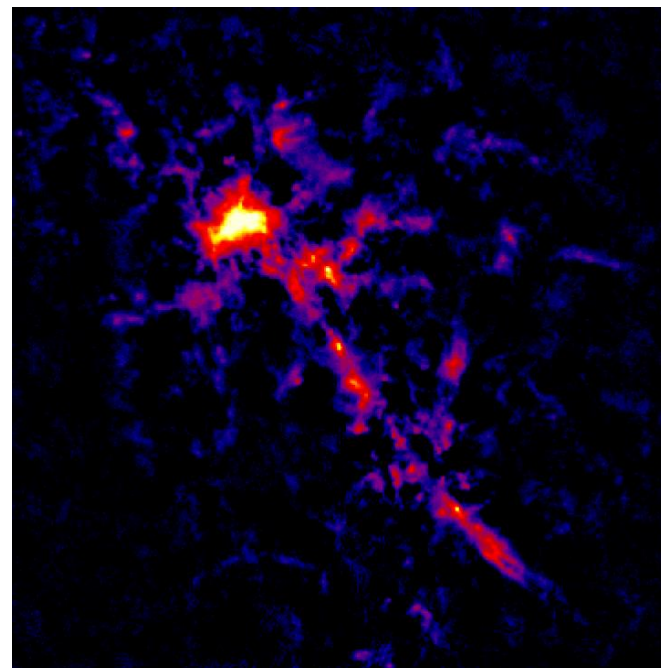
Cosmology: study of the Cosmic Microwave Background

SCUBA2 on the James Clerk Maxwell Telescope (JCMT):

- Transition Edge Sensors, 10240 TESs @ $T \sim 50$ mK
- 0.85 mm (352 GHz) and 0.45 mm (666 GHz)

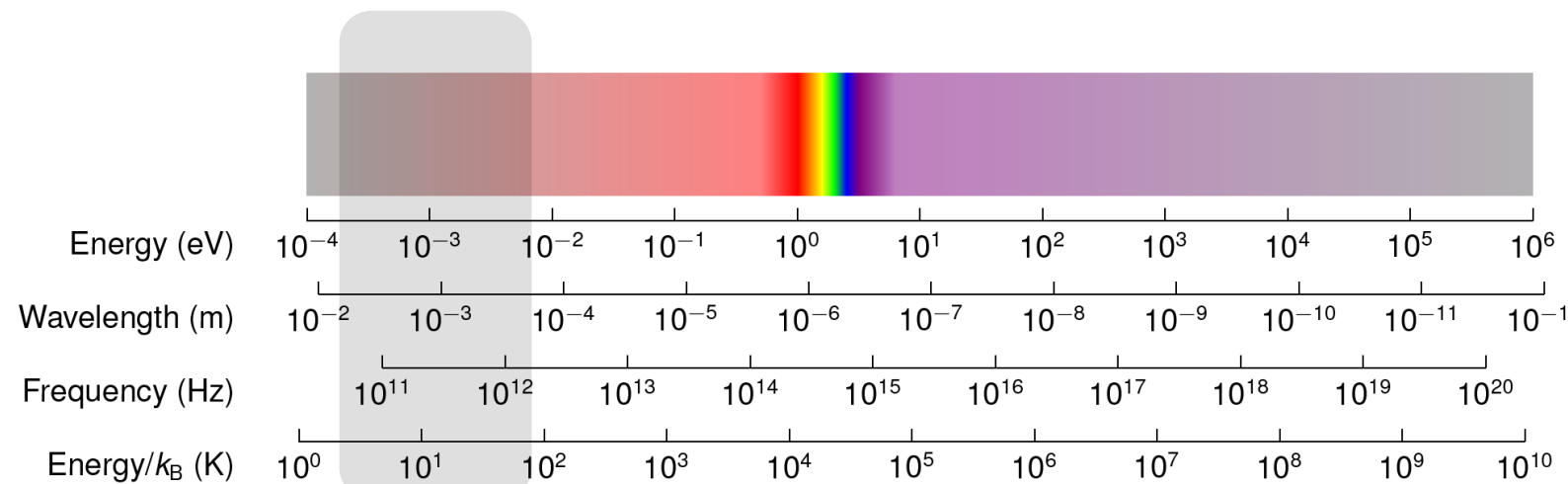


NIST
National Institute of
Standards and Technology
U.S. Department of Commerce



SCUBA2 map of the high-mass star forming region W51 at 850 μm

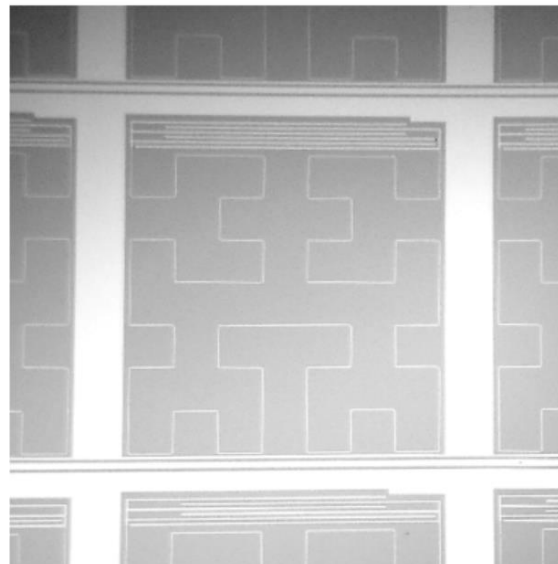
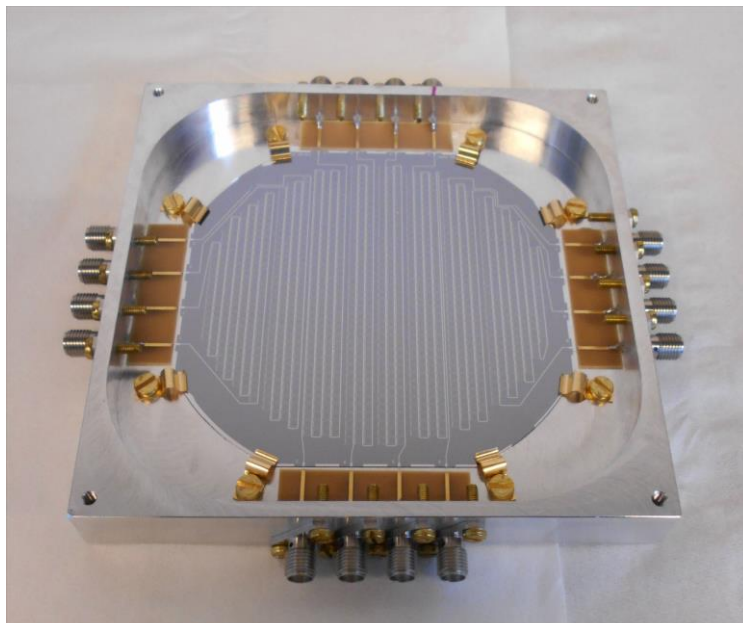
What can LTDs measure - Photons



mm and sub-mm cameras

Astrophysics: studying the generation of stars and galaxies from cold gas

Cosmology: study of the Cosmic Microwave Background

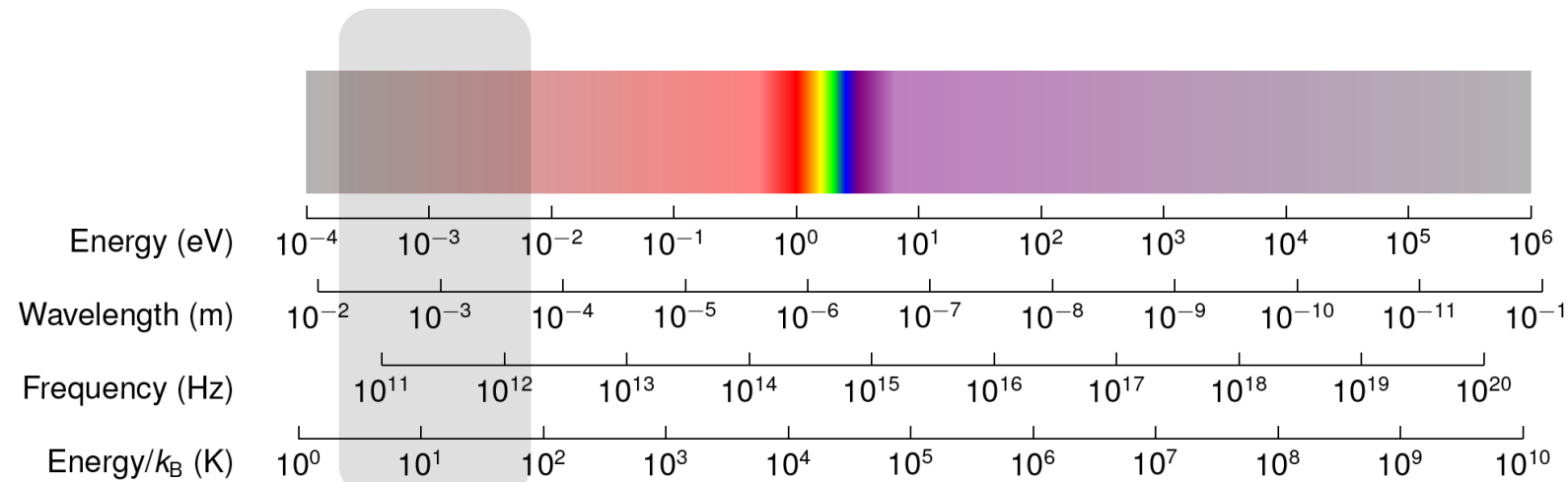


NIKA2 Al Lumped Elements KIDs

- Kinetic Inductance Detector, 2896 KIDs @ $T \sim 150$ mK
- 2 mm (150 GHz) and 1.15 mm (260 GHz)

Pixel size $2.3 \times 2.3\text{mm}^2$

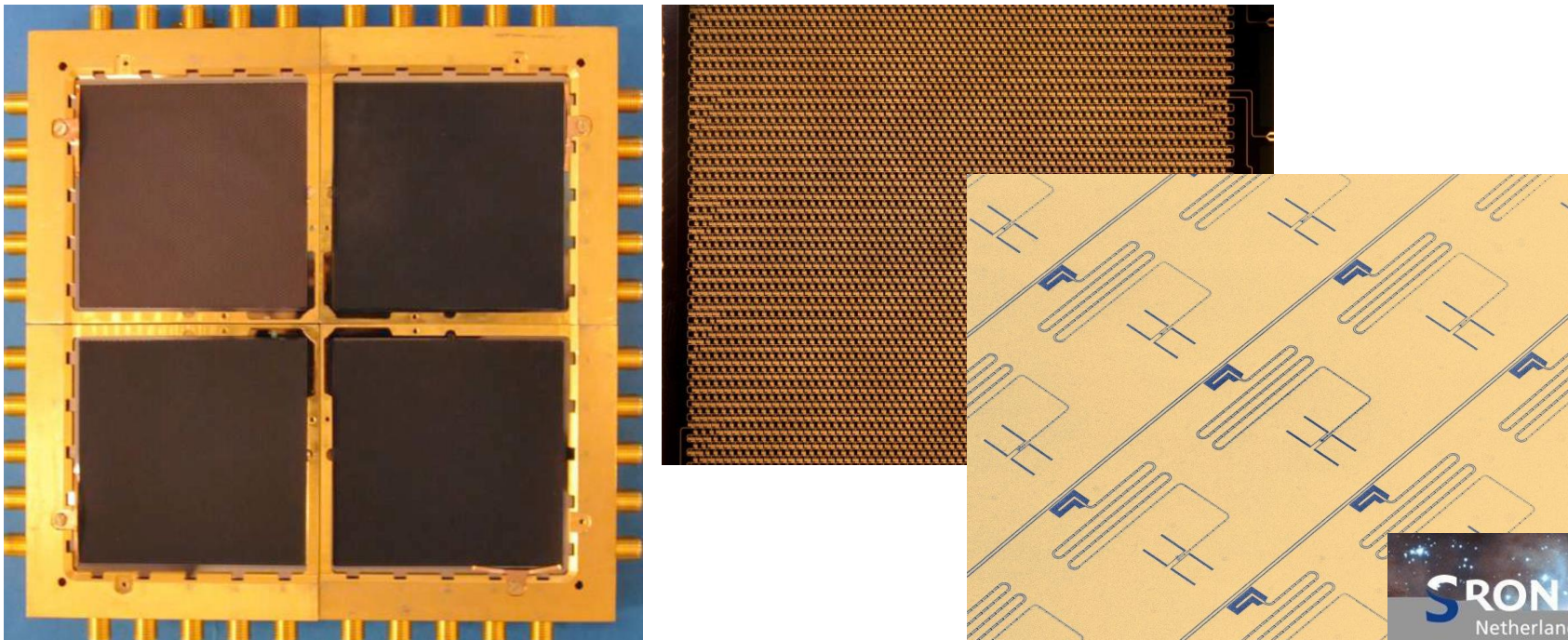
What can LTDs measure - Photons



mm and sub-mm cameras

Astrophysics: studying the generation of stars and galaxies from cold gas

Cosmology: study of the Cosmic Microwave Background



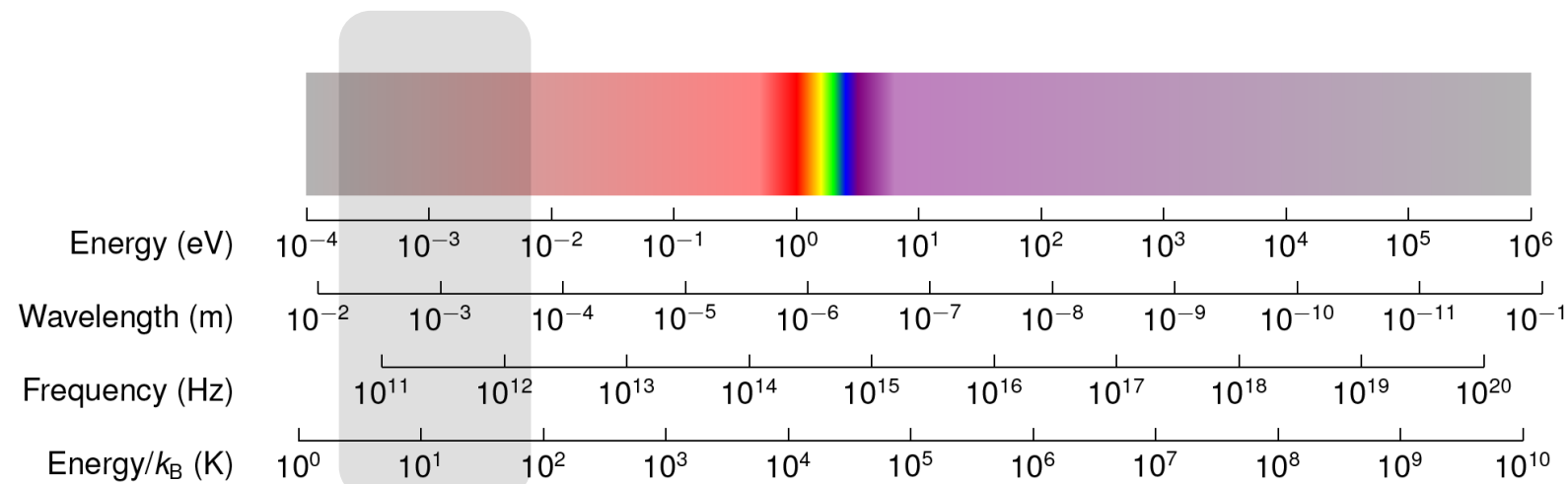
A-MKID (12 m APEX telescope Chile)

Two sub-mm bands (350 and 850 GHz)

Antenna-coupled KID:

- 3,500 pixels @ 0.85mm
- 20,000 pixels @ 0.35mm

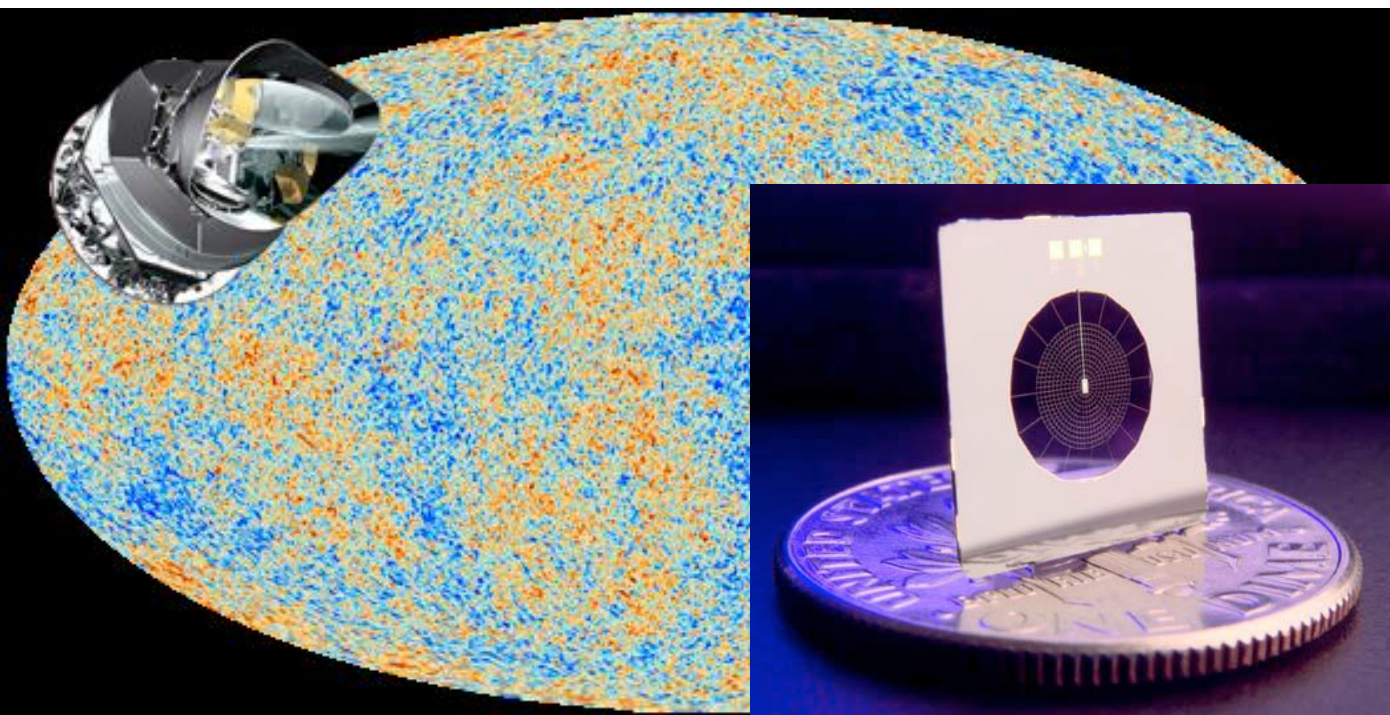
What can LTDs measure - Photons



mm and sub-mm cameras

Astrophysics: studying the generation of stars and galaxies from cold gas

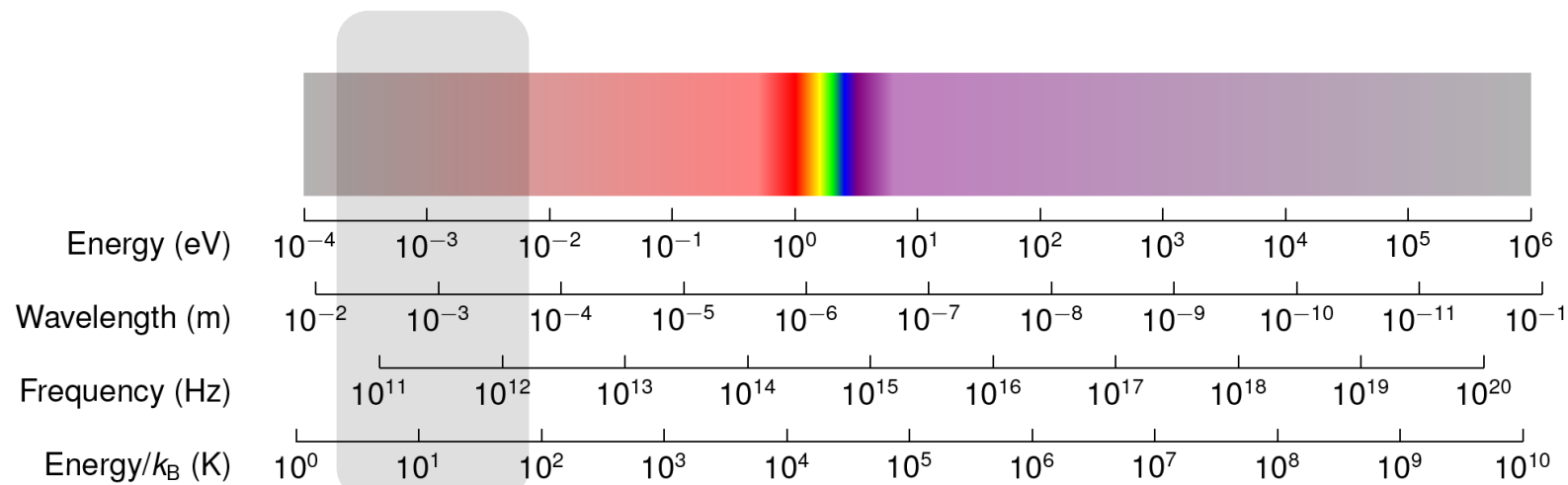
Cosmology: study of the Cosmic Microwave Background



Planck Satellite

High-Frequency Instrument (HFI):
54 Spiderweb absorber coupled to NTD-Ge
bolometers (100mK) for the frequency range
100–857 GHz.

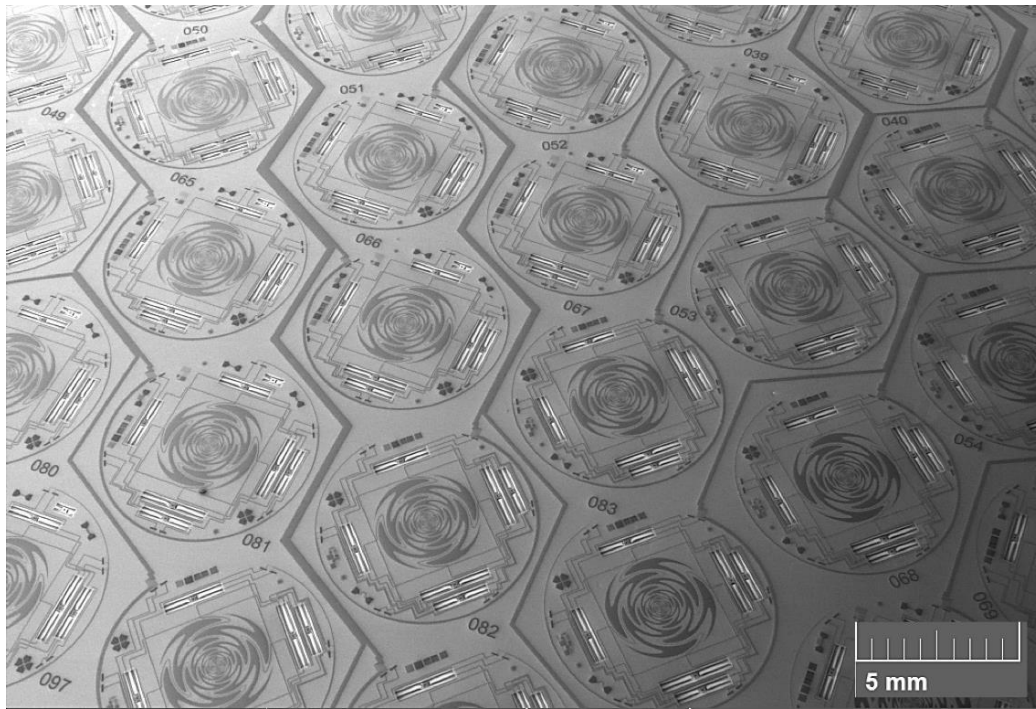
What can LTDs measure - Photons



mm and sub-mm cameras

Astrophysics: studying the generation of stars and galaxies from cold gas

Cosmology: study of the Cosmic Microwave Background



CMB-S4: next-generation ground-based CMB experiment based on antenna coupled TES:

- ~ 500000 detectors (30 - 300 GHz)
- multiple telescopes and sites to map $\gtrsim 70\%$ of sky

Detector development follows work done in ACT (Aiola et al. 2020)

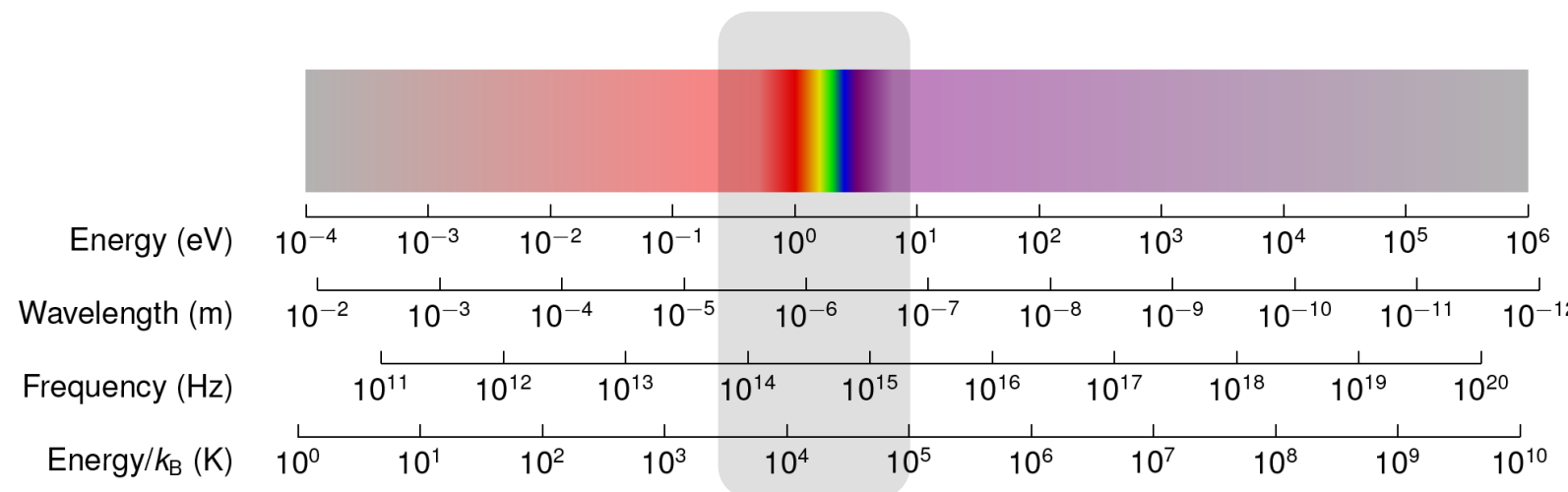
BICEP/Keck (BICEP2/Keck Array Collaborations X 2018)

CLASS (Harrington et al. 2016)

POLARBEAR/Simons Array (Suzuki et al. 2016; Hasegawa et al. 2018)

SPT (Bender et al. 2018; Sayre et al. 2020)

What can LTDs measure - Photons

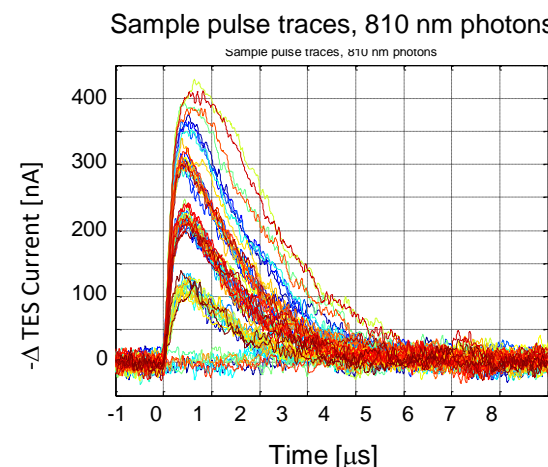
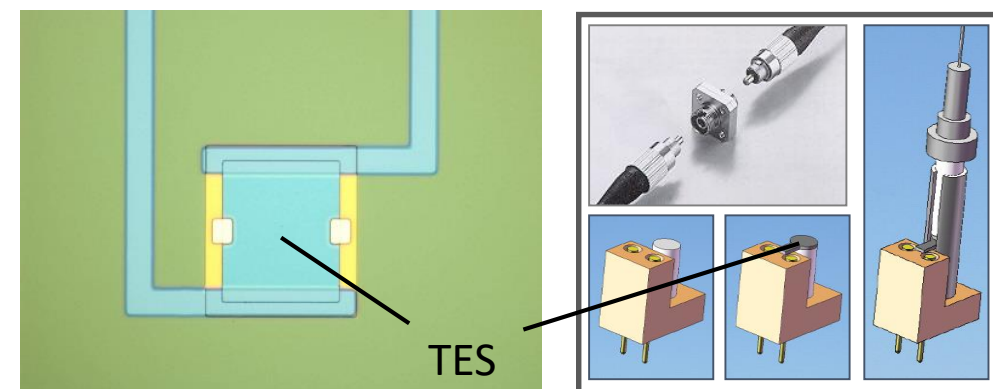


mm and sub-mm cameras

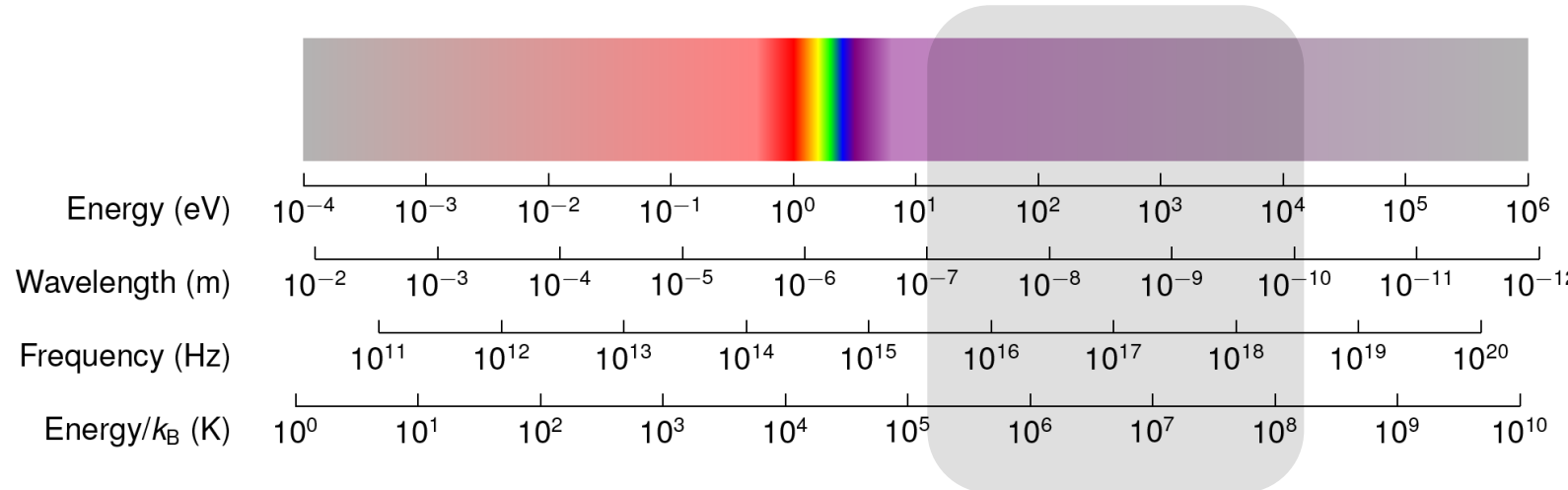
Detection of single NIR and visible photons

Fibre-coupled TES - quantum cryptography

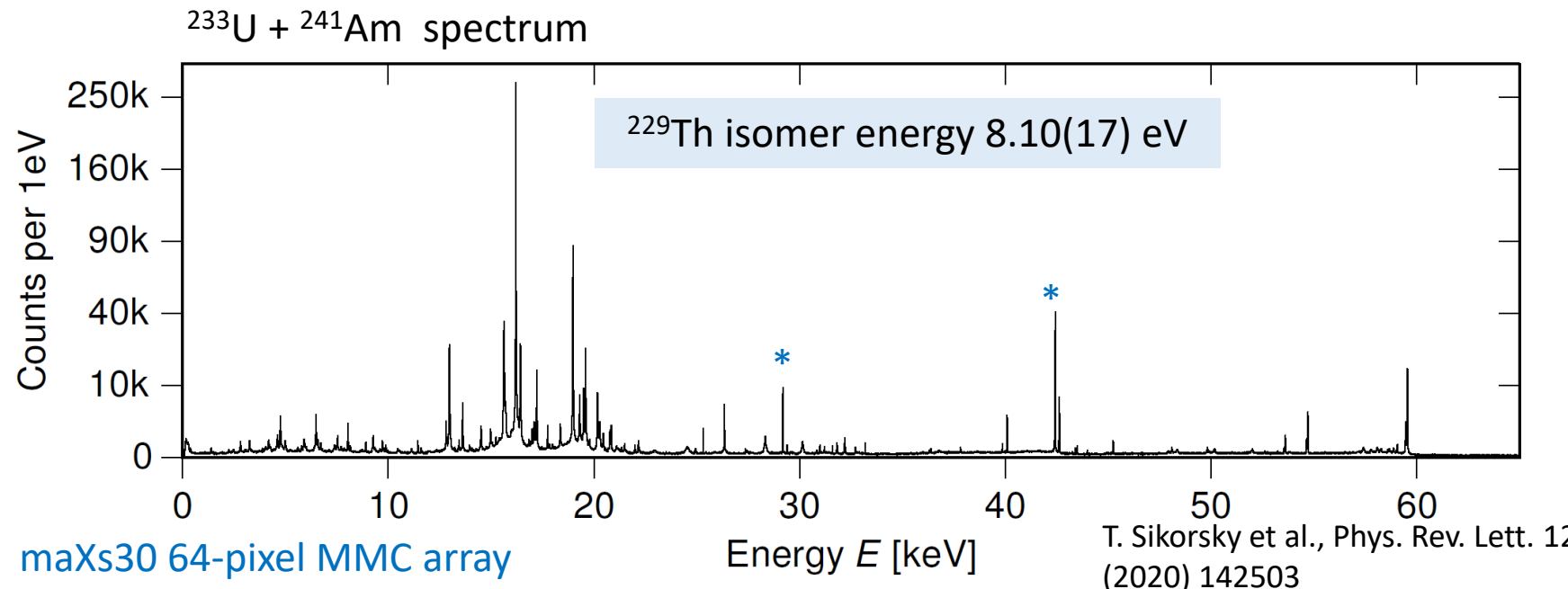
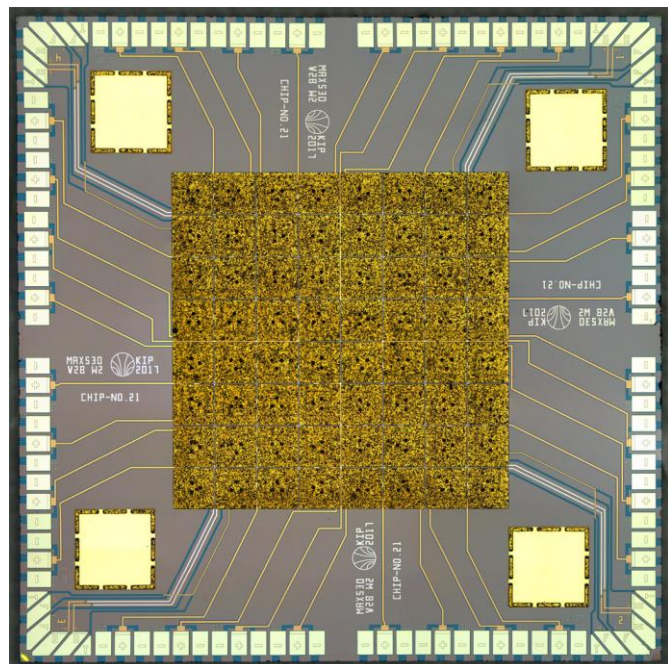
Detection efficiency close to 100%



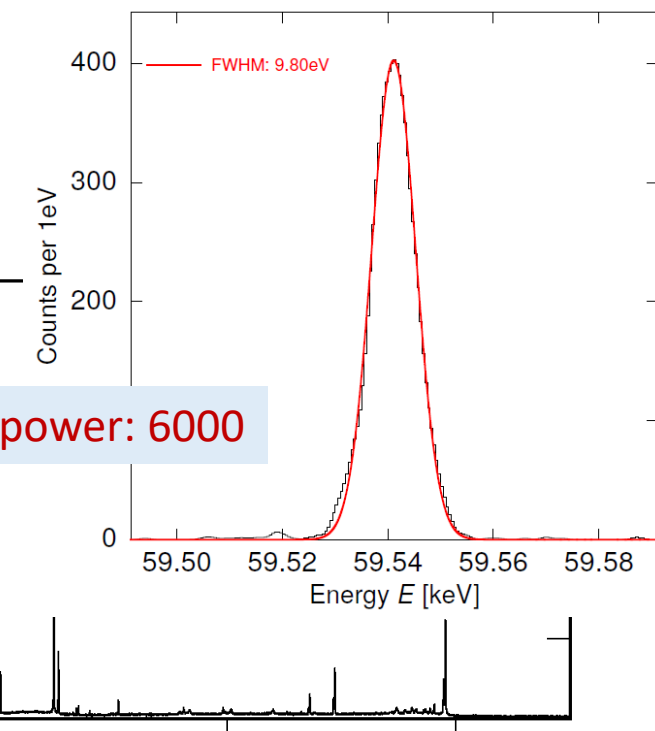
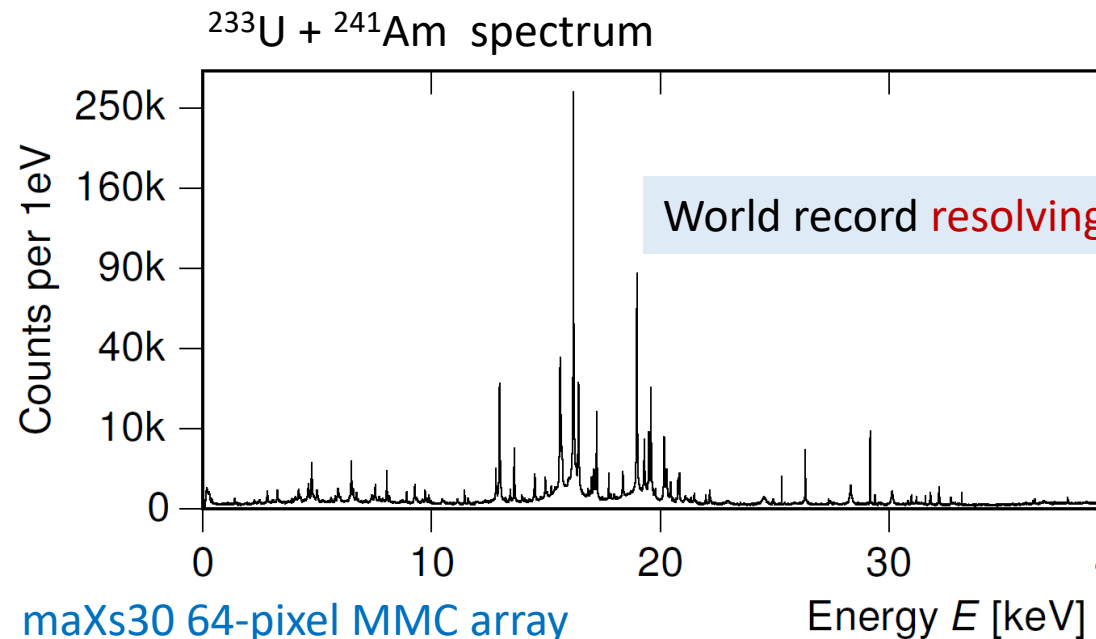
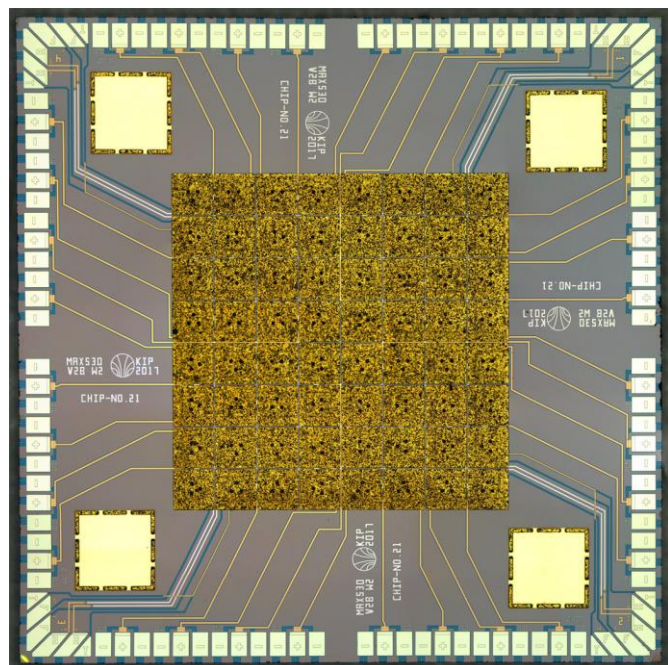
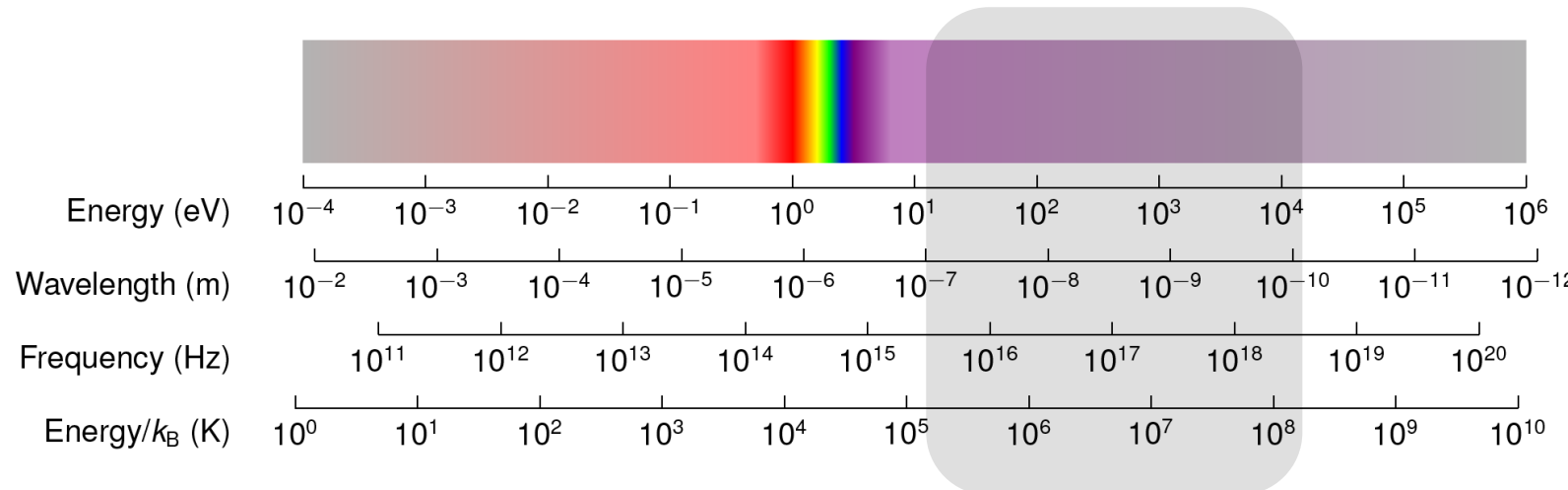
What can LTDs measure - Photons



Single x-ray photons
atomic physics, astronomy, material analysis



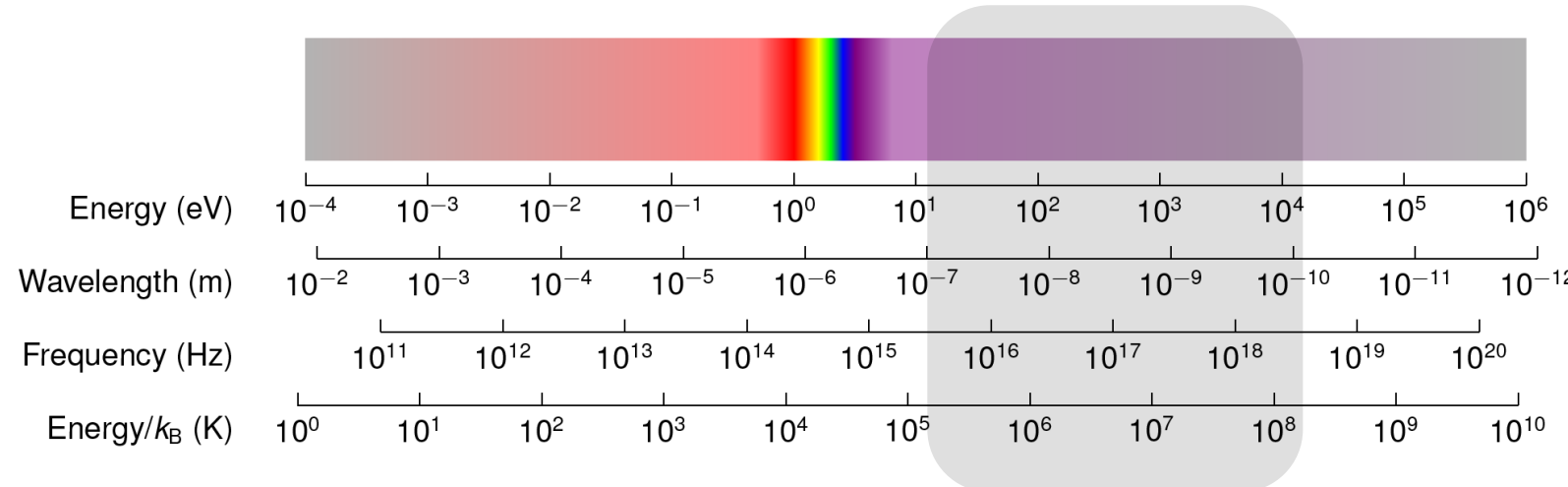
What can LTDs measure - Photons



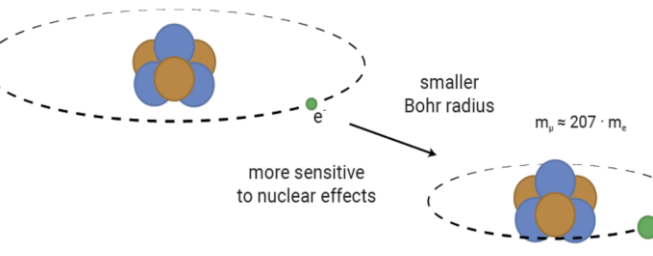
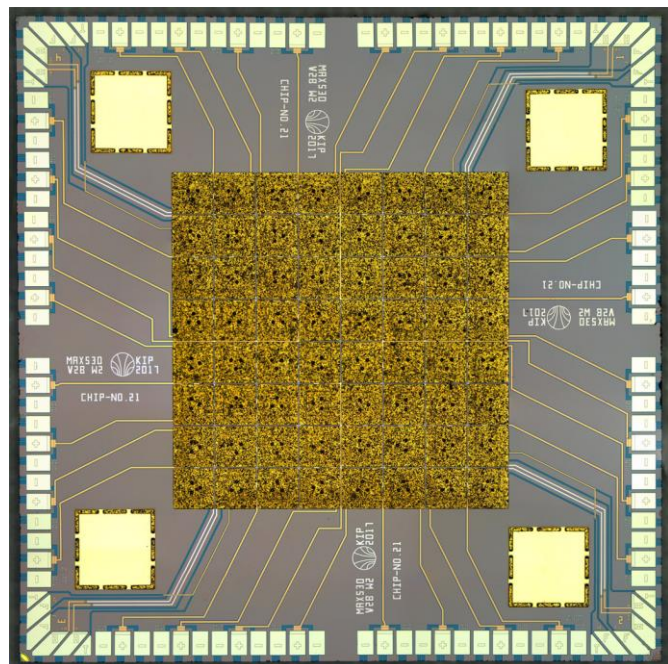
Single x-ray photons
atomic physics, astronomy, material analysis

T. Sikorsky et al., Phys. Rev. Lett. 125 (2020) 142503

What can LTDs measure - Photons

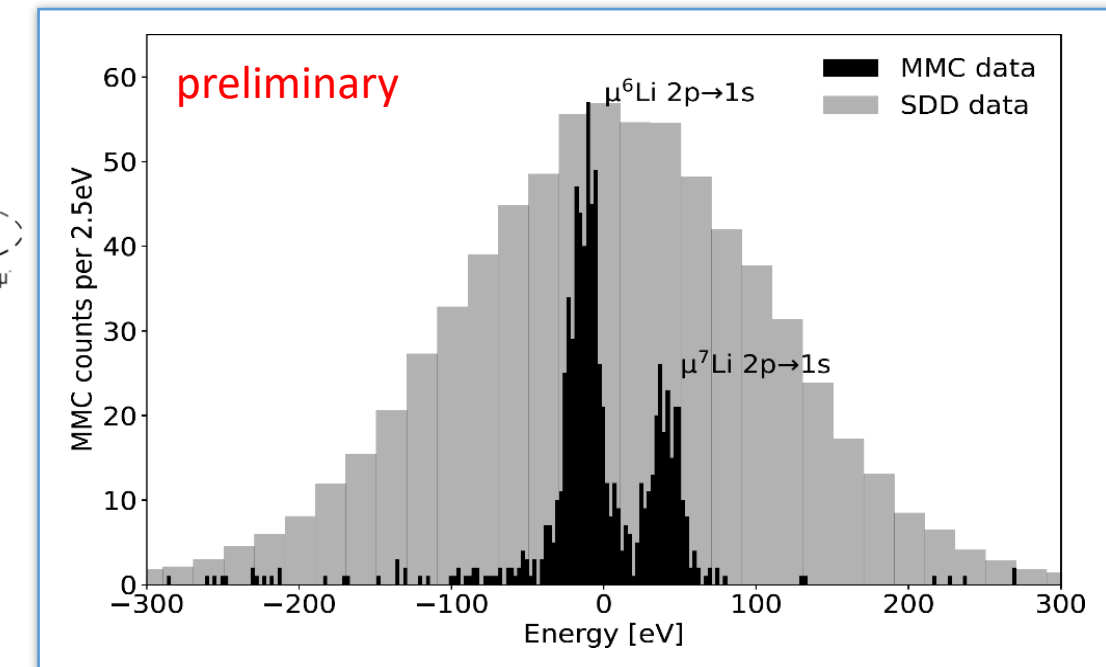


Single x-ray photons
atomic physics, astronomy, material analysis

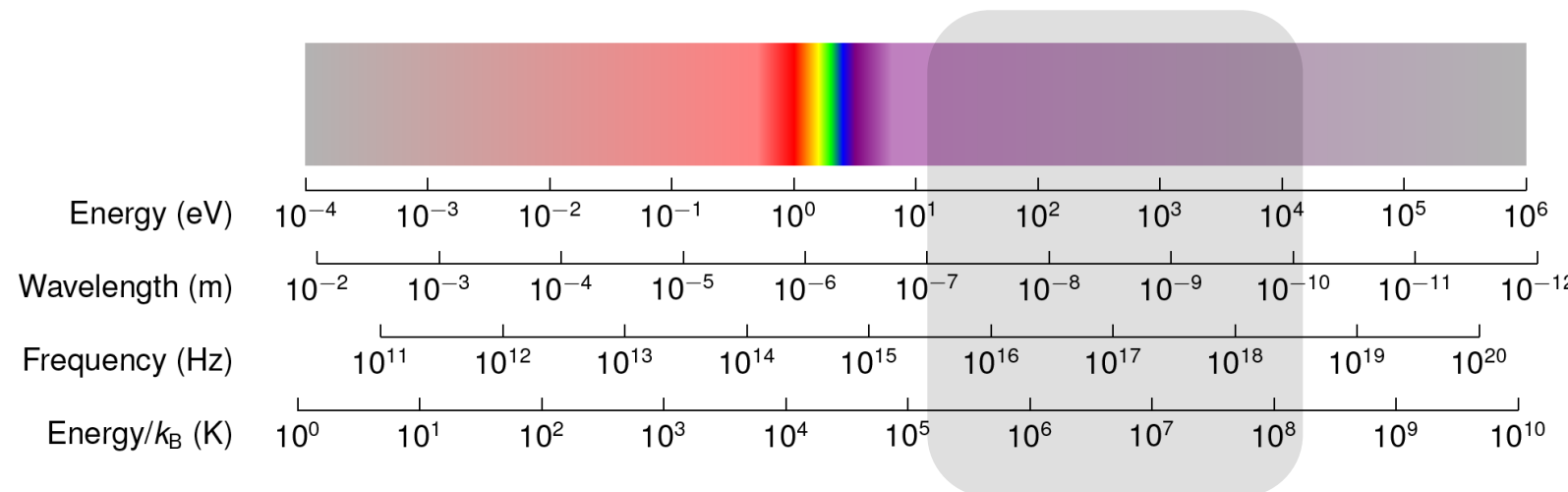


Muonic atoms spectroscopy

maXs30 64-pixel MMC array



What can LTDs measure - Photons

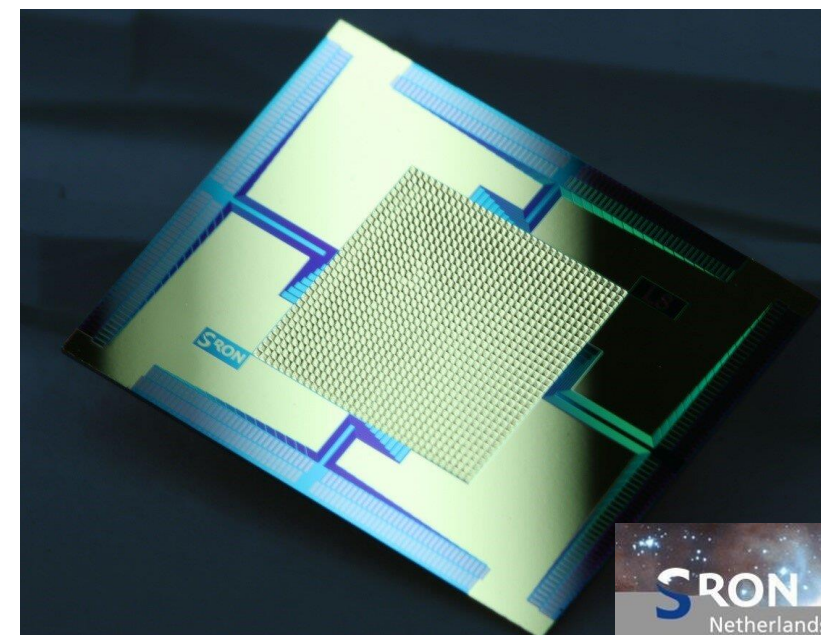


Single x-ray photons
atomic physics, astronomy, material analysis

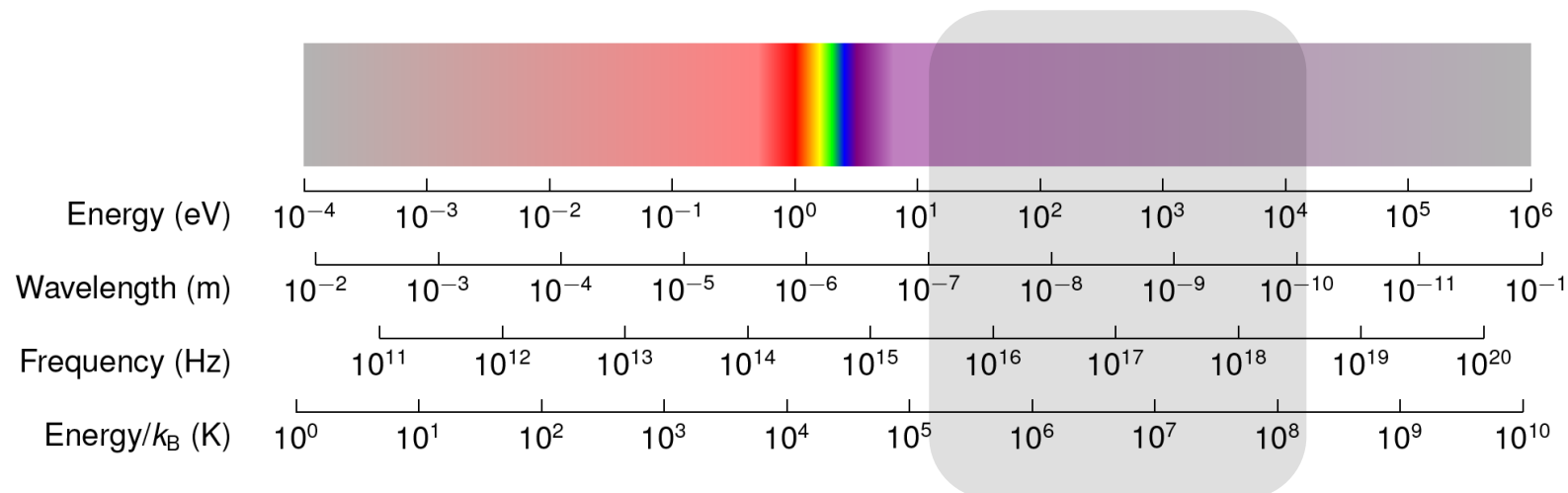
32×32 pixel x-ray camera for the X-IFU

Cryogenic spectrometer, energy band 0.2 – 12 keV

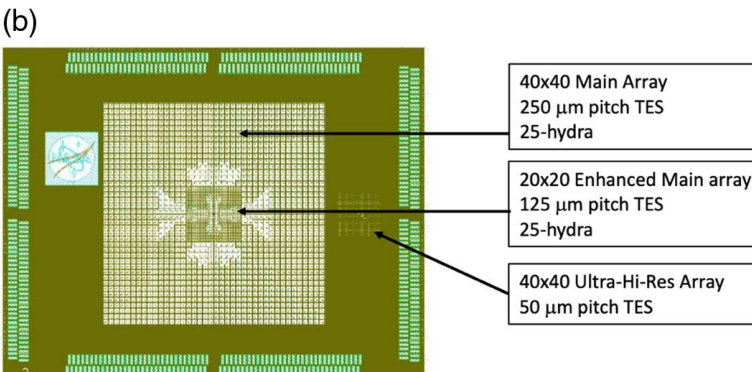
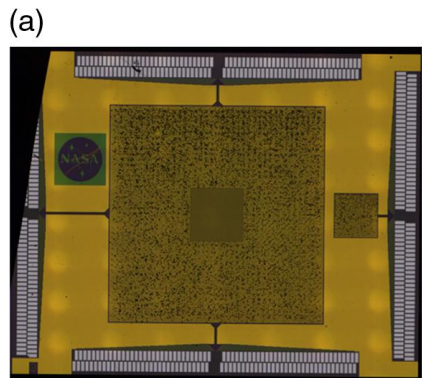
Au absorbers + Ti(35nm)Au(200nm) bilayer $\rightarrow T_c \sim 90\text{mK}$



What can LTDs measure - Photons

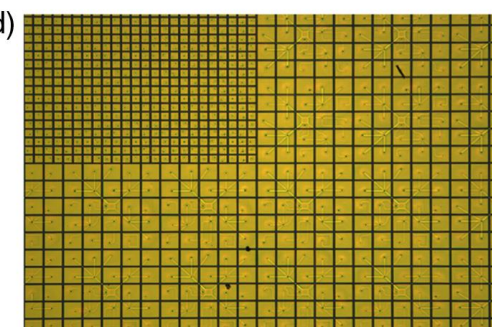
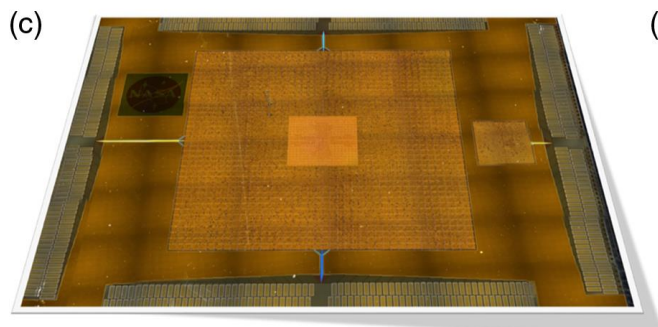


Single x-ray photons
atomic physics, astronomy, material analysis

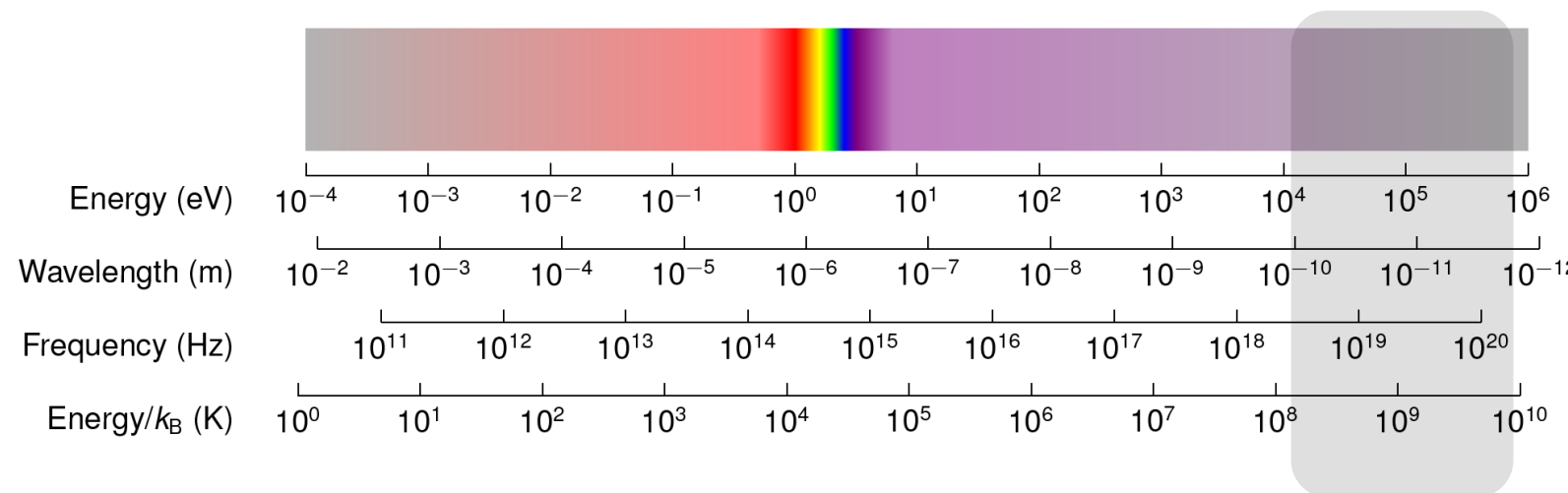


Lynx x-ray microcalorimeter (LXM)

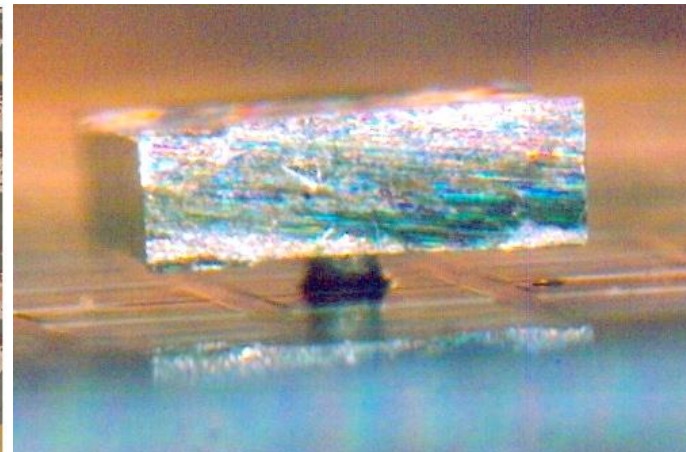
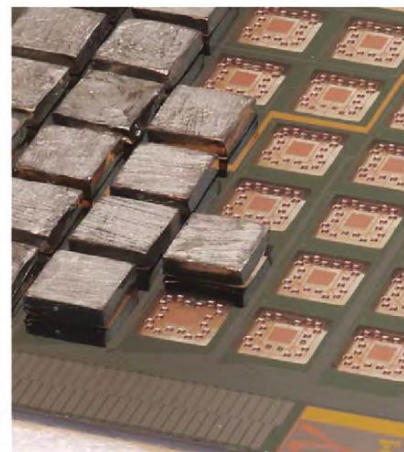
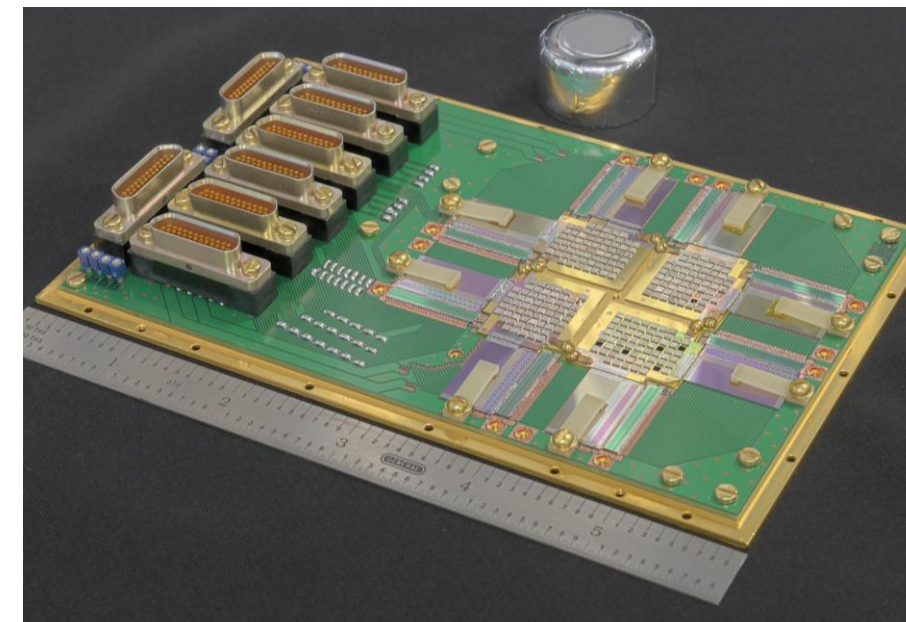
TES (MMC as alternative)



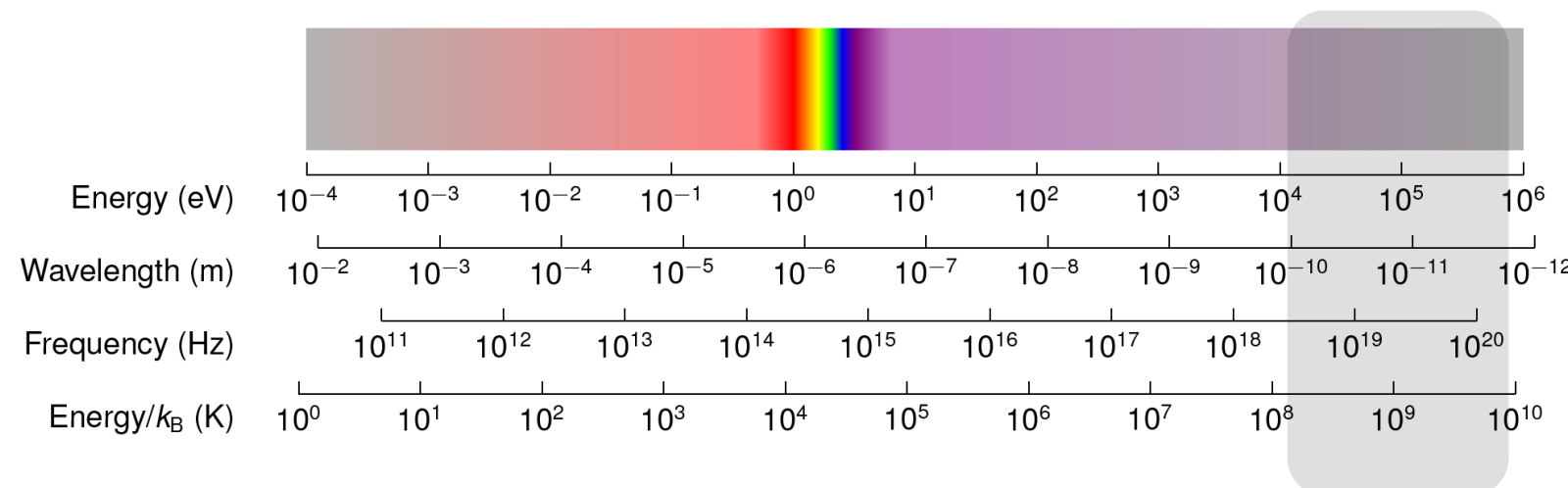
What can LTDs measure - Photons



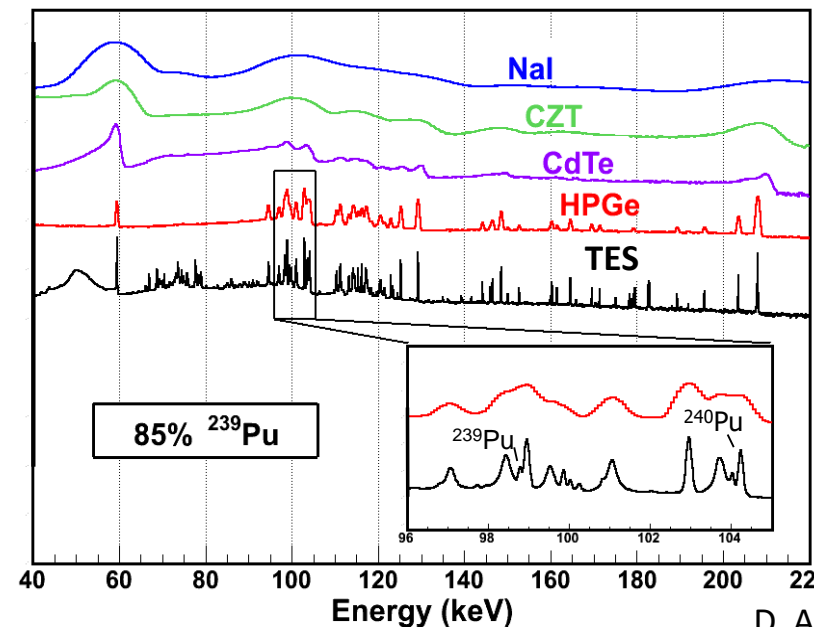
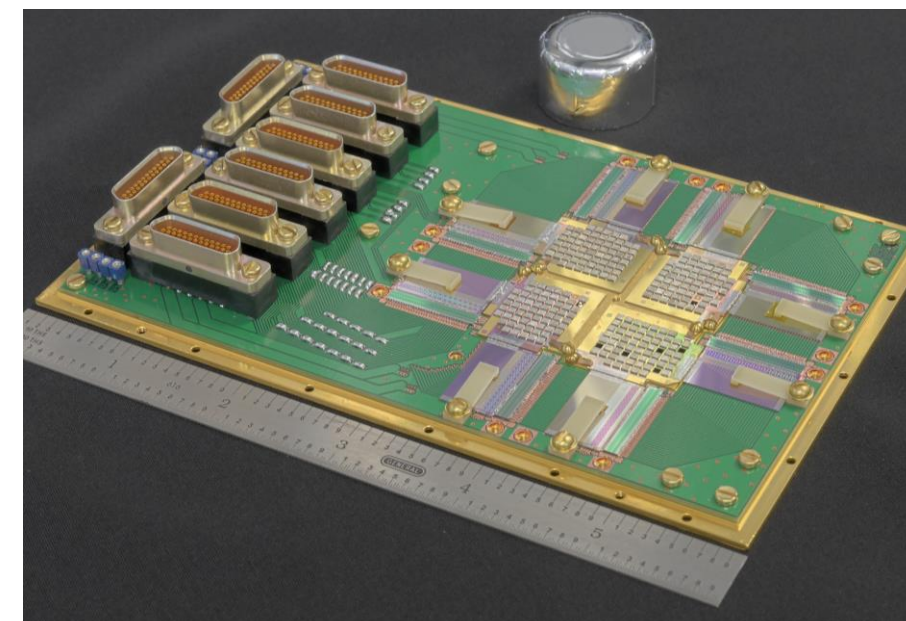
γ - and (α)-detectors
homeland security and nuclear non-proliferation



What can LTDs measure - Photons



γ - and (α)-detectors
homeland security and nuclear non-proliferation



More than a factor 10 better resolving power than typical semiconductor detector

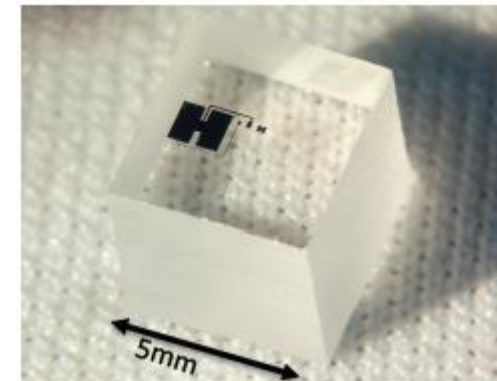
What can LTDs measure – not only photons

Low temperature detector for Neutrino Physics

Neutrinoless double beta decay CUORE, AMoRE, CUPID

Coherent neutrino nucleus scattering NuCLEUS (TES), Ricochet (TES), BullKID (mKID)

Neutrino interaction induces a nuclear recoil



R. Strauss et al., *Eur.Phys.J.C* 79 (2019) 12, 1018

Sterile neutrino searches BeEST (Ta-based STJ)

nuclear recoil following electron capture in ^7Be

Fretwell et al., *Phys. Rev. Lett.* 125, 032701 (2020)

kink in H-3 beta spectrum with LiF + MMC (Exp. in Korea)

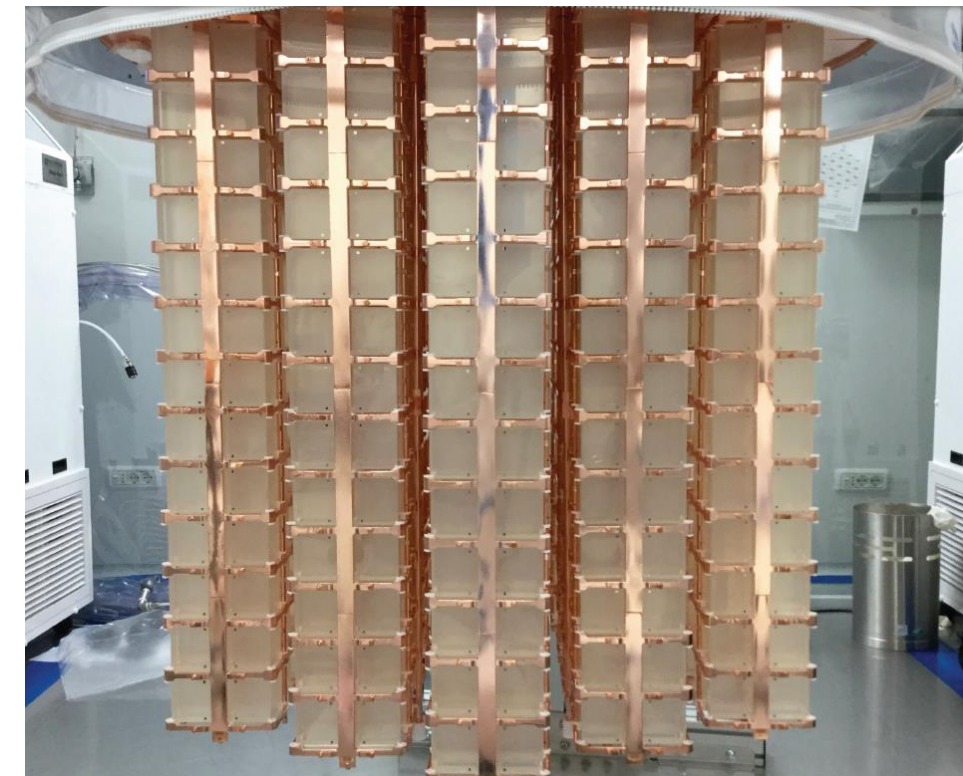
Y.C. Lee et al., *JLTP* 209 (2022) 919

Direct neutrino mass determination ECHo (MMC), HOLMES (TES)

all the energy released upon electron capture in ^{163}Ho ,
besides the one taken away by the neutrino

The ECHo Collaboration *EPJ-ST* 226 8 (2017) 1623

B. Alpert et al, *Eur. Phys. J. C* 75 (2015) 112



What can LTDs measure – not only photons

Phys. Rev. Lett. 120 (2018) 6, 061802

Low temperature detector for Dark Matter direct searches

WIMP produces nuclear recoil → temperature rise + charges

Super CDMS (TES)

EDELWEISS NTD-Ge

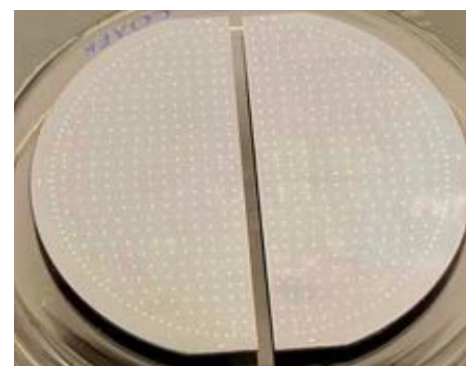
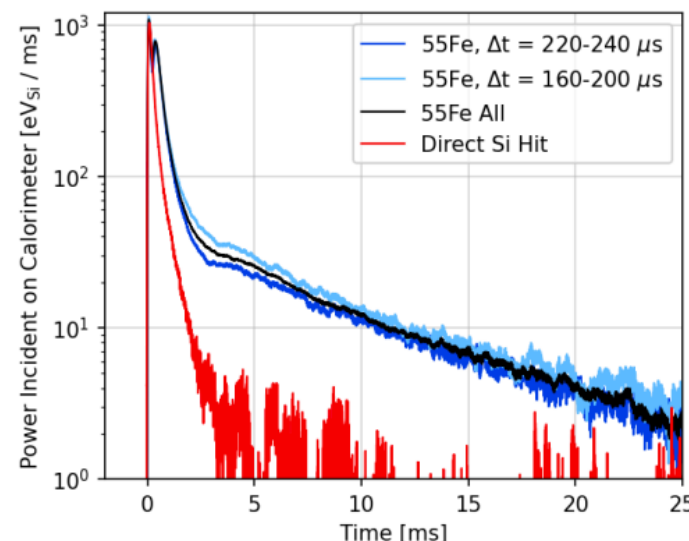
WIMP produces nuclear recoil → temperature rise + light

CRESST (TES)

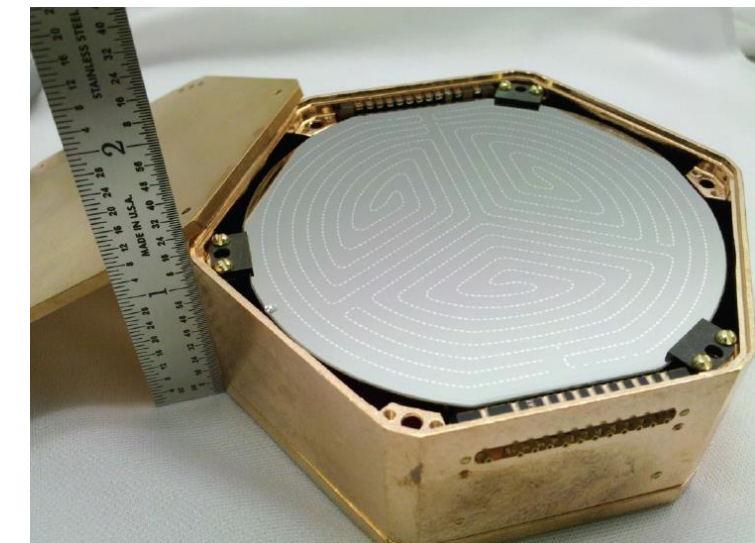
WIMP produces nuclear recoil → light + evaporation + de-excitation

HeRALD (TES)

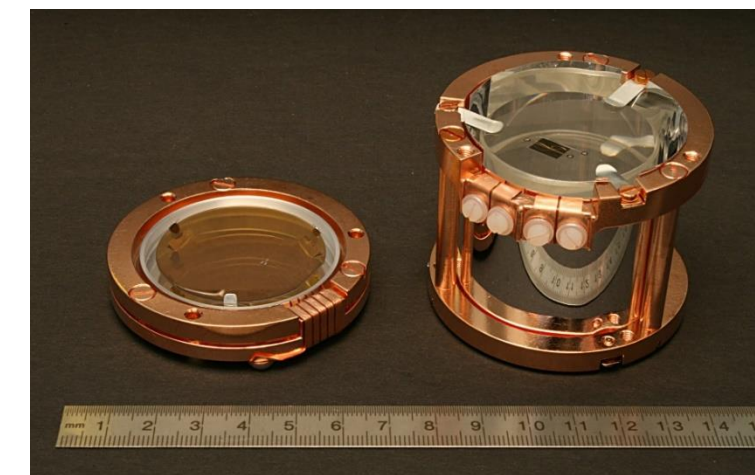
DELight (MMC)



R. Anthony-Petersen et al. (SPICE/HeRALD Collaboration)
Phys. Rev. D 110 (2024) 072006



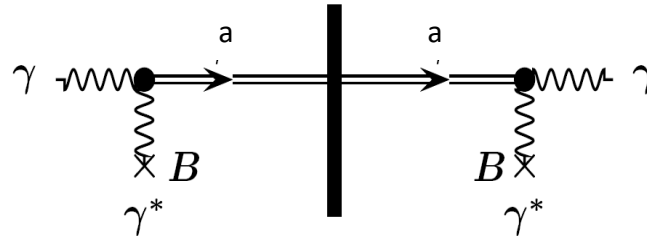
Phys. Rev. D 100 (2019) 10, 102002



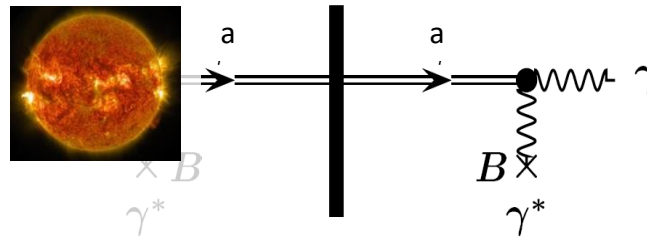
What can LTDs measure – not only photons

Low temperature detector for axion searches

- Purely laboratory experiments
“light-shining-through-walls”,
optical photons

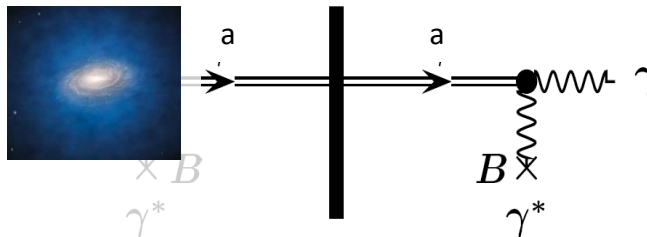


- Helioscopes**
ALPs emitted by the sun,
X-rays,



•

- Haloscopes**
looking for dark matter constituents,
microwaves.

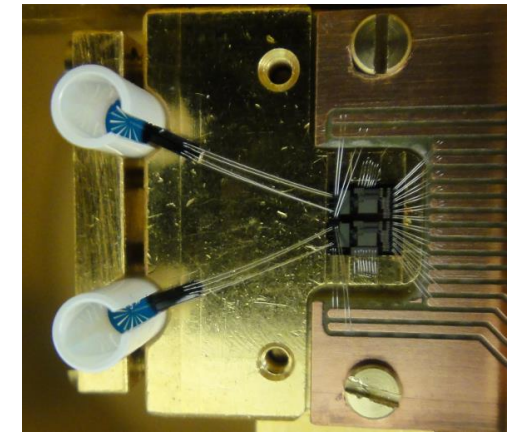
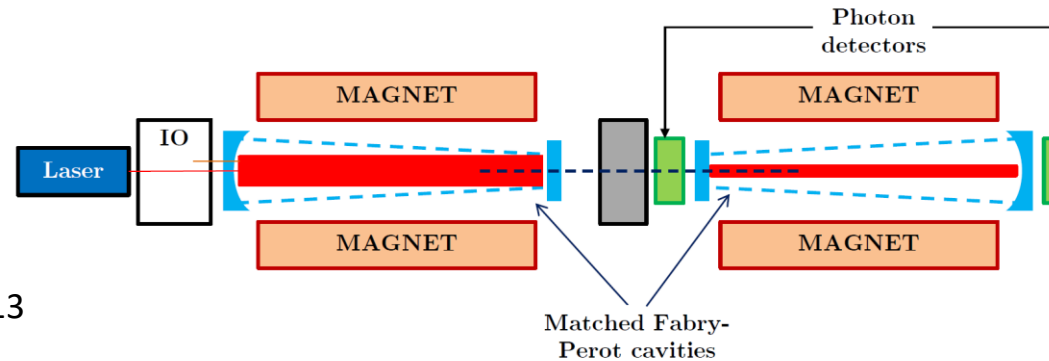


What can LTDs measure – not only photons

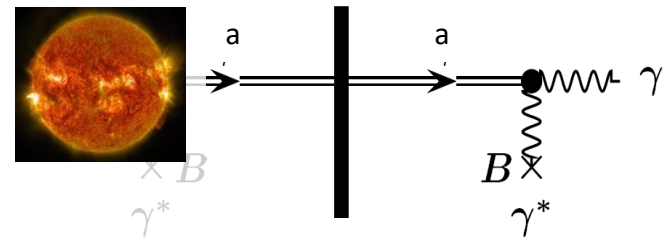
Low temperature detector for axion searches

- Purely laboratory experiments
“light-shining-through-walls”,
optical photons
ALPS experiment

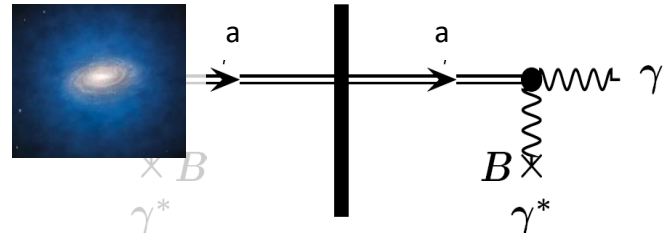
R. Bähre et al., J. Instrum., 8(09):T09001, 2013



- Helioscopes**
ALPs emitted by the sun,
X-rays,



- Haloscopes**
looking for dark matter constituents,
microwaves.

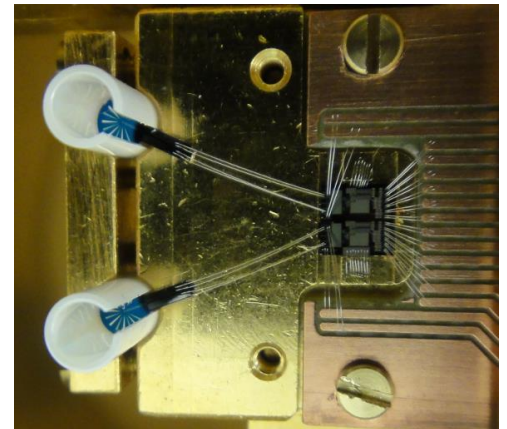
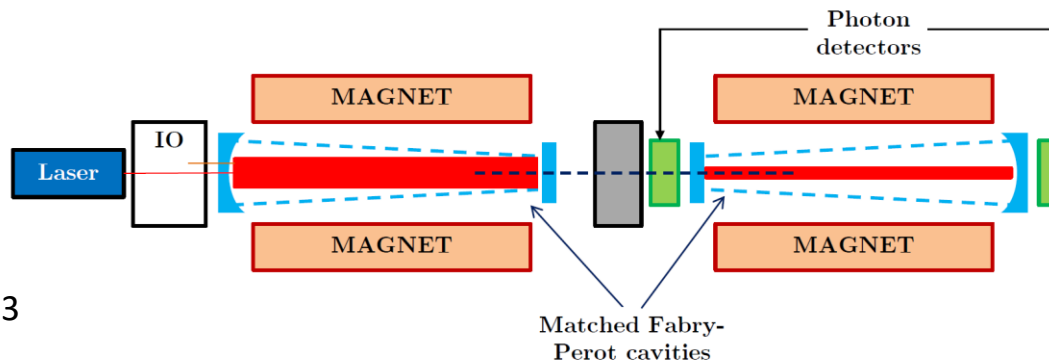


What can LTDs measure – not only photons

Low temperature detector for axion searches

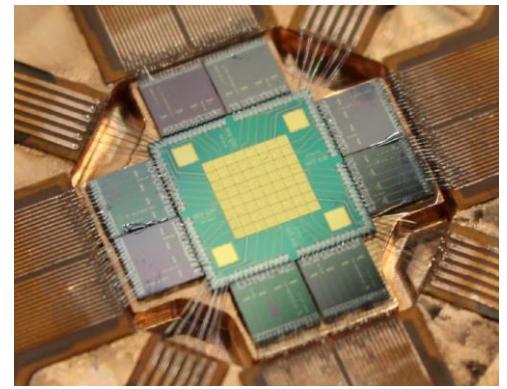
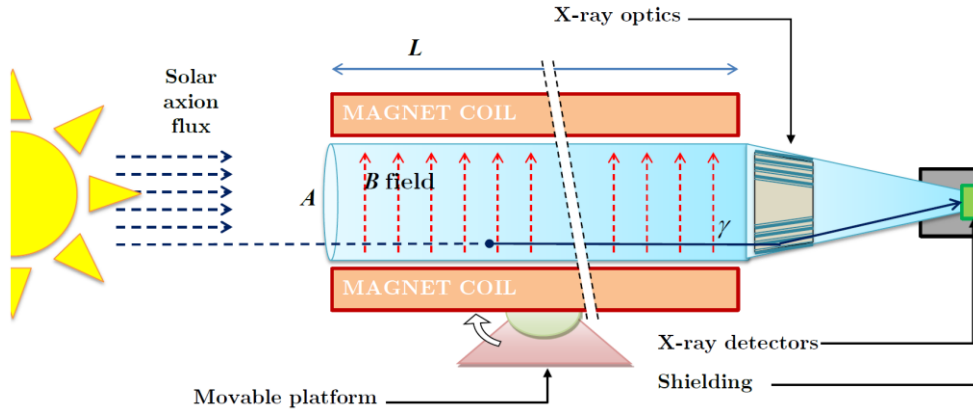
- Purely laboratory experiments
“light-shining-through-walls”,
optical photons
ALPS experiment

R. Bähre et al., J. Instrum., 8(09):T09001, 2013

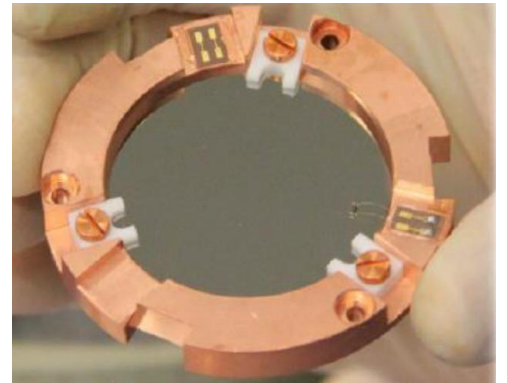
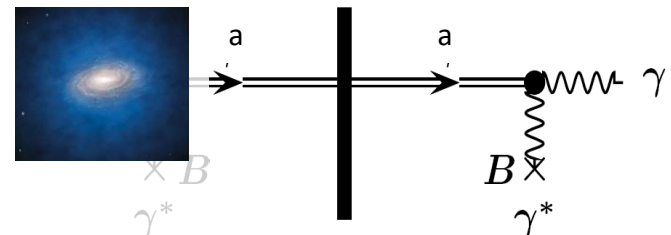


- Helioscopes**
ALPs emitted by the sun,
X-rays
(baby)IAXO

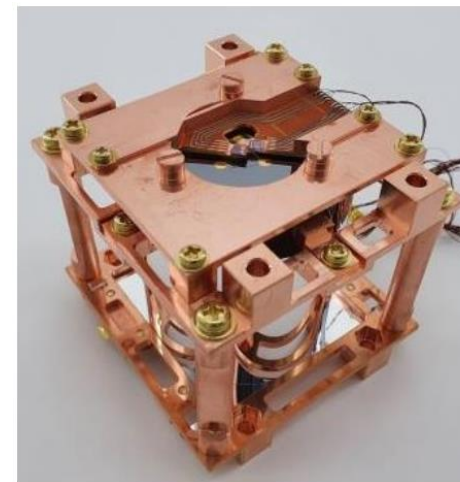
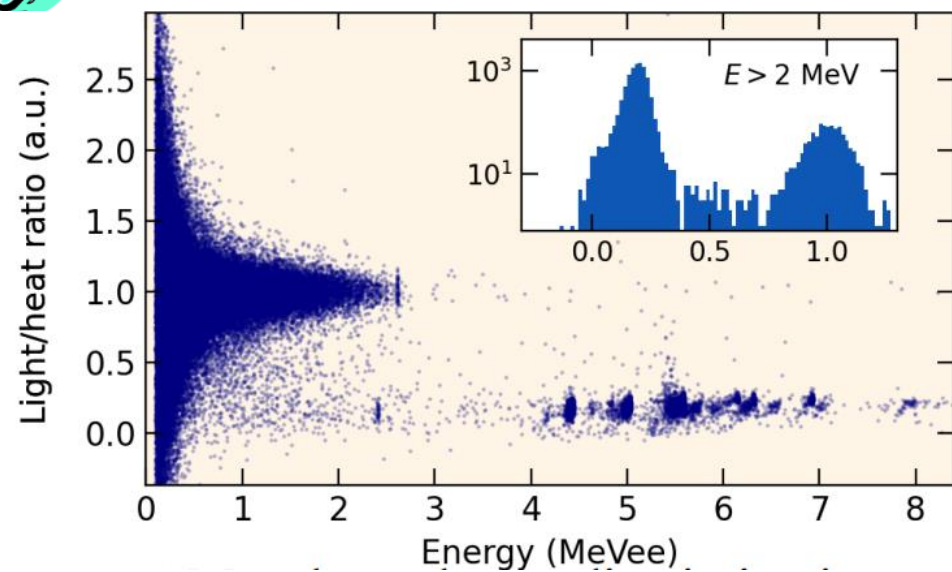
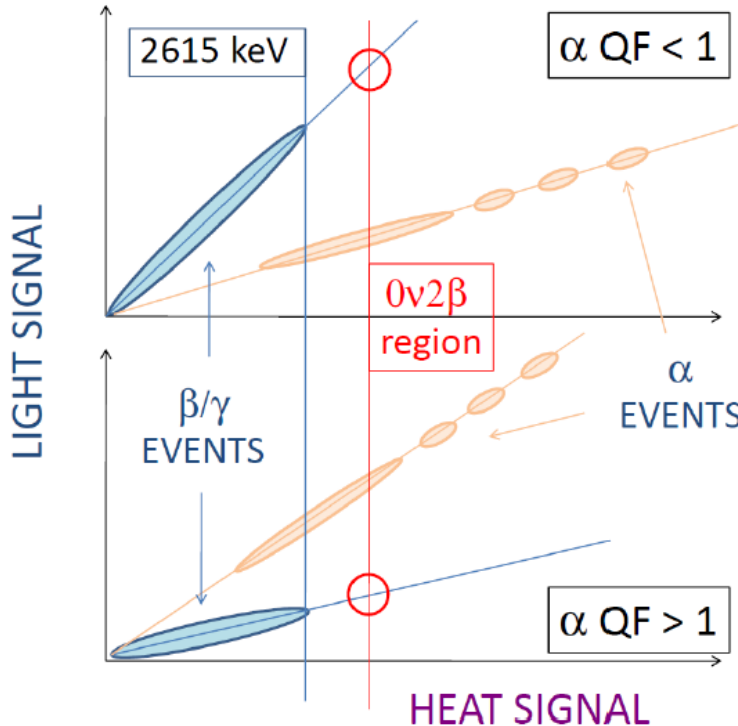
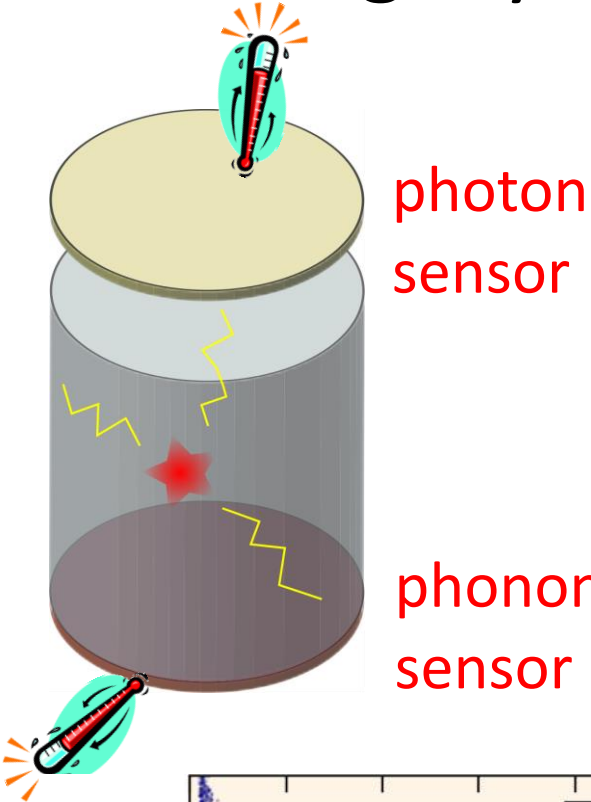
The IAXO Coll., JHEP 2021, (2021) 137



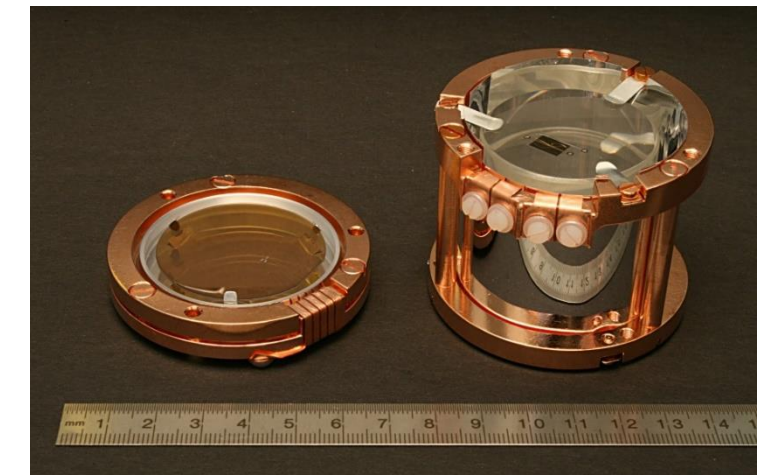
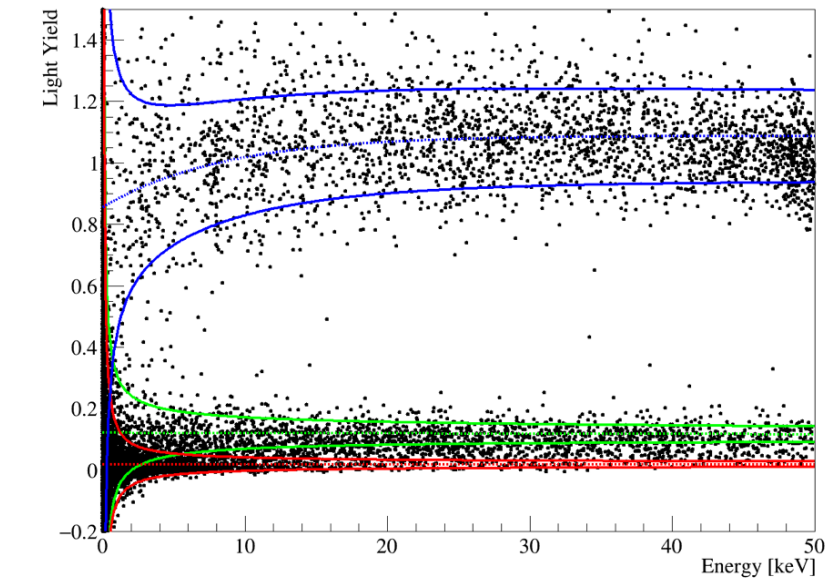
- Haloscopes**
looking for dark matter constituents,
microwaves.



Scintillating crystals

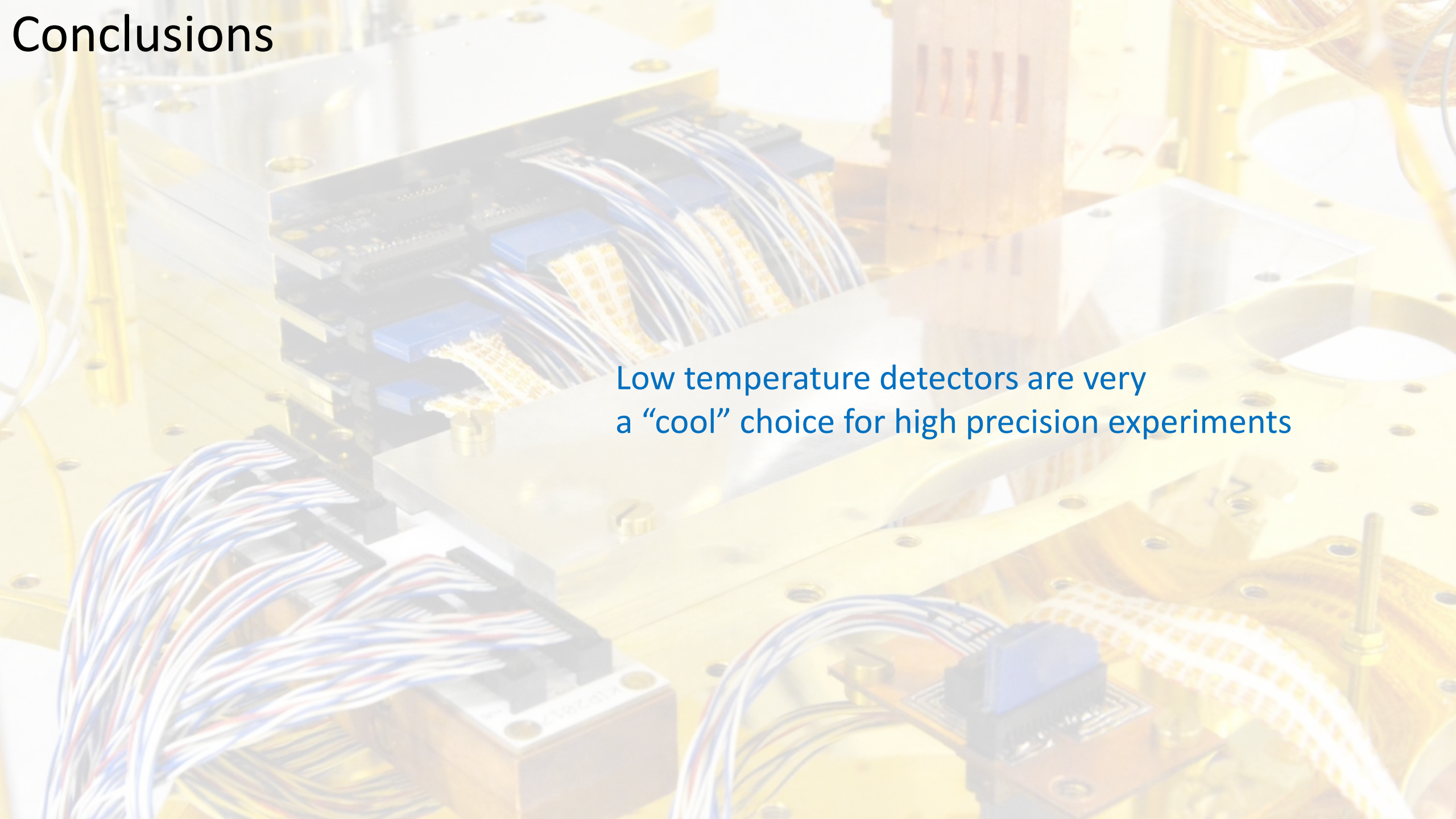


AMoRE Collaboration



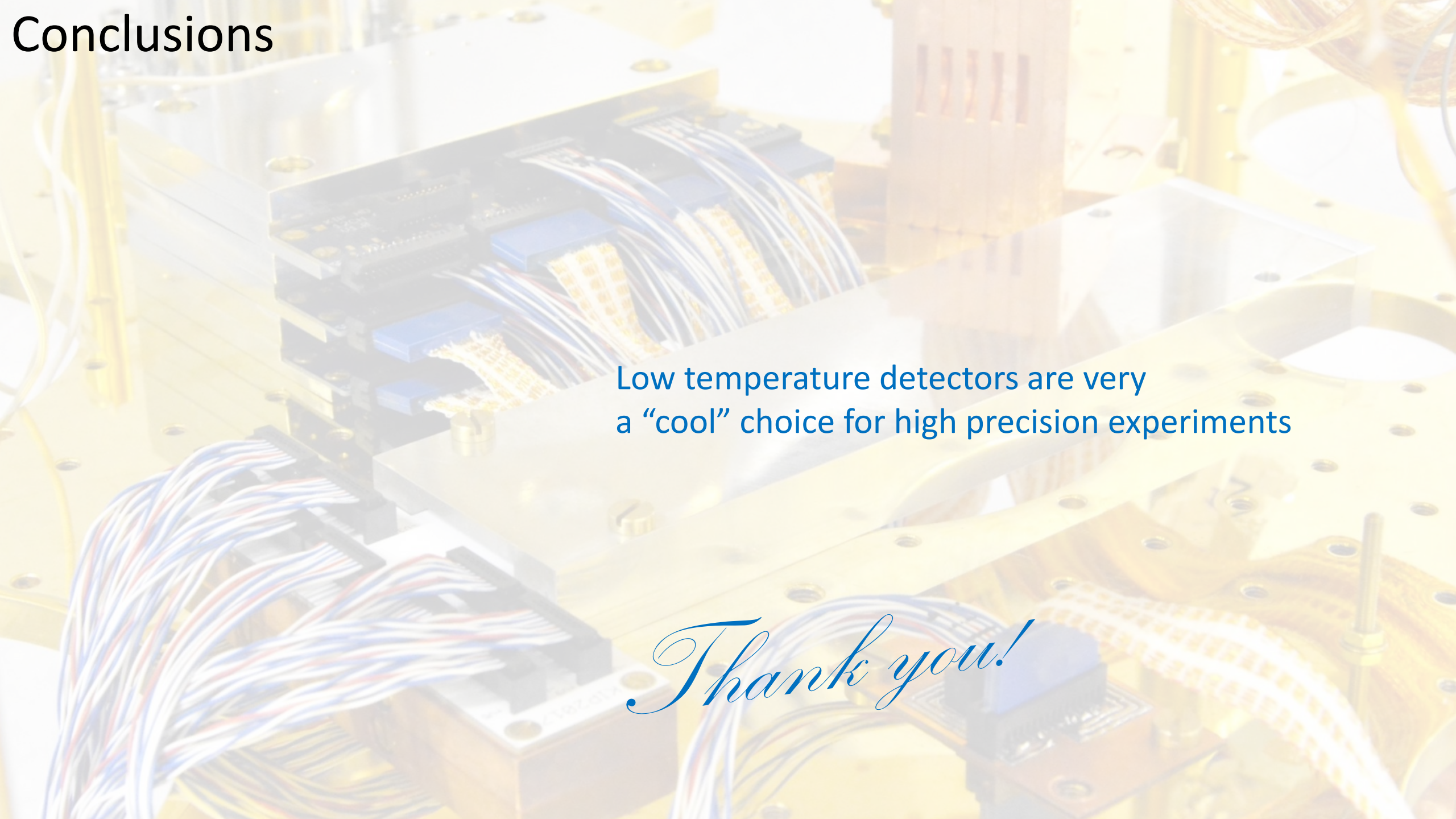
Phys.Rev.D 100 (2019) 10, 102002

Conclusions



Low temperature detectors are very
a “cool” choice for high precision experiments

Conclusions



Low temperature detectors are very
a “cool” choice for high precision experiments

Thank you!